300 Copies

NTIS-25
Bin - 128
S.P. - 125




LETC/TPR-80-1761

# TAR SAND EXTRACTION BY STEAM STIMULATION AND STEAM DRIVE—MEASUREMENT OF PHYSICAL PROPERTIES

By
William R. Lindberg

September 10, 1980 (revised)
Date Published

Work Performed Under Contract No. AS20-79LC01761

Laramie Energy Technology Center
Laramie, Wyoming

R348

TECHNICAL INFORMATION CENTER
UNITED STATES DEPARTMENT OF ENERGY

## DISCLAIMER

## DISCLAIMER



Available from the National Technical Information Service, U. S. Department of Commerce, Springfield, Virginia 22161.

Price: Paper Copy $9.00
Microfiche $3.50

Printed in the United States of America
USDOE Technical Information Center, Oak Ridge, Tennessee

LETC/TPR-80-1761
Distribution Category UC-91

Annual Report
to
Laramie Energy Technology Center

# Tar Sand Extraction by Steam Stimulation and Steam Drive - Measurement of Physical Properties

Task Order 028

For the period 10/1/78 to 11/1/79

William R. Lindberg
Principal Investigator
Dept. of Mechanical Engineering/RMIEE
University of Wyoming
January 15, 1980

TABLE OF CONTENTS

## LIST OF FIGURES

Page

## ABSTRACT

The measurement of the following thermophysical properties of Utah tar sands is in progress: thermal conductivity, specific heat relative permeability, and viscosity (of the recovered bitumen). During the report period (10/1/78 - 11/1/79), experimental procedures have been developed and a basic data set has been measured.

Additionally, standard core analysis has been performed for four drill sites in the Asphalt Ridge, Utah area.

## INTRODUCTION

The presence of large quantities of tar-sand deposits in the United States has encouraged research in the area of techniques for recovery of this resource. Recovery techniques (especially in-situ) must be modelled and evaluated on the basis of known properties of the tar-sand field. This evaluation procedure applies to field tests, laboratory tests and numerical modelling efforts.

Recovery techniques in western tar-sands depend on combustion and thermal/chemical techniques to either gasify the bitumen or increase the mobility of the bitumen so it may be brought to the well-head. In all these cases, the thermophysical properties of thermal conductivity, specific heat, and bitumen viscosity are seen to be important properties which strongly effect the recovery process. These properties are not routinely measured in any core analysis, so the present research was initiated to provide a data base of site-specific measurements of these properties. This data base will also be used to investigate

the predictability of these properties from standard core analysis results. The predictability of these properties will prove useful in both numerical modelling efforts and in the evaluation of future potential recovery sites.

Techniques for the measurement of these properties are not standardized and depend on the range of the property value. Even then, the technique chosen will also depend on economics, required accuracy, time required for the measurement, available sample size, anticipated degree of anisotropy and equipment currently on hand. Each measurement system will be discussed in the individual measurement sections, but a brief summary of the measurement technique used to measure each property is shown in Table 1 below.

| Property | Expected Range | Experimental Technique | Principal Reference for Technique |
|---|---|---|---|
| Specific Heat | .2-.6 j/kg-°K | Controlled Transient | Krischer (1954) |
| Viscosity | .1-$10^5$ poise | Capillary Tube | ASTM D 2171-6 |
| Thermal Conductivity | .5-2. W/$m^2$-°K | Comparitor Method | Tye (1969) |
| Relative Permeability | 0 - 1 | Capillary Pressure Measurement (Via mecury injection) | Burdine (1953) |

Table 1 - Measurement Technique Summary

A summary of the progress to date of the individual measurements is as follows:

Standard Core Analysis and Zone Identification

The standard core analysis for four Utah tar sand drilling sites has been performed during this period. All data from this analysis is included in this report (or is referenced). The data from these studies include: density, bitumen-sand-water content, and porosity and permeability (for both the saturated and extracted core samples). Core samples were analysed at one foot intervals for each of the four wells. Examination of this data enabled an identification of zones where properties did not vary significantly within each zone. An example of this zone identification is shown in Figure 5, where the oil saturation is plotted against depth for well 3T3. The zones of this well are identified on this figure as well.

For the non-standard tests, representative samples from each of the zones discussed above are studies to determine the variability of each property as a function of composition. The corresponding zone for each sample will be identified. The initial measurements are concentrated on samples from each zone, more detailed studies may be required after the initial studies are completed.

Specific Heat:

Seven regions of core have been measured for specific heat as a function of temperature (Regions 1, 3, 4, 5, 7, 8, 9, see Table II). A polynomial curve-fit of the data has been done for each region. As an example, Region 8, of well 3T3 at a depth of 556 feet yields a specific heat of: $C = 772.2 + 3.991T - 1.0109(10^{-2})T^2$

| Region | Well | Depth |
|---|---|---|
| 1 | 3T4 | 418 to 443 |
| 2 | 3T4 | 476 to 495 |
| 3 | 3T4 | 500 to 541 |
| 4 | 3T4 | 543 to END |
| 5 | 3T3 | 410 to 452 |
| 6 | 3T3 | 465 to 483 |
| 7 | 3T3 | 488 to 535 |
| 8 | 3T3 | 539 to END |
| 9 | 3T2 | 445 to 475 |
| 10 | 3T2 | 486 to 512 |
| 11 | 3T2 | 522 to 564 |
| 12 | 3T2 | 565 to 609 |

Table 2 - Identified Regions of Wells
3T2, 3T3, 3T4

where C is in joules/kg-°C and T is in °C. The specific heat of a low-tar and high-tar region as a function of temperature is shown in Figure 1.

Viscosity:

A quantity of bitumen recovered from Asphalt Ride, Utah outcrops has been prepared for testing. A curve of the visocity of 1.4% toluene bitumen is shown in Figure 2. It is seen that the viscosity changes from $4.8 \cdot 10^4$ poise at 20 °C to o.67 poise at 148.8 °C. A systematic study of the effect of solvent, asphaltene and maltene on the viscosity of the bitumen is in progress.

Thermal Conductivity

Five regions have been tested for the thermal conductivity of tar sand as a function of temperature. The results of two tests are shown in Figure 4. The average thermal conductivities for the two samples are 1.51 and 1.65 $W/m^2$-°K. To date, very little temperature dependence on thermal conductivity has been found. The effect of water saturation and axial loading has not been evaluated to date.

Relative Permeability

Various samples of extracted core have been tested for capillary pressure as a function of saturation. From this data, relative permeability is predicted using Burdine's (1953) theory. An example of the results is shown in Figure 4, where the four curves correspond to quite different core samples.

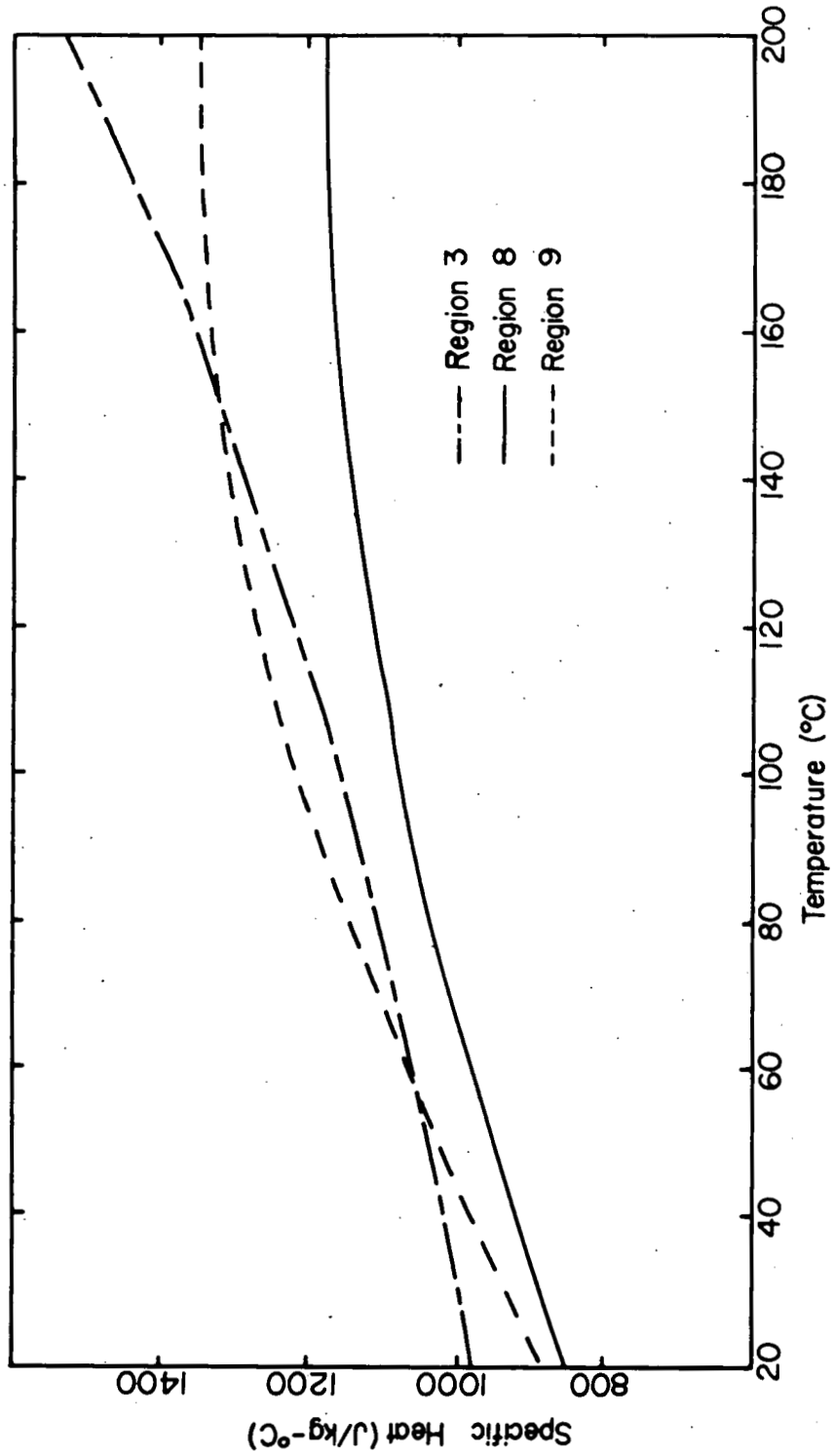


Figure 1. Specific heat as a function of temperature for three zones (zones 3, 8, and 9).

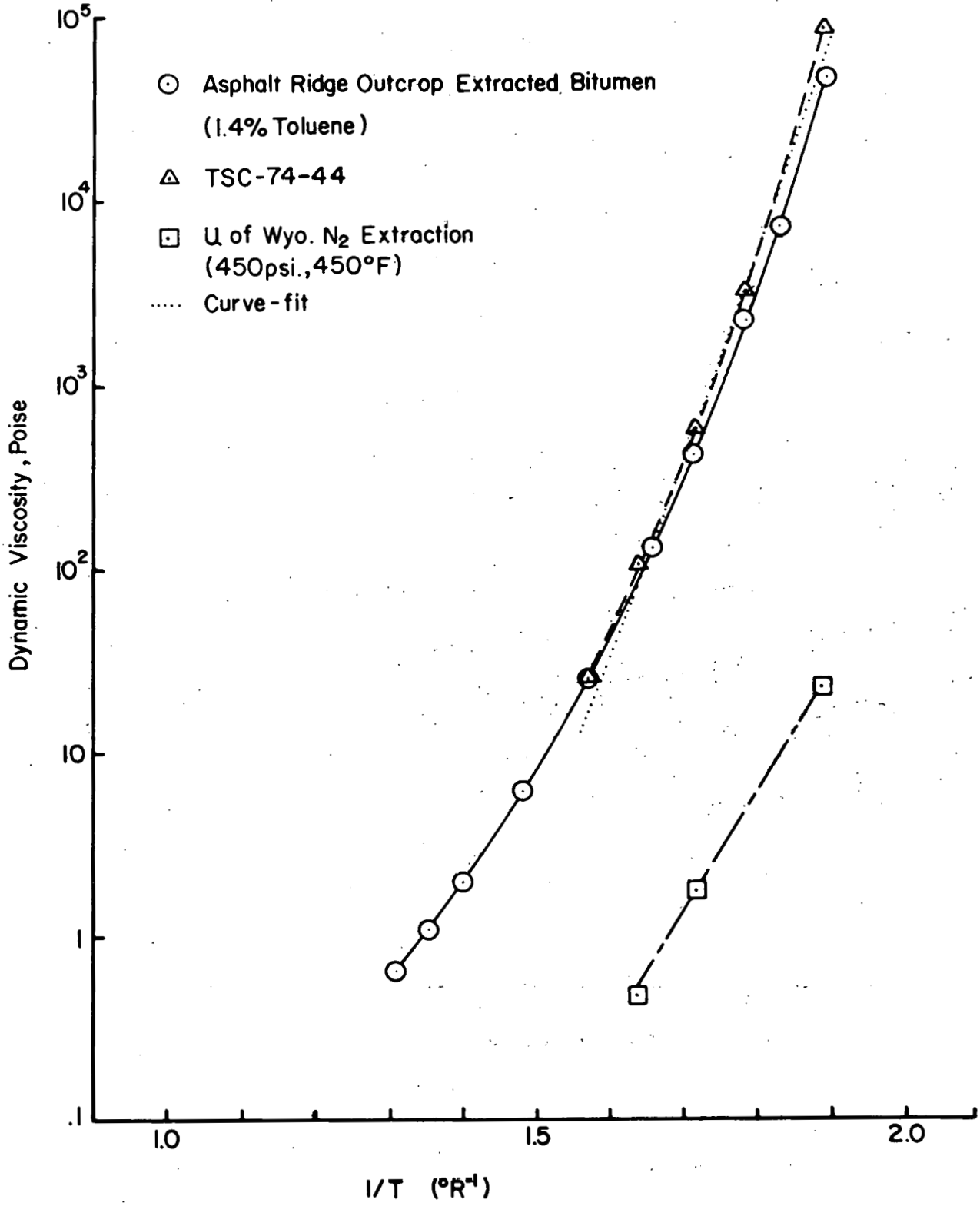


Figure 2. Measured viscosities of various tar sand bitumen products.

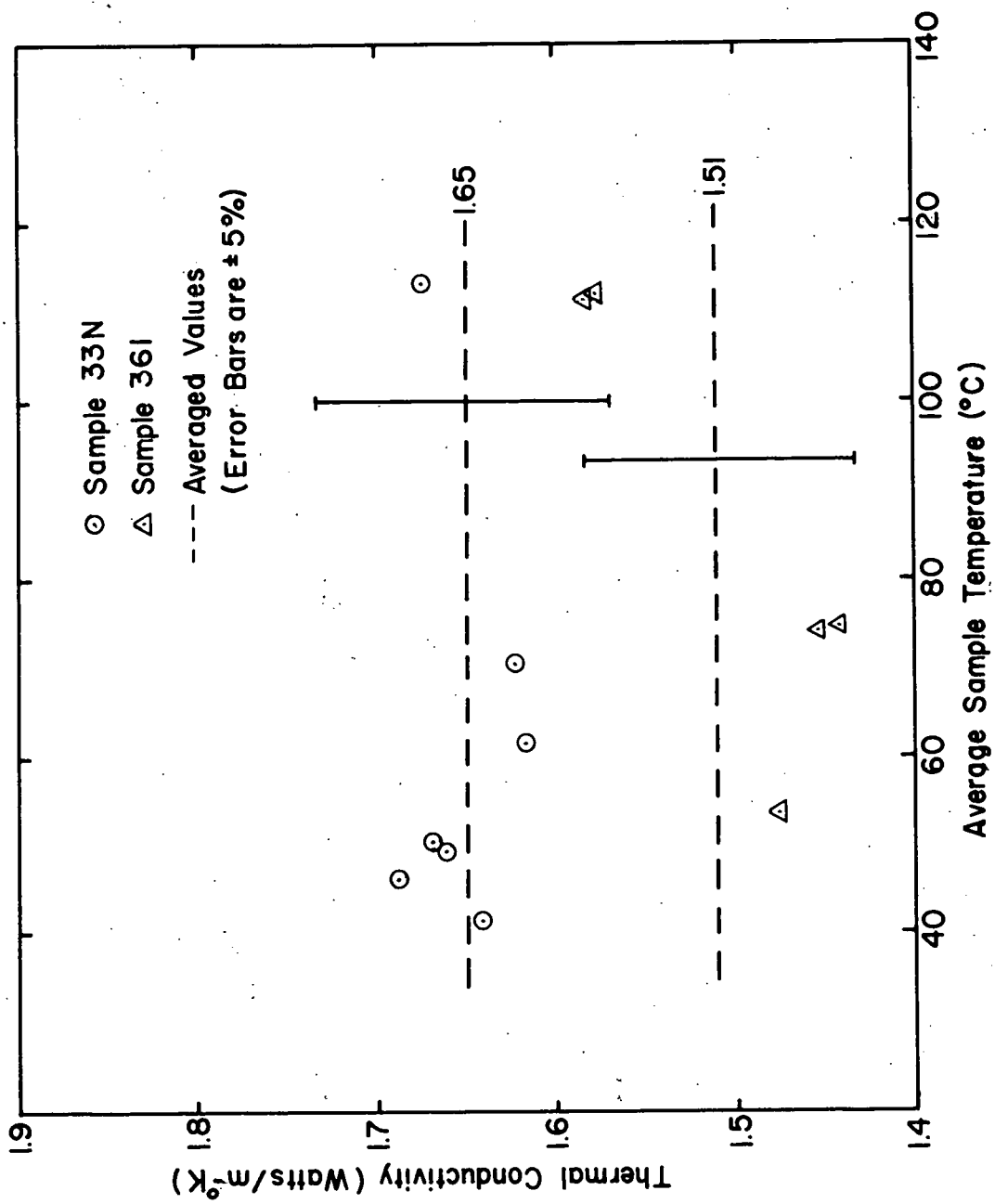


Figure 3. Thermal conductivity as a function of temperature for two tar sand samples.

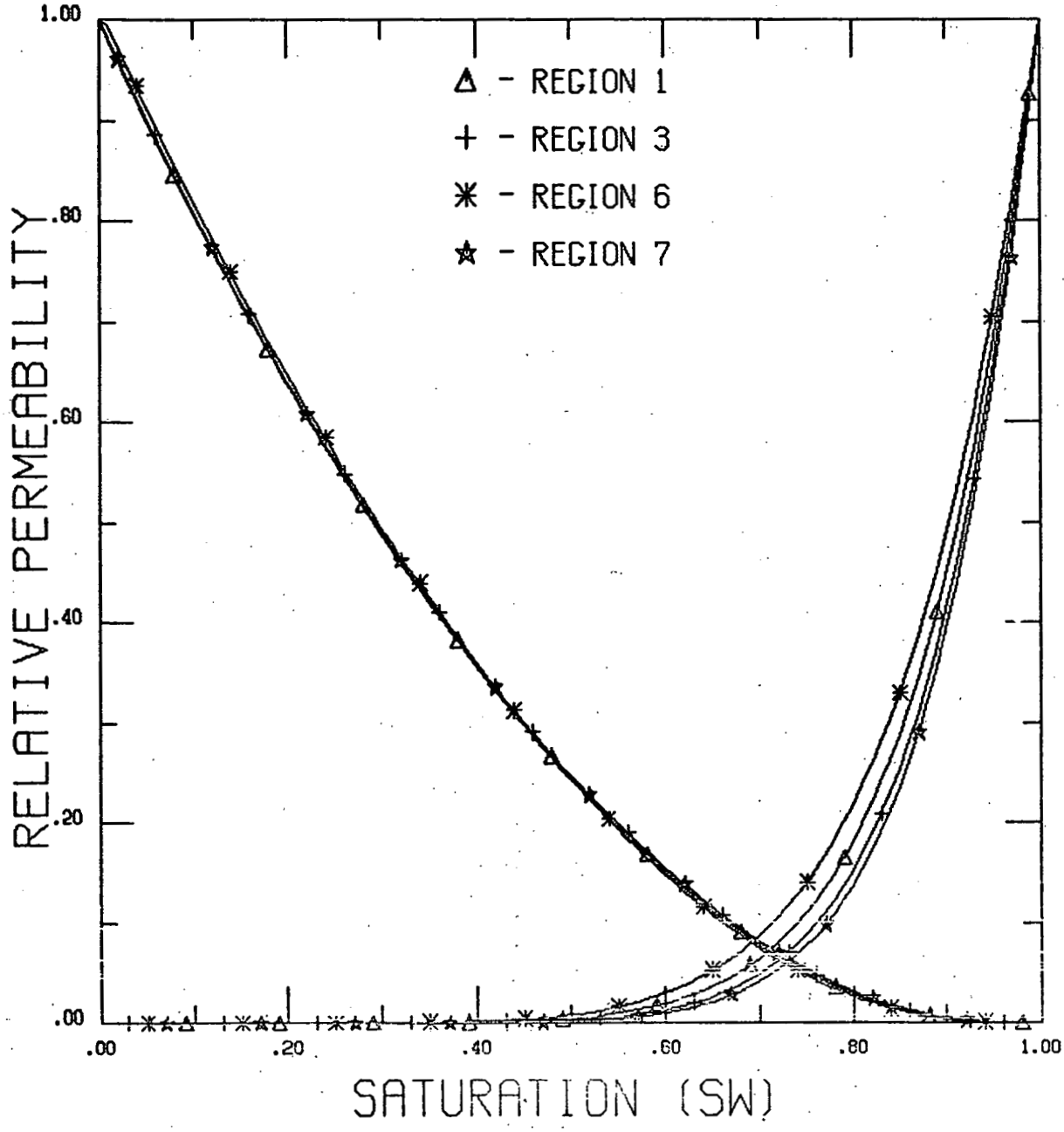


Figure 4. Relative permeability curves for four regions, as predicted from capillary pressure measurements.

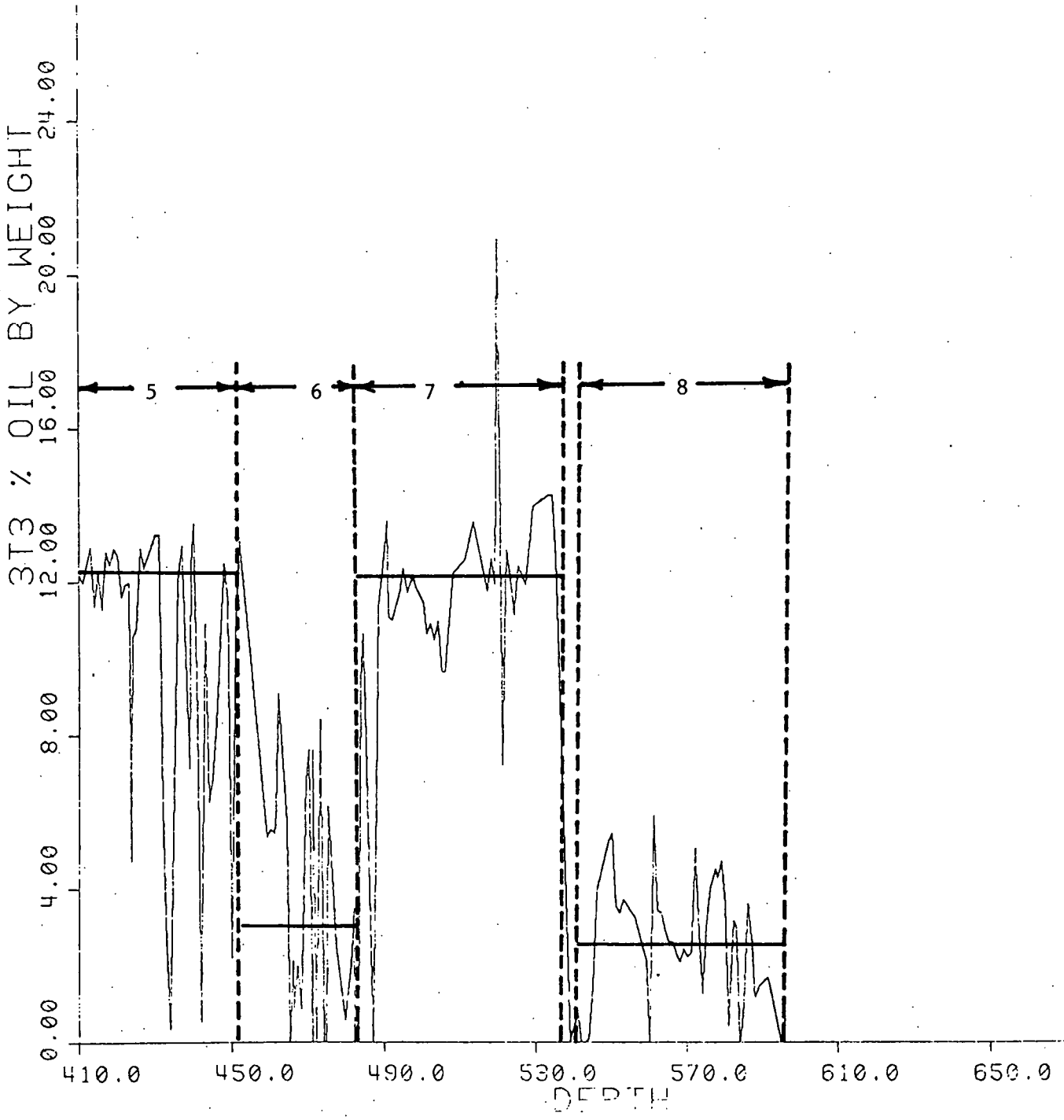


Figure 5. Percent oil saturation for Well 3T3. Identified zones are indicated in Table II. The layers between zones are predominately low oil, shale layers.

## TECHNICAL DISCUSSIONS

### Standard Core Analysis and Zone Identification

Standard core analysis has been performed for the well cores 3T1, 3T2, 3T3, and 3T4. A map showing the location of these cores is shown in Figure 6. These tests were performed at the Laramie Energy Technology Center using that facility's equipment. The density, oil-water-sand content, permeability of saturated and extracted cores and porosity of the saturated and extracted cores were found using standard core analysis techniques.

The results of these studies are summarized in Figure 10. The numerical results are on file at the Department of Mechanical Engineering, University of Wyoming, the Rocky Mountain Institute of Energy and Environment, University of Wyoming and the Laramie Energy Technology Center.

The computer program used for reducing the laboratory data is included in this report as Appendix I. This program was written for a Hewlett Packard 2100 series mini-computer.

An examination of Figures 10a, 10b, and 10c, (oil content for wells 3T2, 3T3 and 3T4) shows distinct zones of high oil content and layered beds of shale-like material. These natural divisions enabled four zones for each well to be identified and these zones are labeled on Figure 10. These regions are also summaried in Table II as a function of depth. The identified region numbers are included in each property test. The average value of selected properties are tabulated for each zone in Table III. It is seen that the variability

LOCATION
OF TEST HOLES
NE¼SE¼ SECTION 23,
T4S R20E SLM

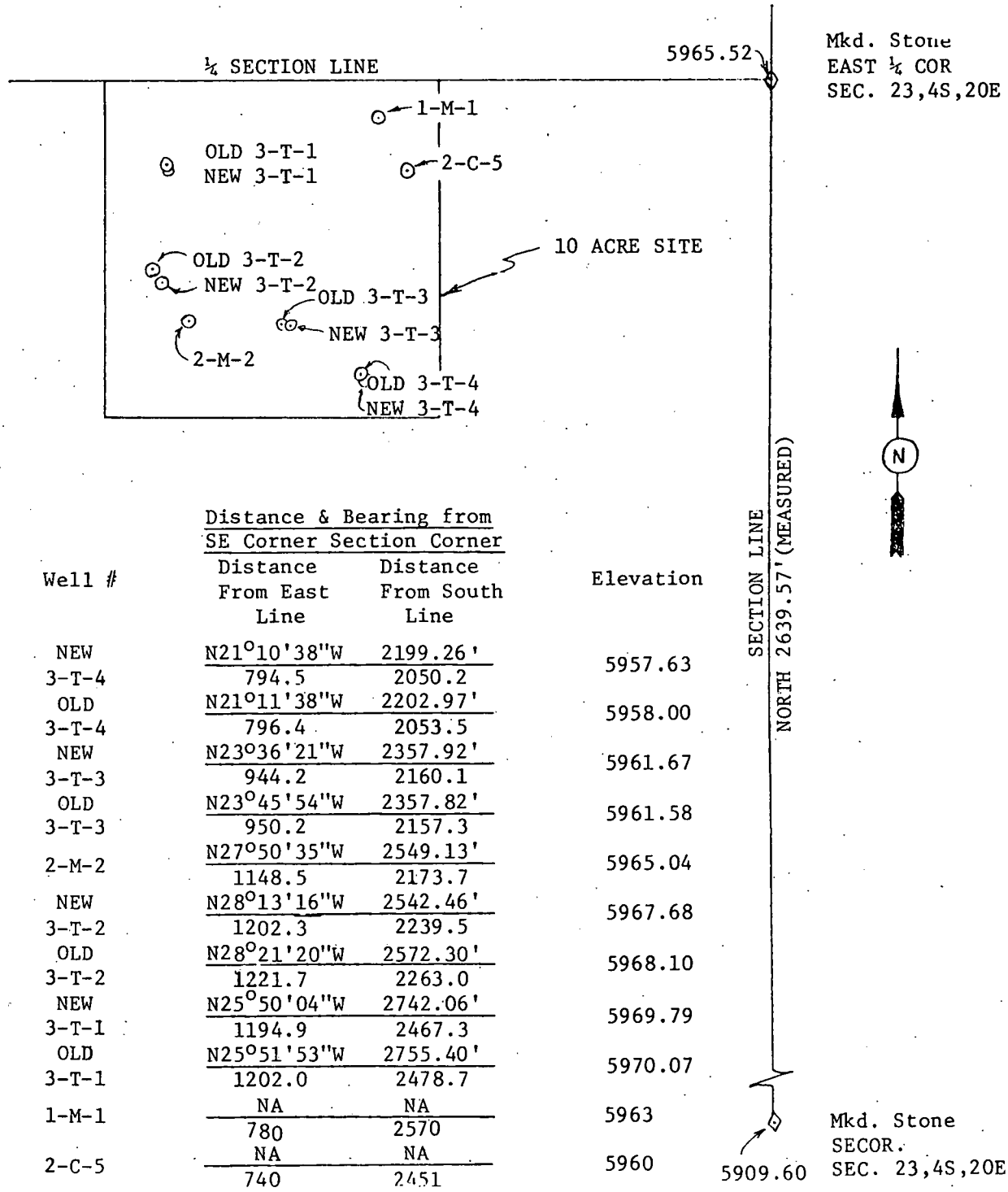


| Well # | Distance & Bearing from SE Corner Section Corner: Distance From East Line | Distance From South Line | Elevation |
|---|---|---|---|
| NEW 3-T-4 | N21°10'38"W | 2199.26' | 5957.63 |
| | 794.5 | 2050.2 | |
| OLD 3-T-4 | N21°11'38"W | 2202.97' | 5958.00 |
| | 796.4 | 2053.5 | |
| NEW 3-T-3 | N23°36'21"W | 2357.92' | 5961.67 |
| | 944.2 | 2160.1 | |
| OLD 3-T-3 | N23°45'54"W | 2357.82' | 5961.58 |
| | 950.2 | 2157.3 | |
| 2-M-2 | N27°50'35"W | 2549.13' | 5965.04 |
| | 1148.5 | 2173.7 | |
| NEW 3-T-2 | N28°13'16"W | 2542.46' | 5967.68 |
| | 1202.3 | 2239.5 | |
| OLD 3-T-2 | N28°21'20"W | 2572.30' | 5968.10 |
| | 1221.7 | 2263.0 | |
| NEW 3-T-1 | N25°50'04"W | 2742.06' | 5969.79 |
| | 1194.9 | 2467.3 | |
| OLD 3-T-1 | N25°51'53"W | 2755.40' | 5970.07 |
| | 1202.0 | 2478.7 | |
| 1-M-1 | NA | NA | 5963 |
| | 780 | 2570 | |
| 2-C-5 | NA | NA | 5960 |
| | 740 | 2451 | |

Figure 6. Laramie Energy Technology Center Tar Sands Field Site, Vernal, Utah.

is quite significant and that the zone identification is too coarse for anything except "first look" purposes.

It should be noted that a few porosity calculations may be incorrect. Since the mercury pyncnometer could not be calibrated after each core and a variable degree of sand would accumulate in the cylinder, negative porosities resulted on occasion. The graphs indicate these points as being zero.

Viscosity

Viscosity measurements are continuing on bitumen extracted from Utah open pit sites. The past few months have been used to extract a quantity of bitumen by roto-evaporation and filtering. The quantity extracted is 1400 ml.

The viscosity regions of study are to include the following: (1) non-Newtonian effects at selected temperatures ranging from 20°C to 204°C, (2) Arrhenius plots for varying degrees of asphaltene content and toluene dilution content.

Cannon-Manning capillary-tube viscosity equipment is being used since both non-Newtonian and high temperature measurements are desired. Additionally, the large range of dynamic viscosity which the bitumen exhibits as a function of temperature may be accommodated with this equipment.

To date, the tests which have been performed are on bitumen from (a) sample TSC-74-44, (a toluene extracted sample), (b) University of Wyoming extraction tests using nitrogen at 450°F and 450 psi., and (c) toluene-extracted samples from Asphalt Ridge, Utah outcrops (this is the material to be used in the subsequent detailed testing program).

The results of these tests are shown in Figure 2. The Arrhenius plots show a marked deviation from linearity above 200°F, but below that temperature, a first estimate for the viscosity-temperature dependence is of the form:

$$\mu = (3.26 \cdot 10^{-17}) \exp(2.85 \cdot 10^{4}/T)$$

where $\mu$ is in poise and T is in °R. This curve-fit is for the 1.4% toluene-diluted sample.

The rheological behavior of the tested bitumen indicated that the material is very nearly Newtonian and only the slightest tendency toward Bingham-type behavior has been observed. These observations are well-borne out in Figures 7a, b, and c. A least-squares best-fit to the shear-strain rate curves has been applied and the slope-intercept values are shown on the figures. The calculated slopes of the lines are in excellent agreement with the measured viscosity values of Figure 2.

Since the experimental procedures used for the viscosity tests are standard ASTM procedures, the details may be obtained by referring to ASTM Standard D 2171-66.

Specific Heat

The specific heat of tar sand samples is being measured with an in-house designed and constructed apparatus which is patterned after a system suggested by Krischer (1954). This technique was seen to be suitable after a review of conventional techniques indicated problems with each approach. The advantages of the approach presently being used are: (1) inhomogenieties in the cores require a fairly large sample to adequately represent the "bulk" specific heat, (2) a wide

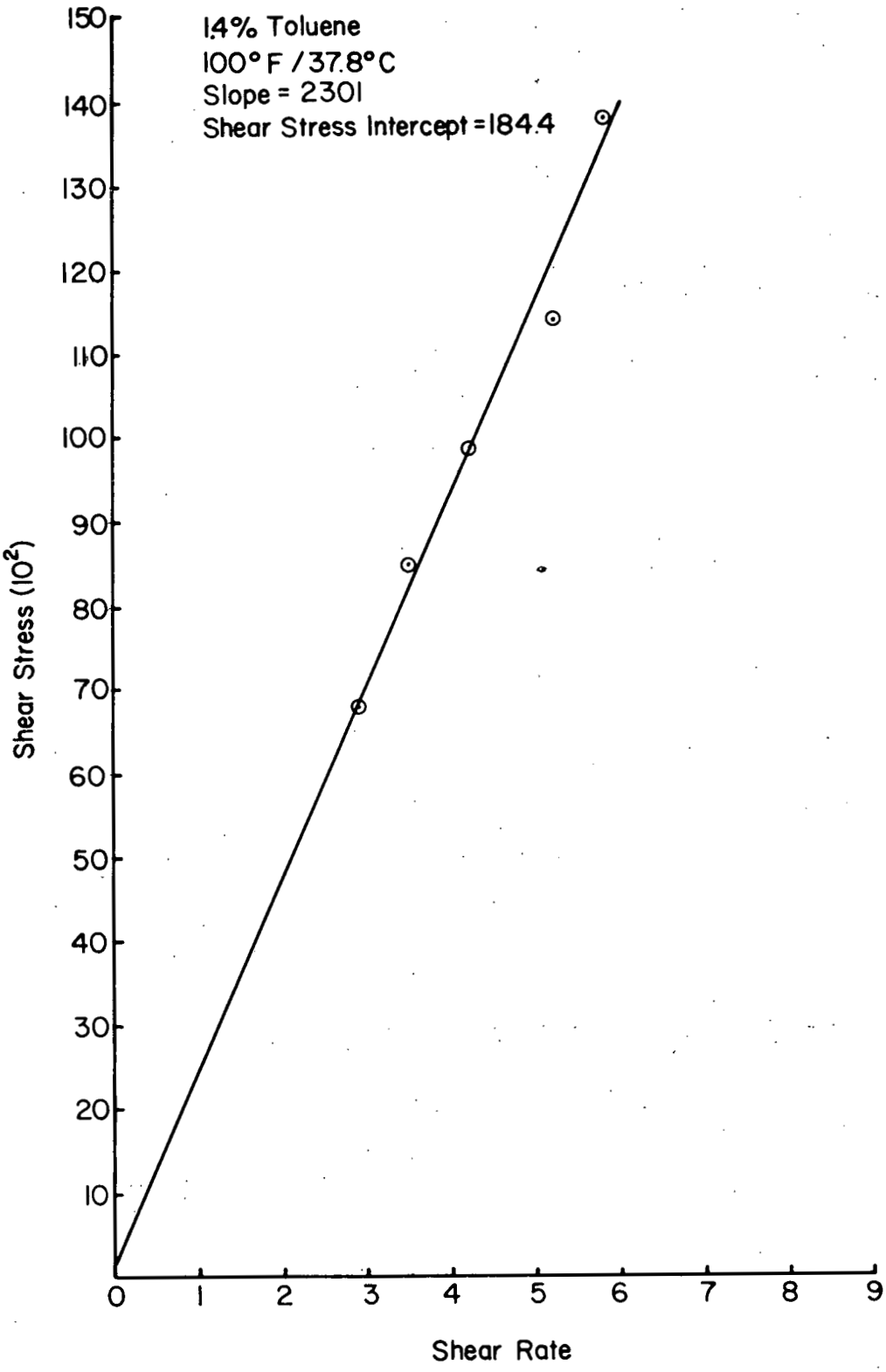


Figures 7. (a)(b)(c) Test of Newtonian behavior of bitumen (toluene extracted, primary sample) with 1.4% toluene present (a) 100°F, (b) 140°F, (c) 275°F.

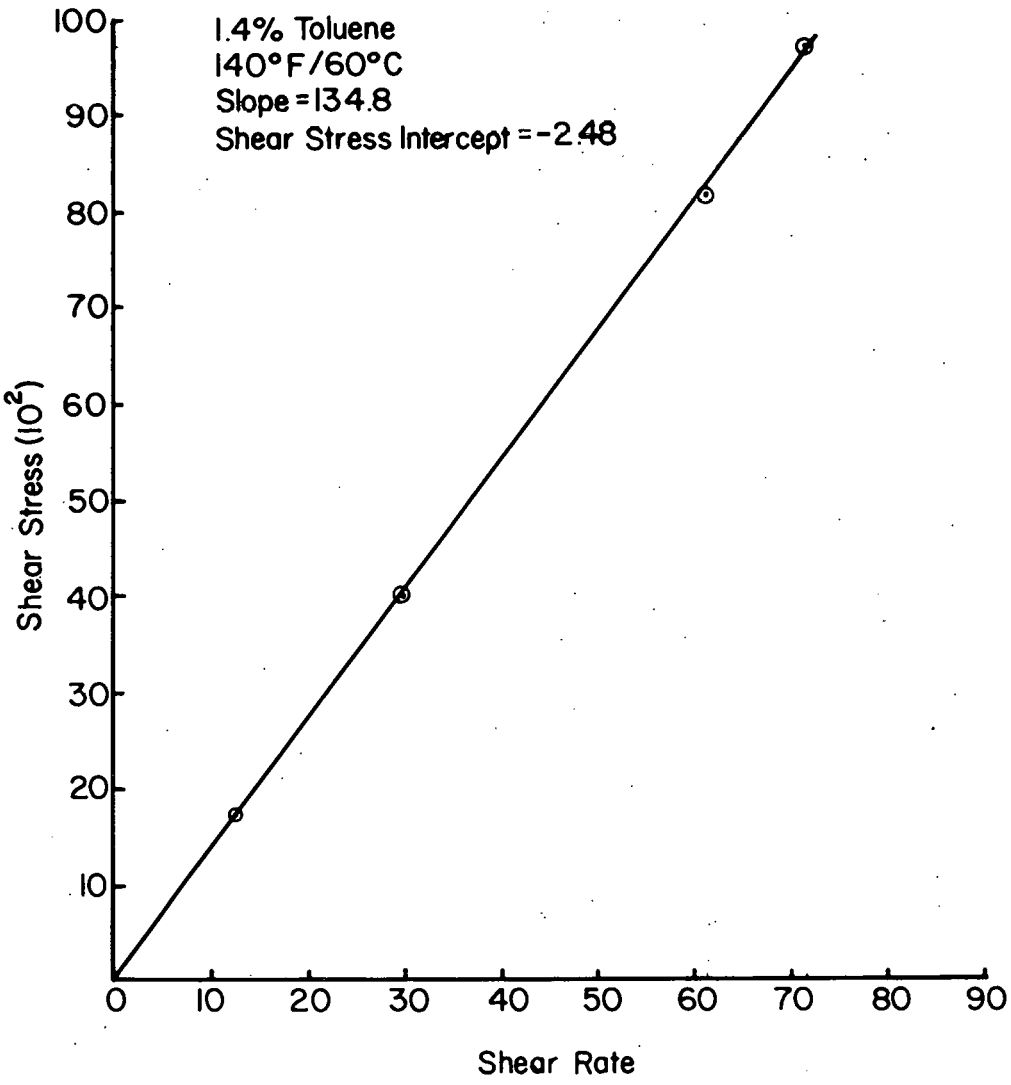
1.4% Toluene
140°F/60°C
Slope = 134.8
Shear Stress Intercept = -2.48
Shear Stress ($10^2$)
100
90
80
70
60
50
40
30
20
10
0
10
20
30
40
50
60
70
80
90
Shear Rate

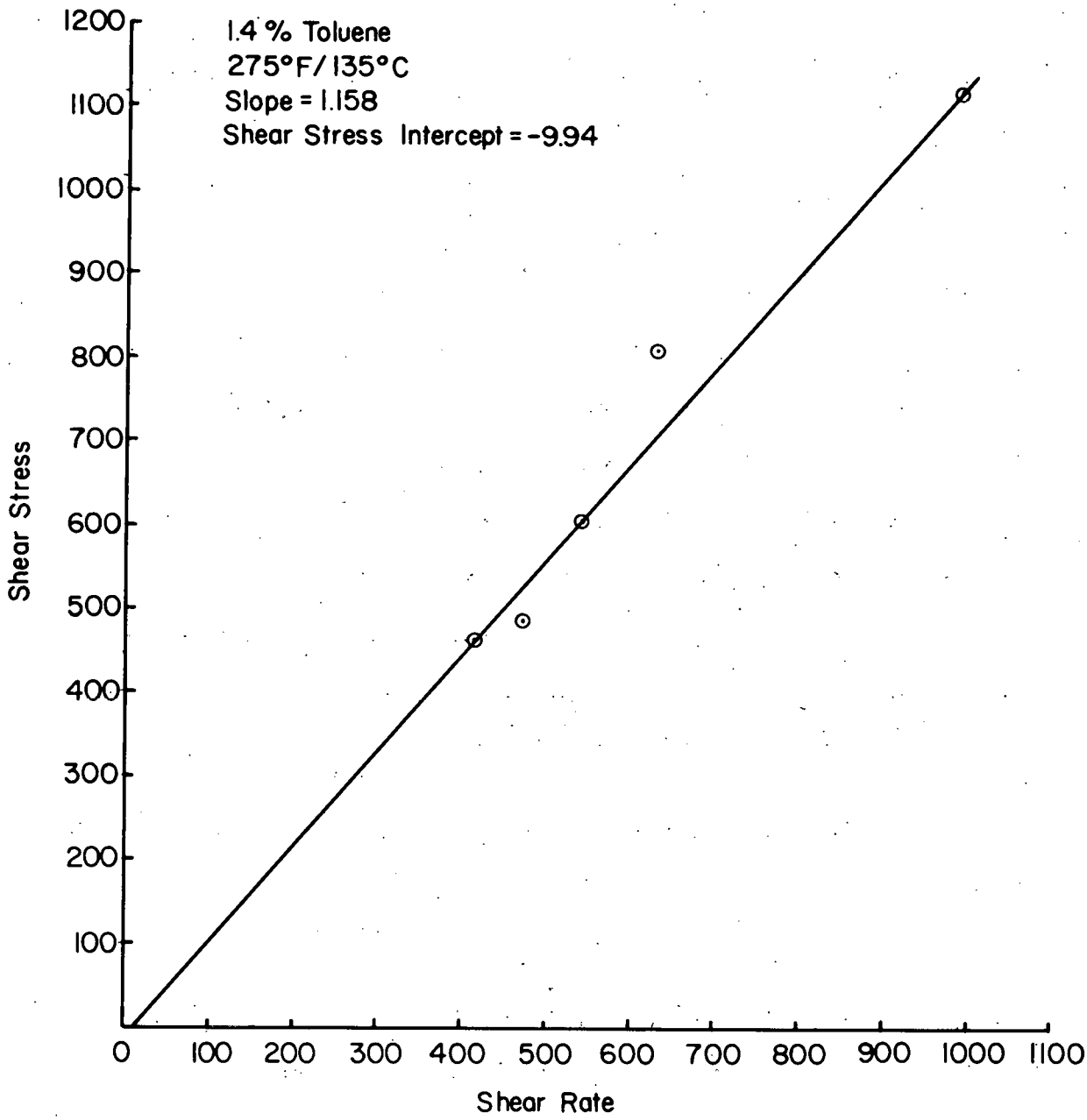
1.4 % Toluene
275°F/135°C
Slope = 1.158
Shear Stress Intercept = -9.94
Shear Stress
Shear Rate
1200
1100
1000
900
800
700
600
500
400
300
200
100
0
100
200
300
400
500
600
700
800
900
1000
1100

range of temperatures was desired to examine the sample's dependence on temperature, (3) a lack of detailed information on related properties dictated a technique which did not require this corrolary information.

A detailed summary of the theory and procedure of the technique is included in Appendix II. Since the approach is somewhat unconventional, calibration tests and repeatability tests have been made in some detail for the initial sample tests. The results (as summarized in Appendix II) indicate the technique is viable and applicable to the range of specific heats being measured.

As the discussion in Appendix II indicates, the apparatus is arranged as shown in Figure 8. The two central heaters provide a constant heat flux, q, to the four adjacent samples, which in turn transiently heat up with time. The other heaters are used to guard the boundaries from heat losses. After approximately 30 minutes, the system has evolved into a quasi-steady state wherein the temperature distribution within the samples is as follows:

$$T(x,t) = \frac{q\ t}{\rho\ C_p L} + \frac{q\ L}{k}\ \left(\frac{3x^2 - L^2}{6L^2}\right)$$

If this equation is differentiated with respect to time at a fixed measurement, x, one obtains:

$$C_p = \frac{q}{\rho\ L}\ \left(\frac{dt}{dT}\right). \qquad (1)$$

The experiment thus involves monitoring an interior temperature of the sample as a function of time, curve-fitting the resulting temperature-time curve and differentiating the smoothed curve. Equation (1) is

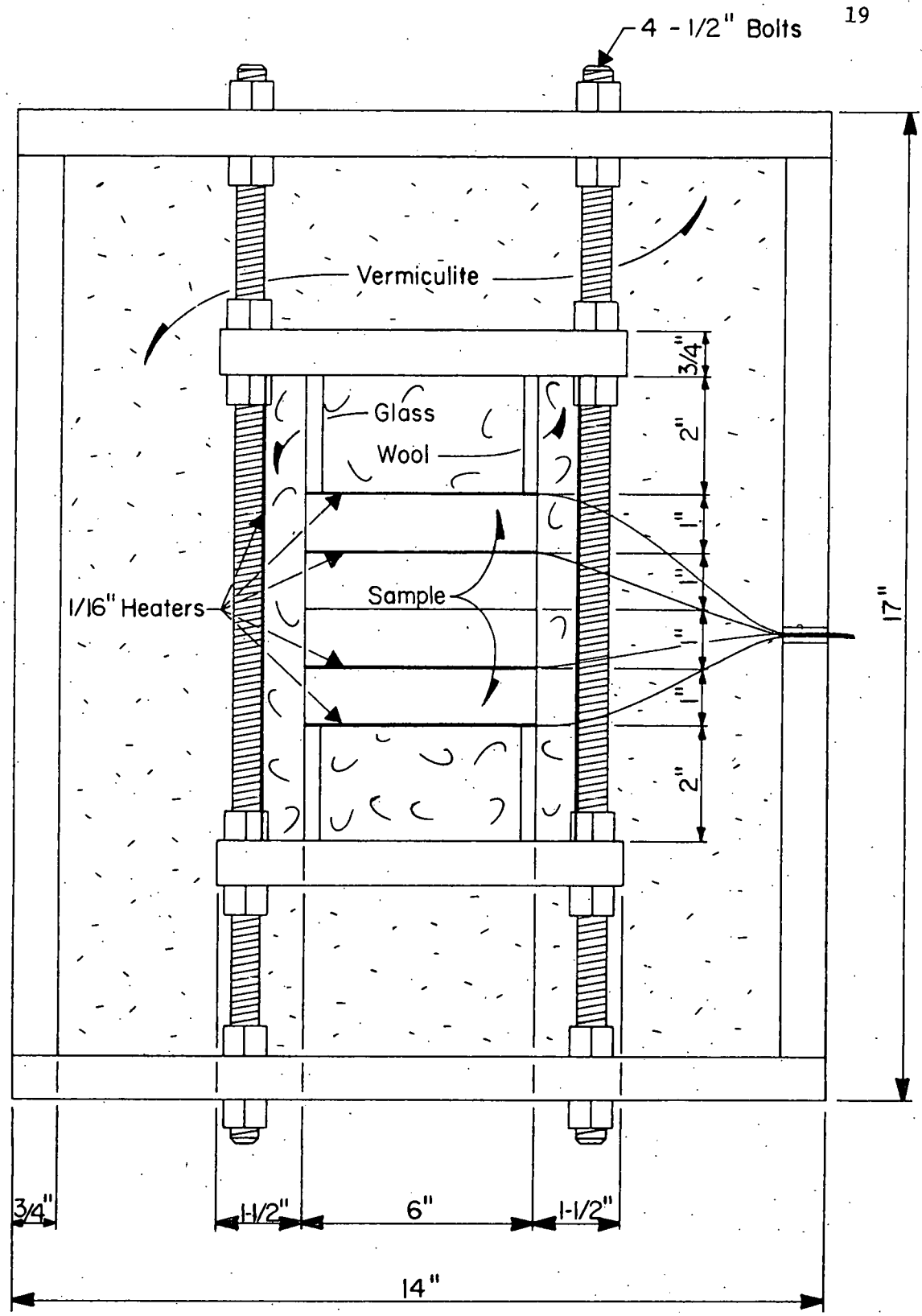


Figure 8. Specific heat apparatus

then applied to determine the specific heat as a function of average temperature of the sample. When this procedure is applied to samples from Region 3 and 8, the specific heat may be written as:

$$(C_p)3 = 8.24(10^{-3})T^2 + 1.295T + 954.2$$

$$(C_p)8 = -1.011(10^{-3})T^2 + 3.99T + 772.2$$

where $C_p$ is in J/kg-°C and T is in °C. The range of validity of these equations is from room temperature up to 200°C. These equations are plotted in Figure 1. It should be noted that Region 3 is a high bitumen content area while Region 8 is quite low in bitumen content. A rough estimate of the constituent properties may be obtained from the specific heat properties of the two regions:

$$(C_p)_i = (C_{p,\text{bitumen}})\, x_{\text{bitumen},i}\, (C_{p,\text{sand}})\, x_{\text{sand},i}$$

were the subscript refers to the sample number and x is the constituent mass fraction. For the two regions (3 and 8) the constituent properties are of the order of 940. j/kg-°C for the sand and 1790 j/kg-°C for the bitumen specific heat. This is a very rough estimate as water content has not been included and the mass fractions are only estimates, however, these values are consistent with published values for sands and asphalts.

It is expected that the initial examination of the eight regions will be completed by 1 January, 1980. This data should provide an adequate data base for examining both tar sand and constituent specific heats as a function of temperature.

Relative Permeability

Relative permeability measurements for tar sand samples have been generated through a multi-step procedure based on theoretical and

empirical results. The theoretical and experimental basis for this procedure is reviewed in Appendix III. The curves were calculated from capillary pressure measurements which were obtained from a memory injection apparatus. This particular technique was selected because of the speed, ease and availability of the mercury injection apparatus, as compared to measuring relative permeability directly. The accuracy of this technique is subject to question, and it appears worthwhile to perform some independent measurements of relative permeability. This independent check is scheduled for the 1979-80 period.

As is indicated in Appendix III, the basic equations (from Burdine, 1954) for calculating the relative permeability for the wetting and non-wetting fluids are:

$$k_{rw} = (S_e)^{\frac{2 + 3\lambda}{\lambda}}$$

$$k_{rnw} = (1 - S_e)^2(1 - S_e^{\frac{2 + \lambda}{\lambda}}),$$

where $S_e$ is the effective saturation and $\lambda$ is a number which characterizes the pore-size distribution of the medium (and is determined from capillary pressure measurements).

The results of tests in four regions for relative permeability are shown in Figure 4. The four regions cover the range of consistency from very loose sandstone to consolidated shale, and it is surprising that the relative permeability curves show such striking similarity. At least three possibilities exist for accounting for this similarity: (1) the pore-size distribution, as reflected in similar values of $\lambda$, is the same order in all four samples, (2) the experimental and numerical

procedure for determining $\lambda$ and $S_e$ is inadequate to resolve the material differences, or (3) Burdine's theory is an inadequate representation of the relevant processes.

Thermal Conductivity

Thermal conductivity measurements are being made using the "comparative method". As is indicated in Appendix III, this method was selected to best suit the requirements of nonhomogeniety and expected range of thermal conductivity. The apparatus is schematically shown in Figure 9.

The main elements of the apparatus are: 1) The stack, which is composed of 1.9 cm diameter elements each 2.86 cm long. The center element is the test sample and the adjacent elements are Pyrex glass of known thermal conductivity. Temperatures at two points along the axis of each element are measured. 2) The heater and heat sink elements provide the required temperature gradient for the system. 3) The guard system, which provides a temperature profile around the stack very close to the stack's temperature profile, thus reducing radial heat losses.

Thermal conductivity of the test sample is thus measured through Fourier's law of conduction:

$$k = \frac{LQ}{A\Delta T}$$

where k is thermal conductivity, L the axial distance between the temperature probes in the sample, A is the cross-sectional area of the sample, Q is the averaged, measured heat flux through the comparator elements adjacent to the sample, and $\Delta T$ is the temperature difference between the two measuring points in the sample.

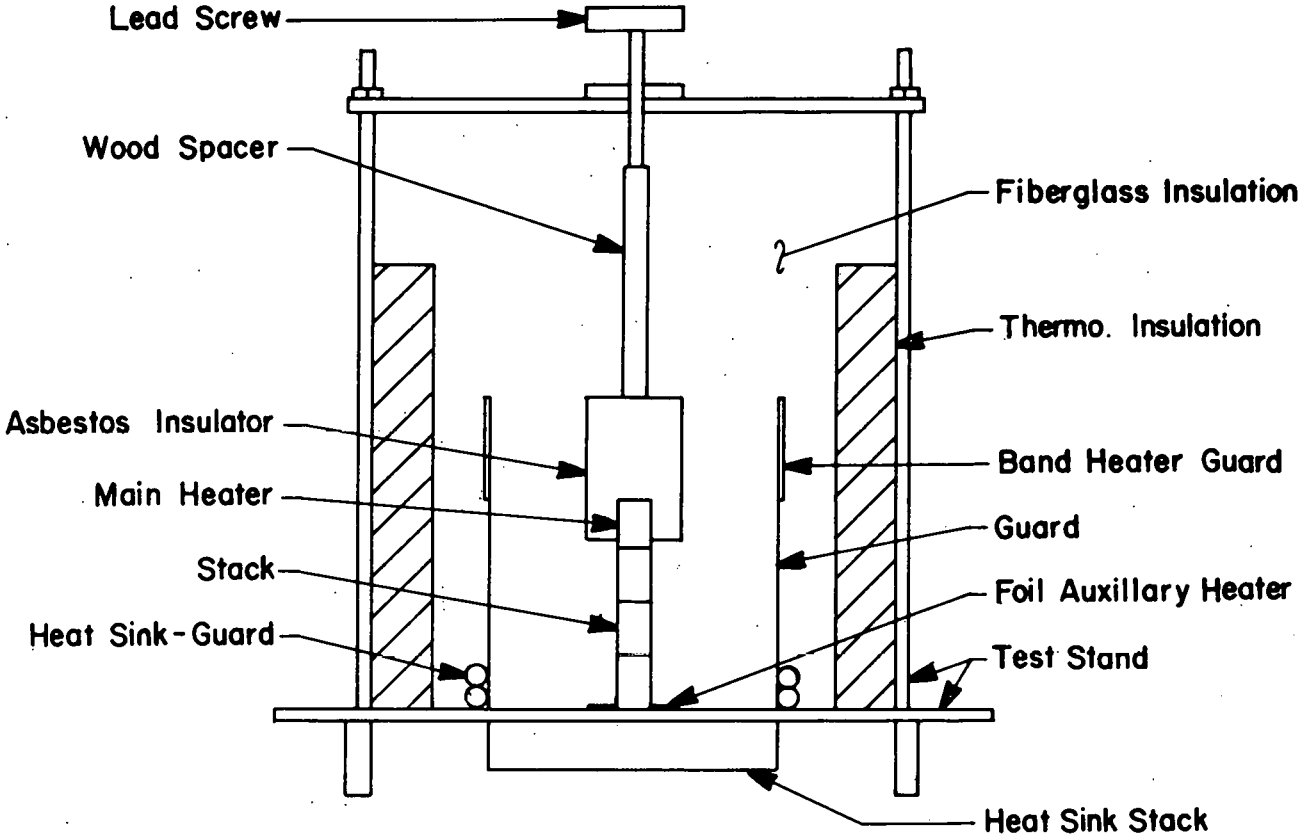


Figure 9. Thermal conductivity test apparatus.

Results of two tests are shown in Figure 3. Both data sets have a variability around the mean of less than $\pm$ 5%. The basic properties of the two samples of Figure 4 are tabulated in Table IV.

TABLE IV

Basic properties of samples 33N and 361 which correspond to thermal conductivity data of Figure 4.

| | Sample No. | |
|---|---|---|
| | 33N | 361 |
| Region No. | 5 | 3 |
| Well No. | 3T3 | 3T4 |
| Depth (ft.) | 443 | 506 |
| Permeability Saturated (md) | 10.6 | 0* |
| Porosity, Saturated (% pore volume) | 4.44 | 4.3 |
| Percent oil (weight) | 12.88 | 13.14 |
| Percent oil (saturation) | 82.7 | 87.6 |
| Percent water (saturation) | 6.04 | 2.03 |
| Density ($gm/cm^3$) | 2.065 | 2.086 |
| Average conductivity (watts/m°K) | 1.65 | 1.51 |

*permeability less than .05 md

The variation in thermal conductivity between the rather similar samples appears to be due to the difference in water content. The apparent increase in thermal conductivity with temperature seems to be attributable to an experimental problem rather than any real trend. This problem, associated with a change in operating mode at higher temperatures, is being addressed at the present.

No attempt has yet been made as to the predictability of thermal conductivity using standard core analysis data. This program is in the beginning stages of a literature search. The methods suggested by Crane and Vachon (1977) Krupiczka (1967), Somerton, Keese and Chu (1971), and Arrand, Somerton and Jomaa (1973), are, however, encouraging. The next few months are also scheduled for testing of the effect on thermal conductivity of water saturation, orientation and applied overburden pressure.

| Region | Well | Depth (Ft) | Density ($lbm/ft^3$) | Permeability Saturated (Millidarcy) | Permeability Extracted (Millidarcy) | Porosity Saturated (% Pore) | Porosity Extracted (% Pore) | %Weight Bitumen | %Weight Water | %Saturation Bitumen | %Saturation Water |
|---|---|---|---|---|---|---|---|---|---|---|---|
| 1 | 3T4 | 428 | 128.09 | 12.8 | 57.4 | 5.25 | 34.55 | 9.81 | .19 | 57.73 | 7.37 |
| 2 | 3T4 | 488 | 136.57 | 6.1 | 187.4 | 3.11 | 29.04 | 8.27 | .07 | 61.91 | 4.24 |
| 3 | 3T4 | 521 | 129.43 | 4.9 | 727.0 | 5.23 | 31.36 | 11.55 | .08 | 76.97 | 3.31 |
| 4 | 3T4 | 554 | 118.04 | 16.0 | 191.8 | 16.32 | 25.28 | 1.92 | .09 | 16.29 | 1.02 |
| 5 | 3T3 | 421 | 129.99 | 4.5 | 413.7 | 2.23 | 30.38 | 11.60 | .08 | 79.77 | 7.81 |
| 6 | 3T3 | 468 | 135.01 | 5.5 | 2.2 | 13.66 | 17.95 | .87 | 2.99 | 10.15 | 56.95 |
| 7 | 3T3 | 501 | 127.61 | 26.6 | 503.2 | 5.65 | 28.39 | 10.60 | .40 | 76.31 | 14.40 |
| 8 | 3T3 | 556 | 119.39 | 445.8 | 508.0 | 23.72 | 29.53 | 3.24 | .38 | 20.67 | 30.42 |
| 9 | 3T2 | 447 | 129.56 | 27.9 | 692.2 | 10.77 | 31.51 | 11.18 | .31 | 71.66 | 5.74 |
| 10 | 3T2 | 507 | 136.80 | 4.1 | 6.2 | 14.96 | 22.84 | .21 | .63 | 1.87 | 9.36 |
| 11 | 3T2 | 535 | 128.01 | 4.6 | 535.7 | 5.13 | 28.13 | 11.32 | .09 | 84.29 | 3.57 |
| 12 | 3T2 | 587 | 118.79 | 395.5 | 437.4 | 24.10 | 29.02 | 2.94 | .02 | 19.77 | .14 |

TABLE III

Figure 10 (a)-(y) Results of standard tests on wells 3T1,3T2, 3T3, and 3T4 (similar to Figure 5).

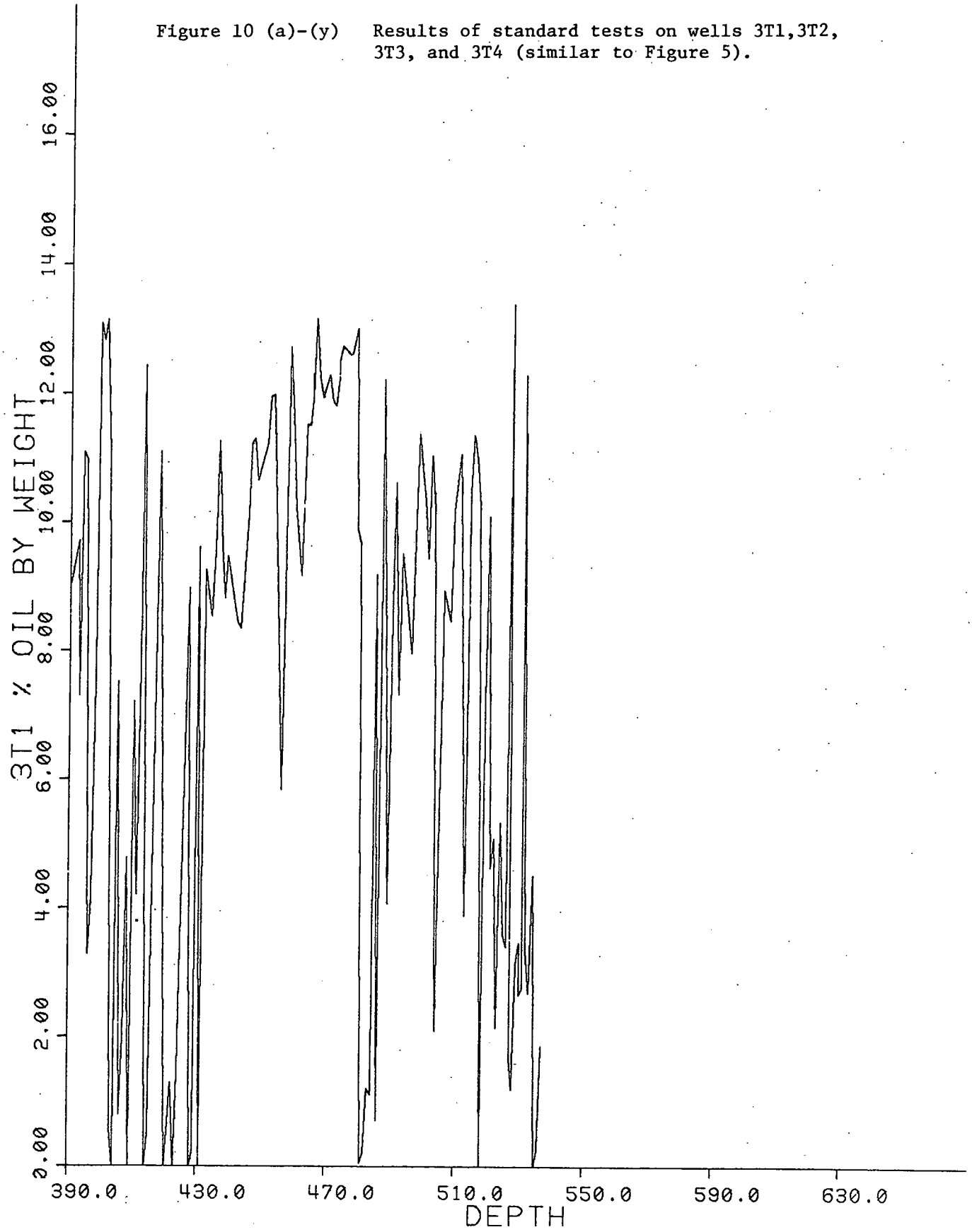

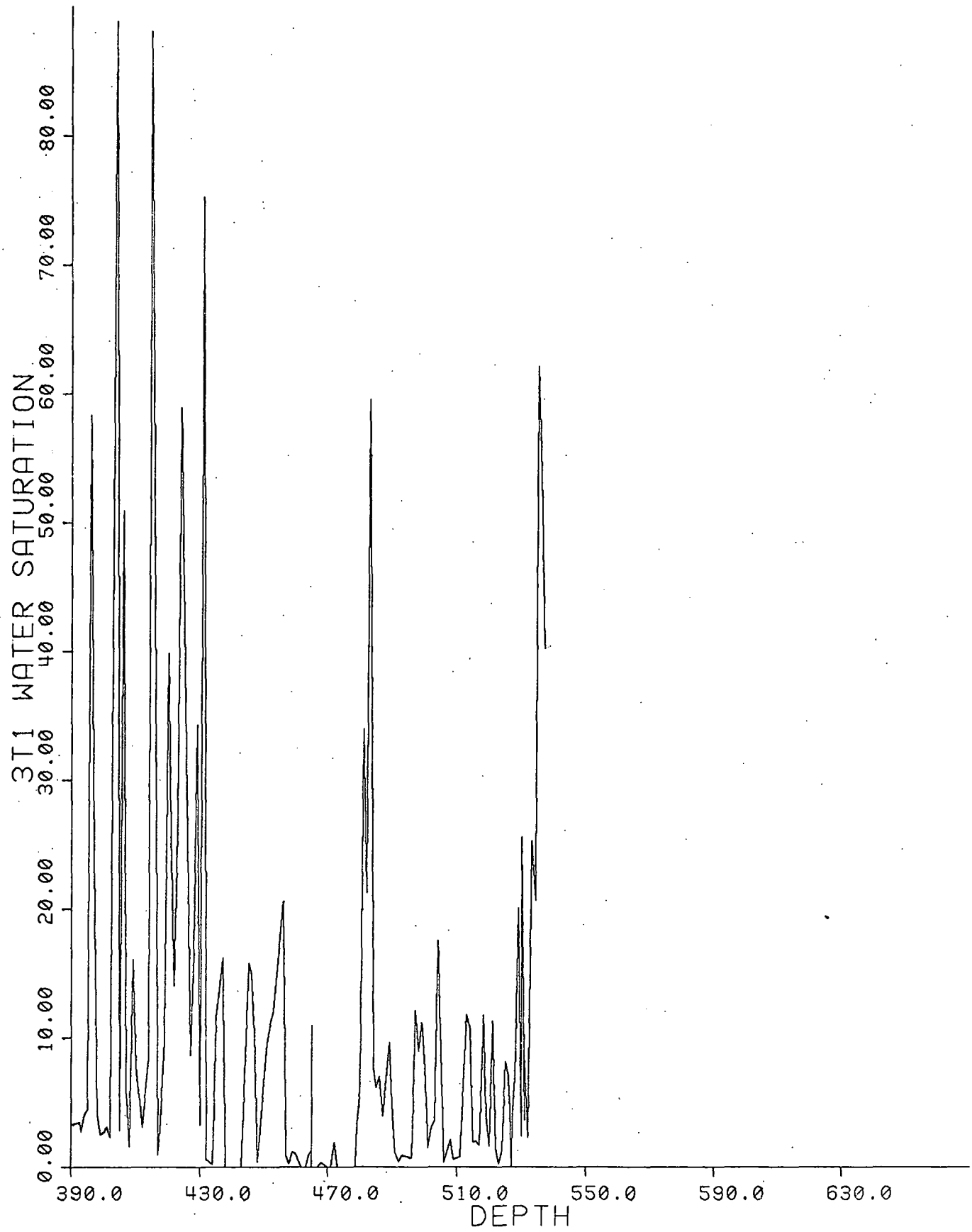
3T1 WATER SATURATION
0.00
10.00
20.00
30.00
40.00
50.00
60.00
70.00
80.00
390.0
430.0
470.0
510.0
550.0
590.0
630.0
DEPTH

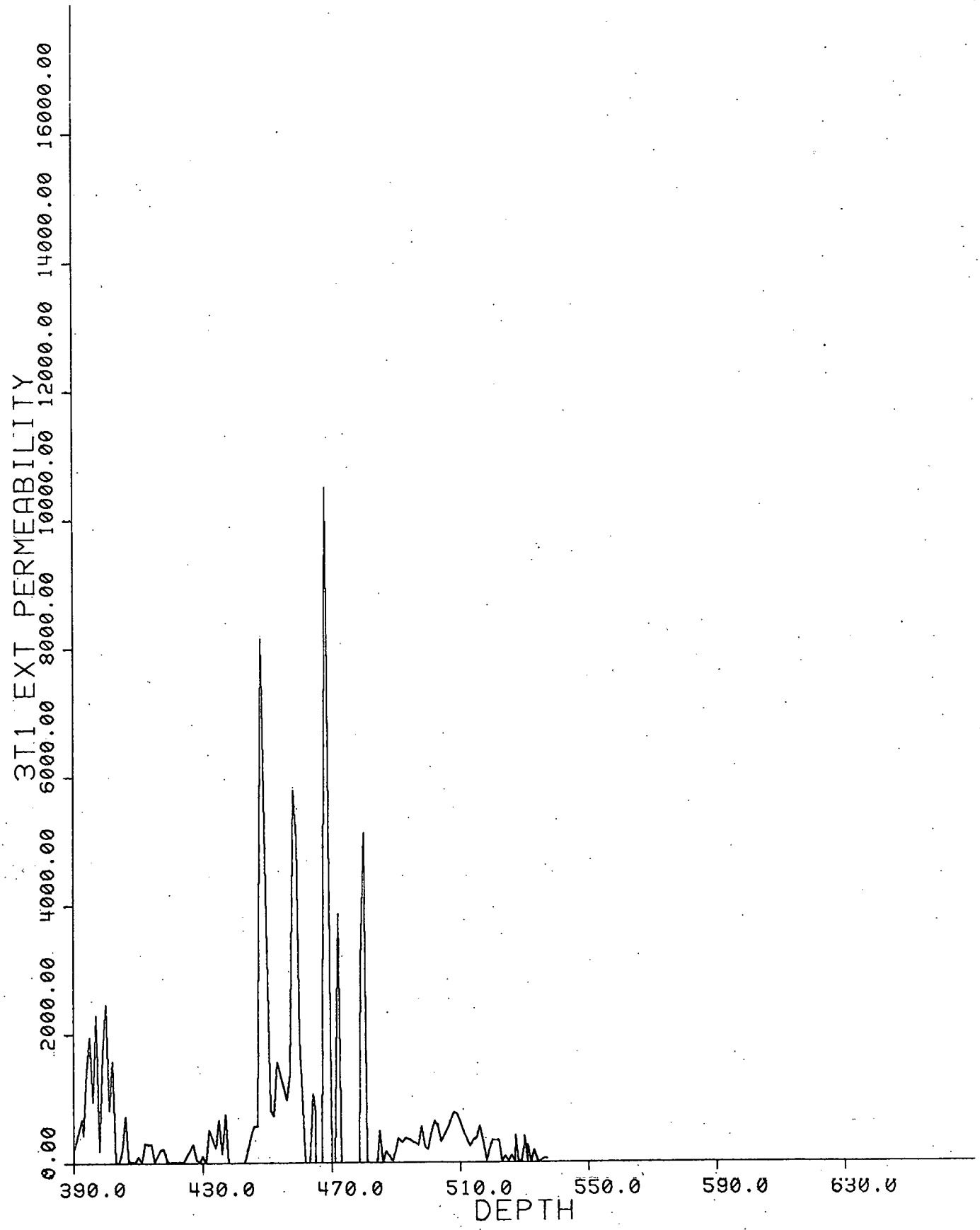
3T1 EXT PERMEABILITY
0.00
2000.00
4000.00
6000.00
8000.00
10000.00
12000.00
14000.00
16000.00
390.0
430.0
470.0
510.0
550.0
590.0
630.0
DEPTH

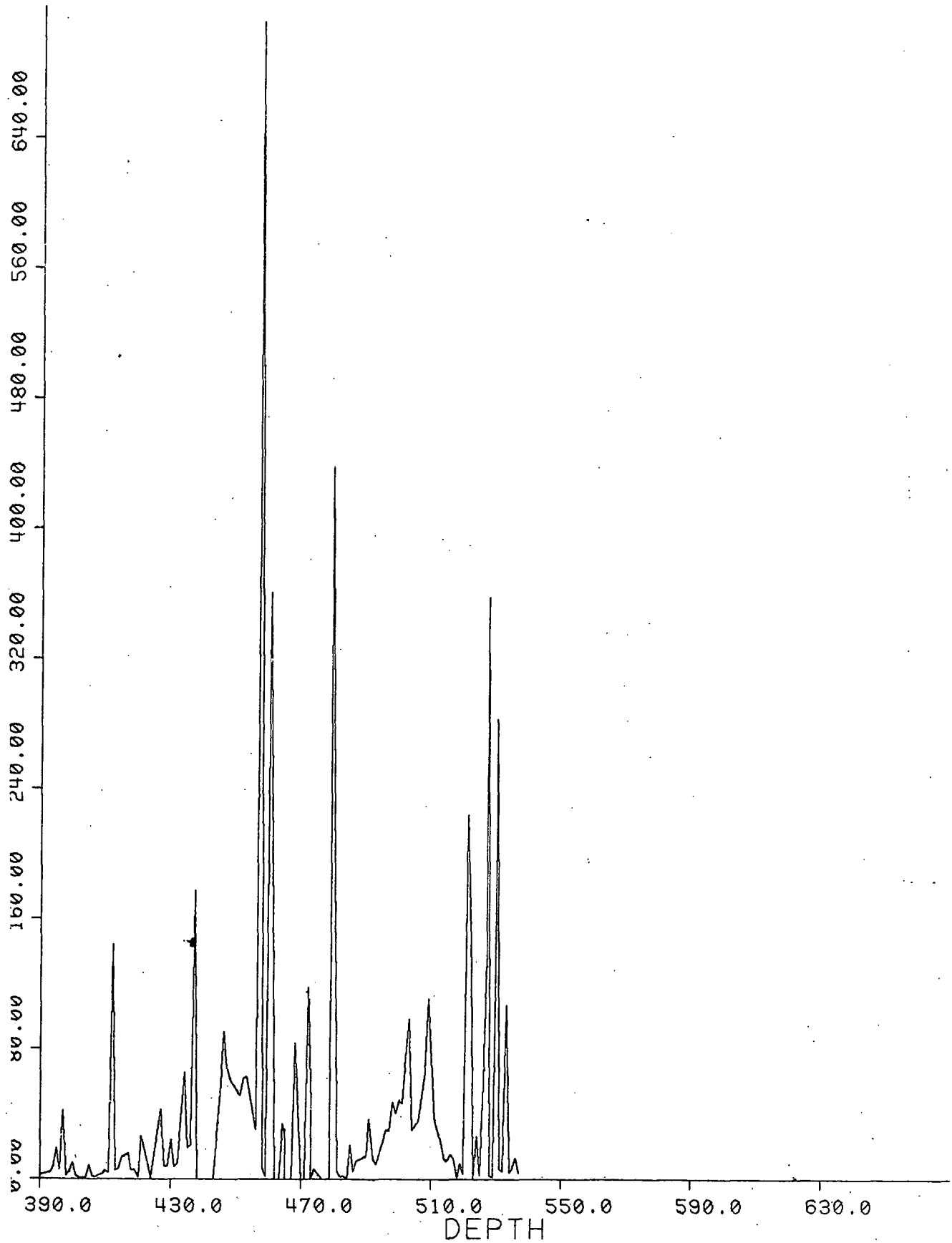
640.00
560.00
480.00
400.00
320.00
240.00
160.00
80.00
0.0
390.0
430.0
470.0
510.0
550.0
590.0
630.0
DEPTH

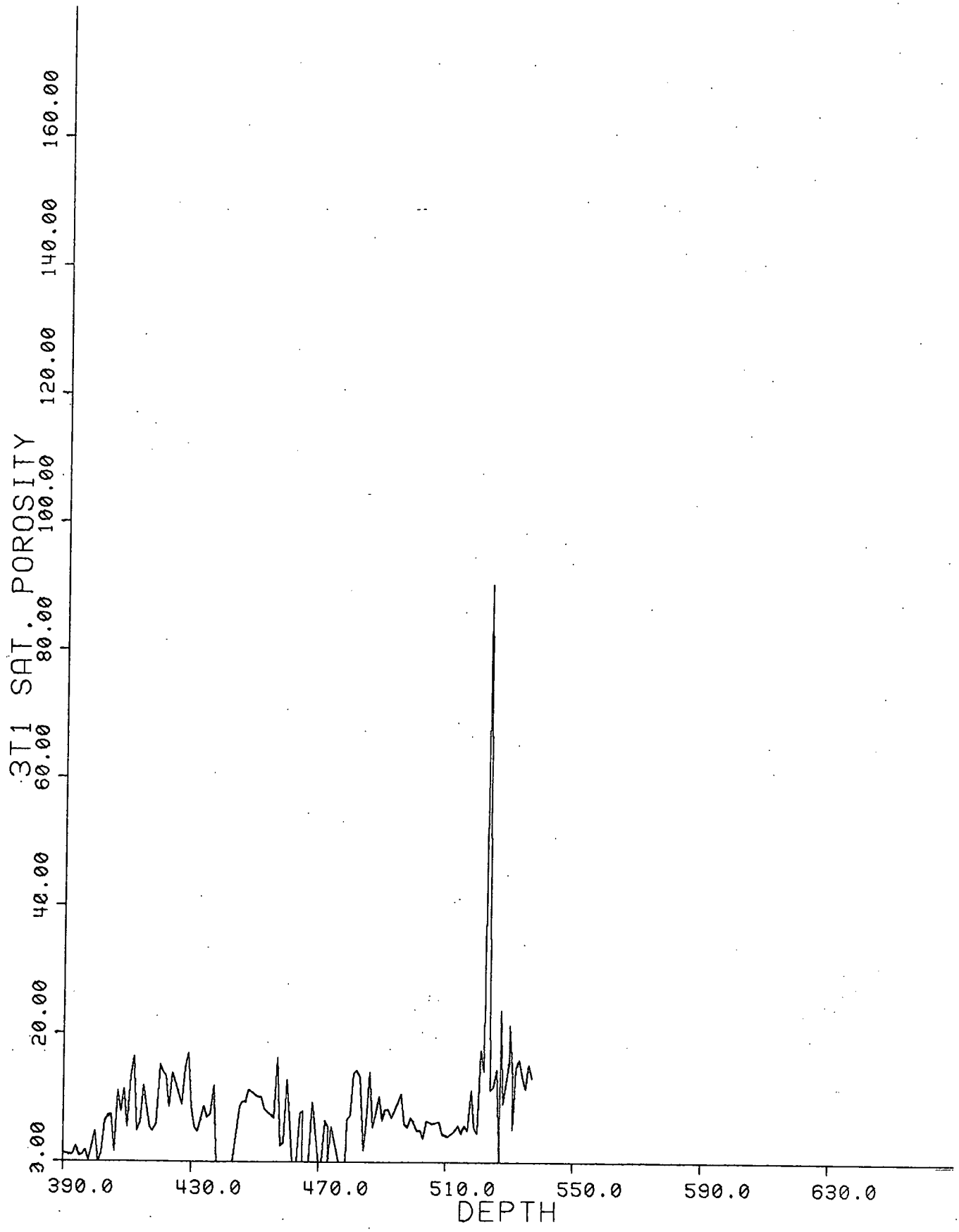
3T1 SAT. POROSITY
3.00
20.00
40.00
60.00
80.00
100.00
120.00
140.00
160.00
390.0
430.0
470.0
510.0
550.0
590.0
630.0
DEPTH

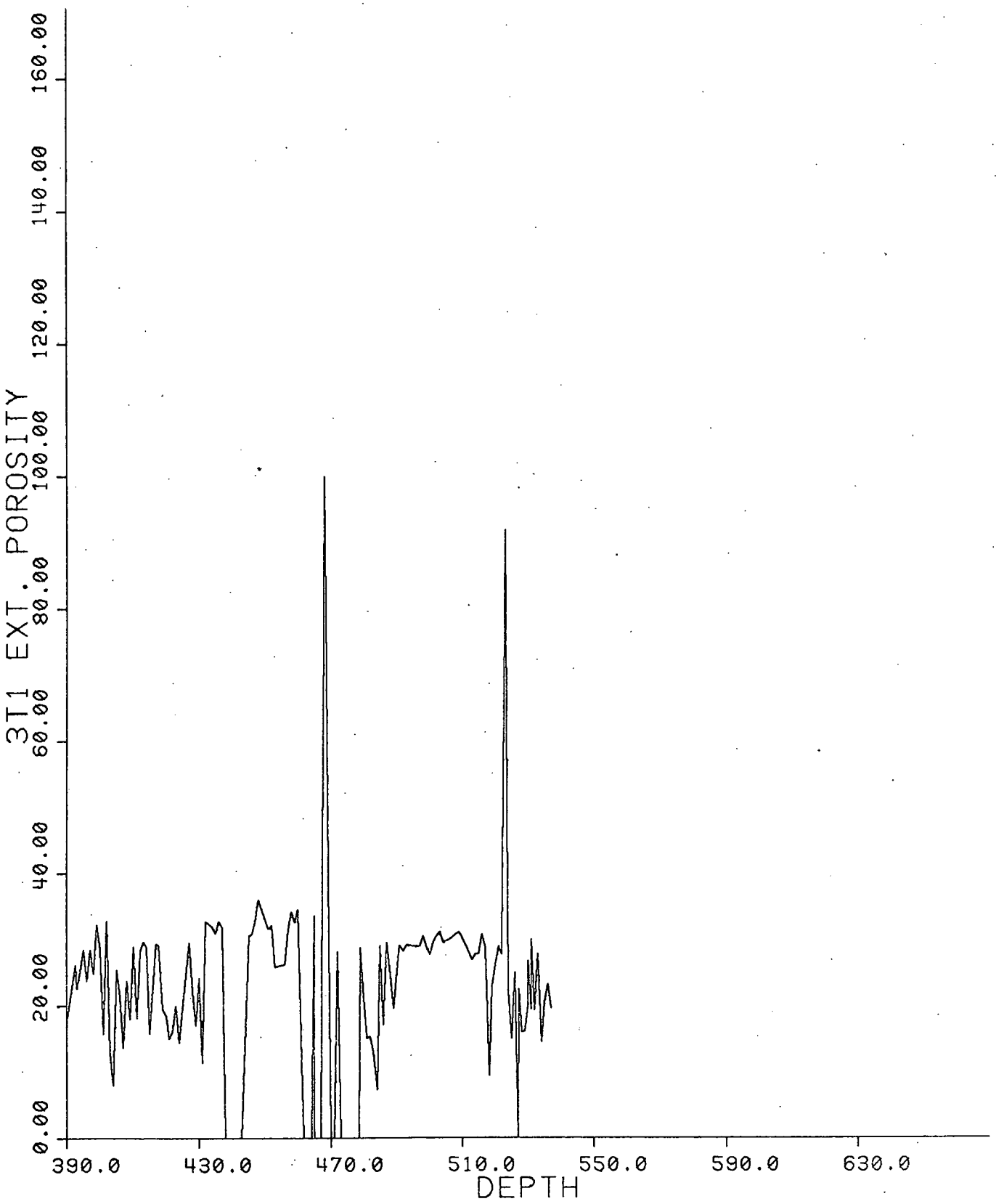
3T1 EXT. POROSITY
0.00
20.00
40.00
60.00
80.00
100.00
120.00
140.00
160.00
390.0
430.0
470.0
510.0
550.0
590.0
630.0
DEPTH

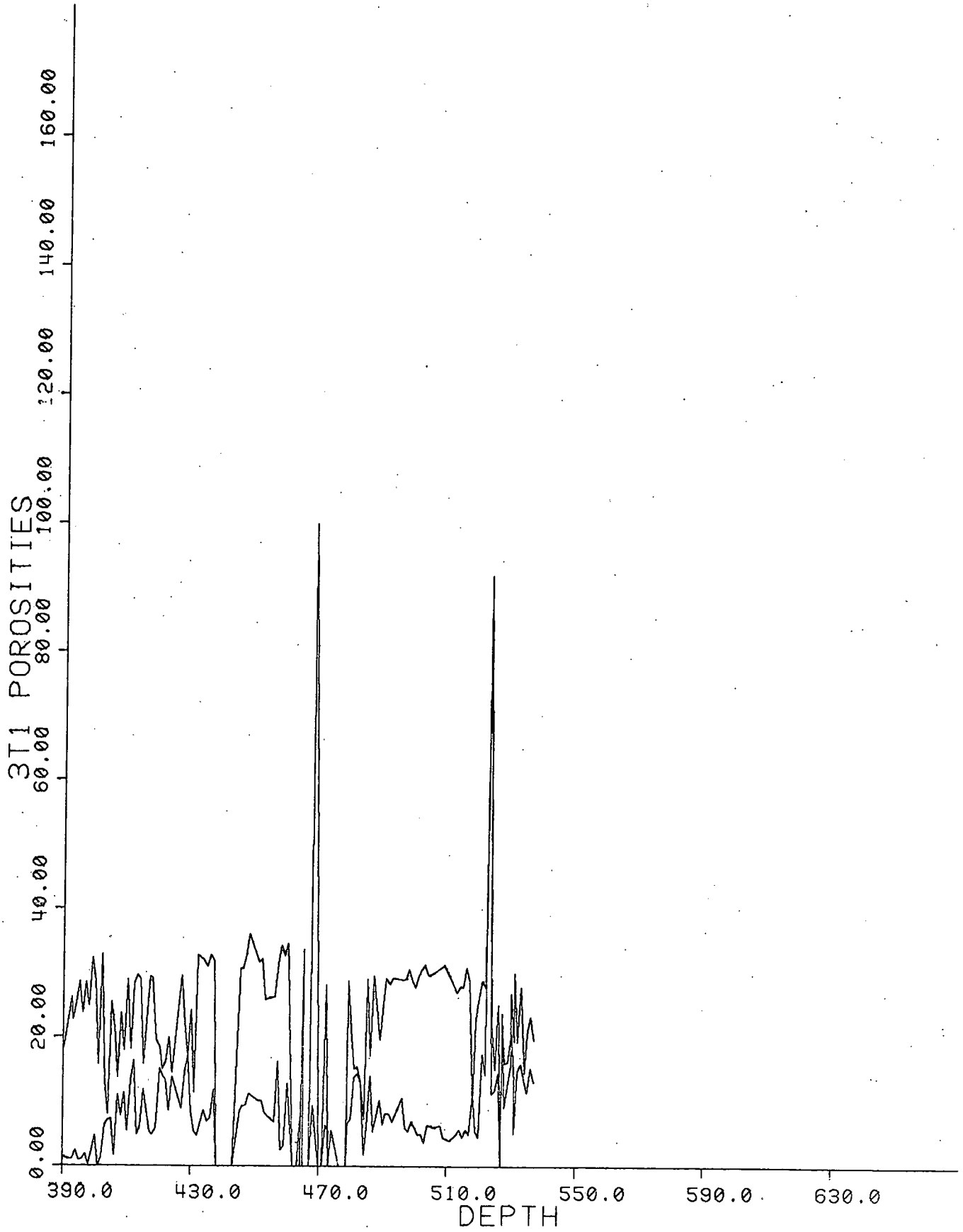
3T1 POROSITIES
0.00
20.00
40.00
60.00
80.00
100.00
120.00
140.00
160.00
390.0
430.0
470.0
510.0
550.0
590.0
630.0
DEPTH

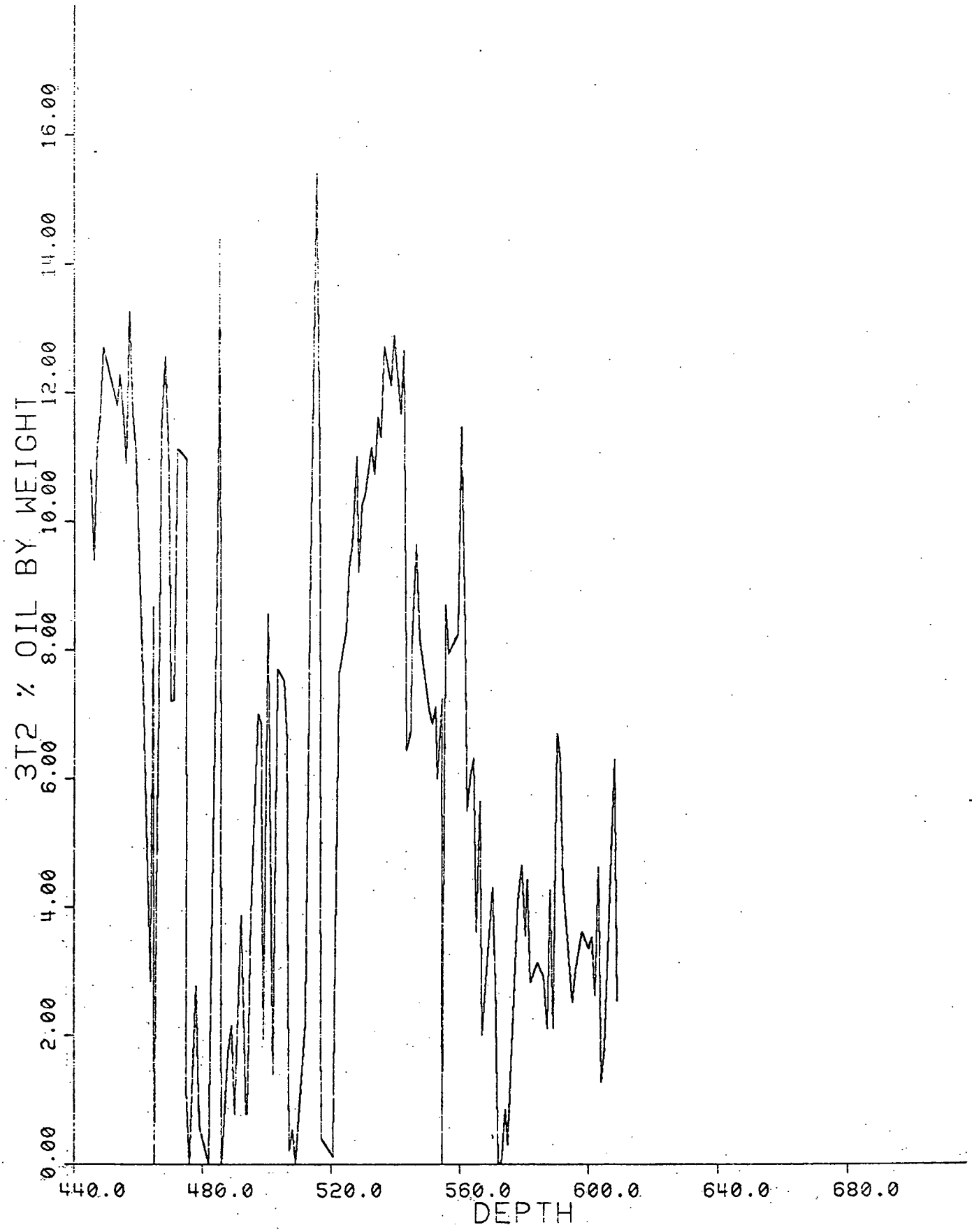
3T2 % OIL BY WEIGHT
0.00
2.00
4.00
6.00
8.00
10.00
12.00
14.00
16.00
440.0
480.0
520.0
560.0
600.0
640.0
680.0
DEPTH

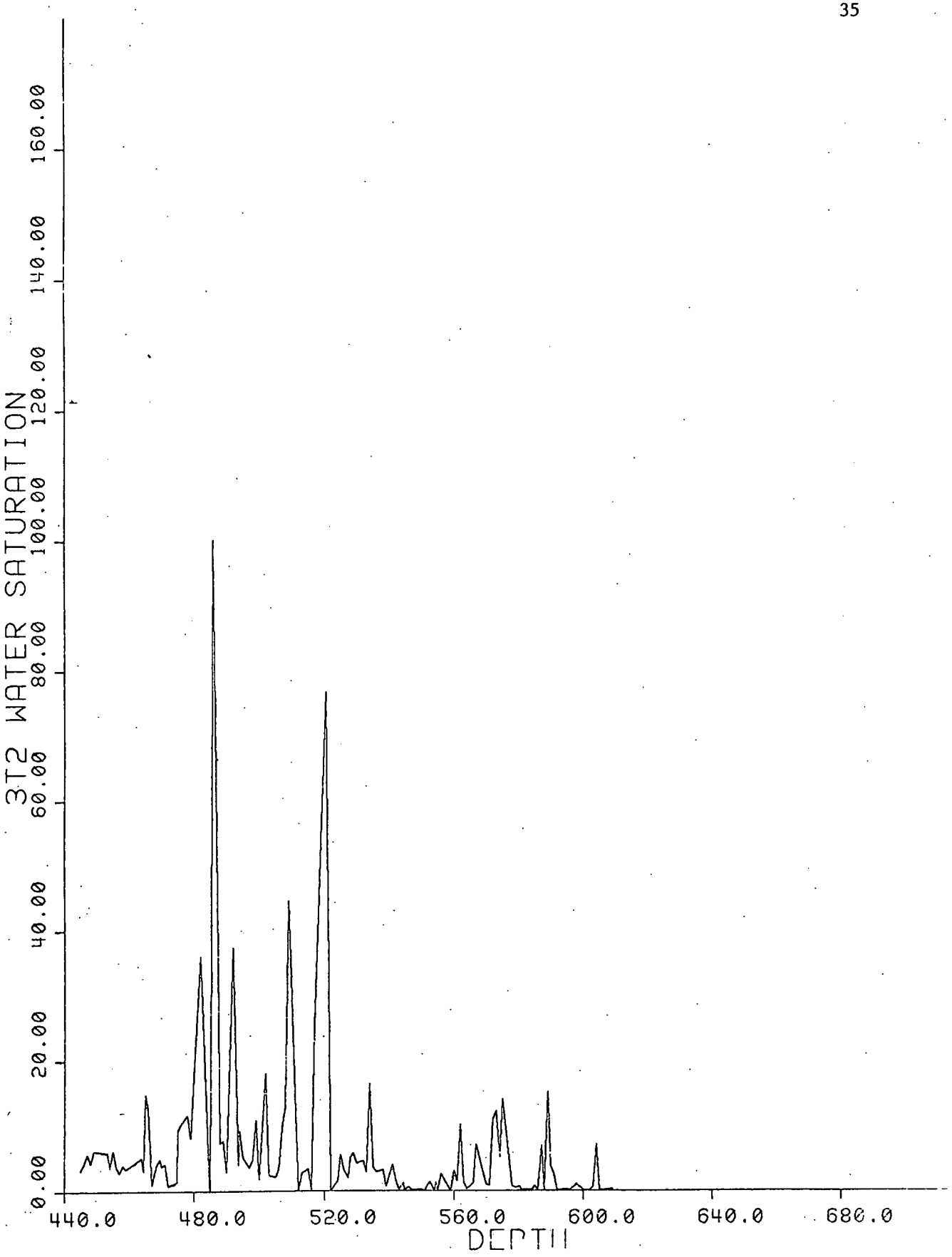
3T2 WATER SATURATION
0.00
20.00
40.00
60.00
80.00
100.00
120.00
140.00
160.00
440.0
480.0
520.0
560.0
600.0
640.0
680.0
DEPTH

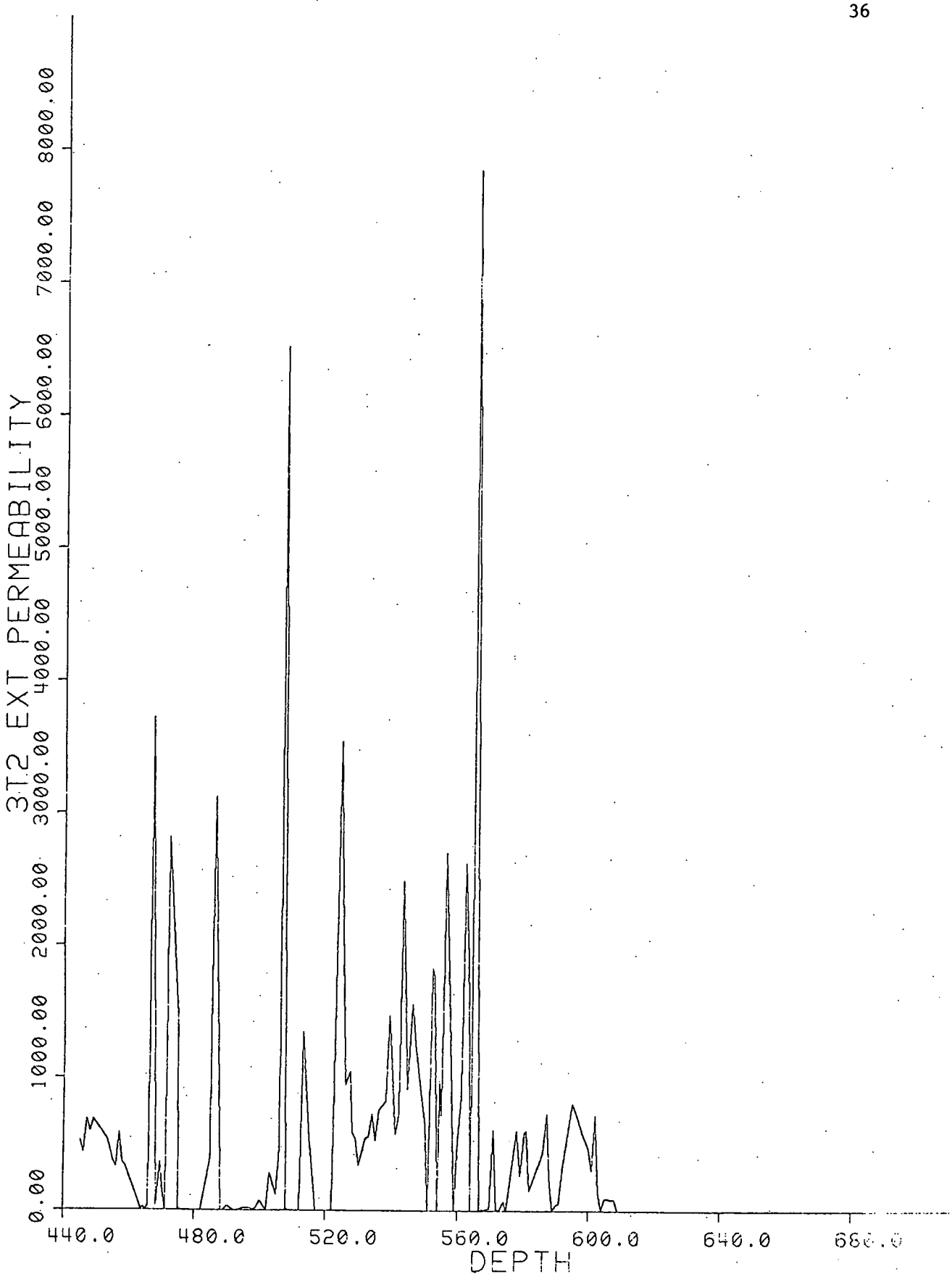
3T2 EXT PERMEABILITY
0.00
1000.00
2000.00
3000.00
4000.00
5000.00
6000.00
7000.00
8000.00
440.0
480.0
520.0
560.0
600.0
640.0
DEPTH

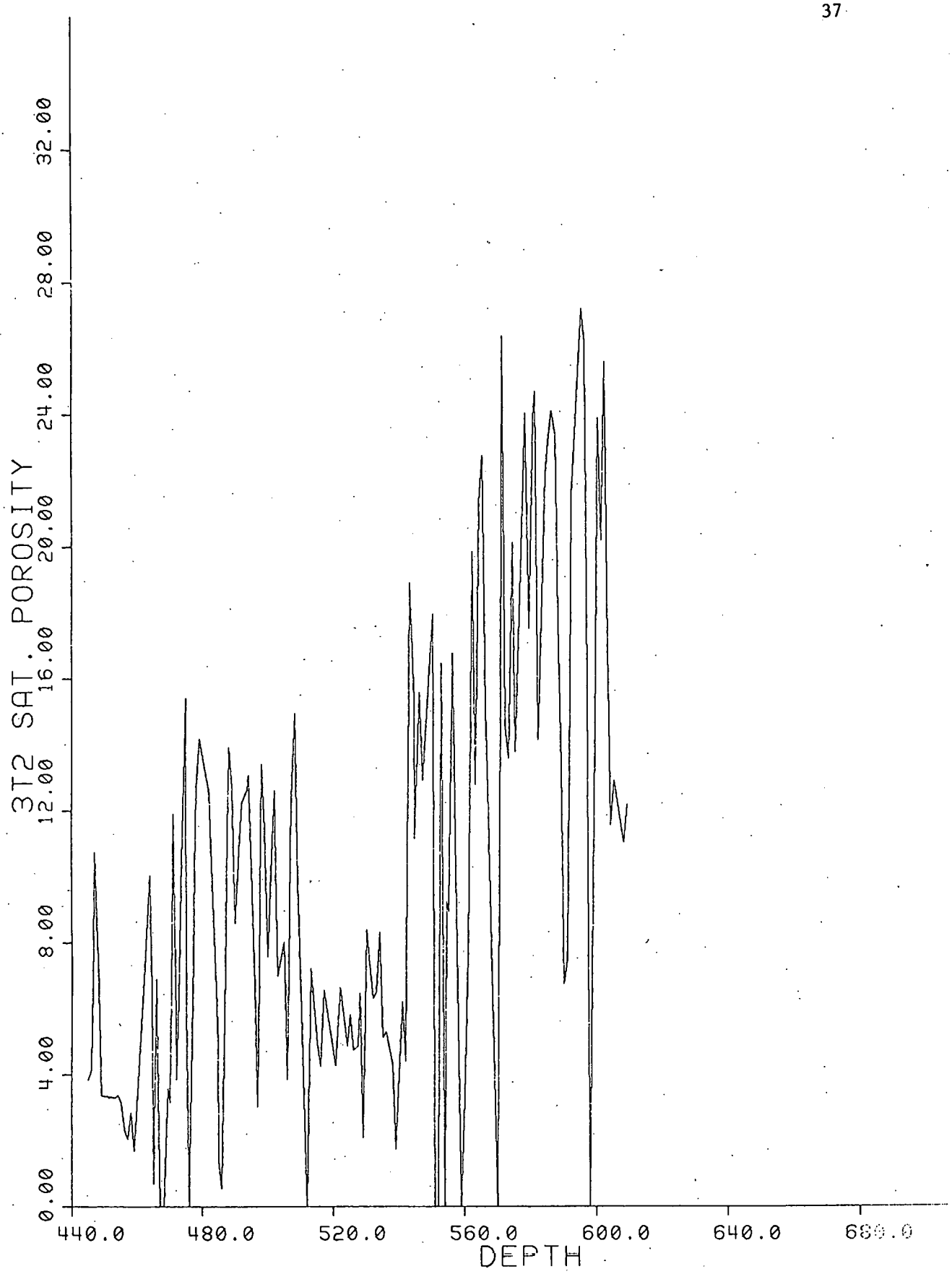
3T2 SAT. POROSITY
0.00
4.00
8.00
12.00
16.00
20.00
24.00
28.00
32.00
440.0
480.0
520.0
560.0
600.0
640.0
680.0
DEPTH

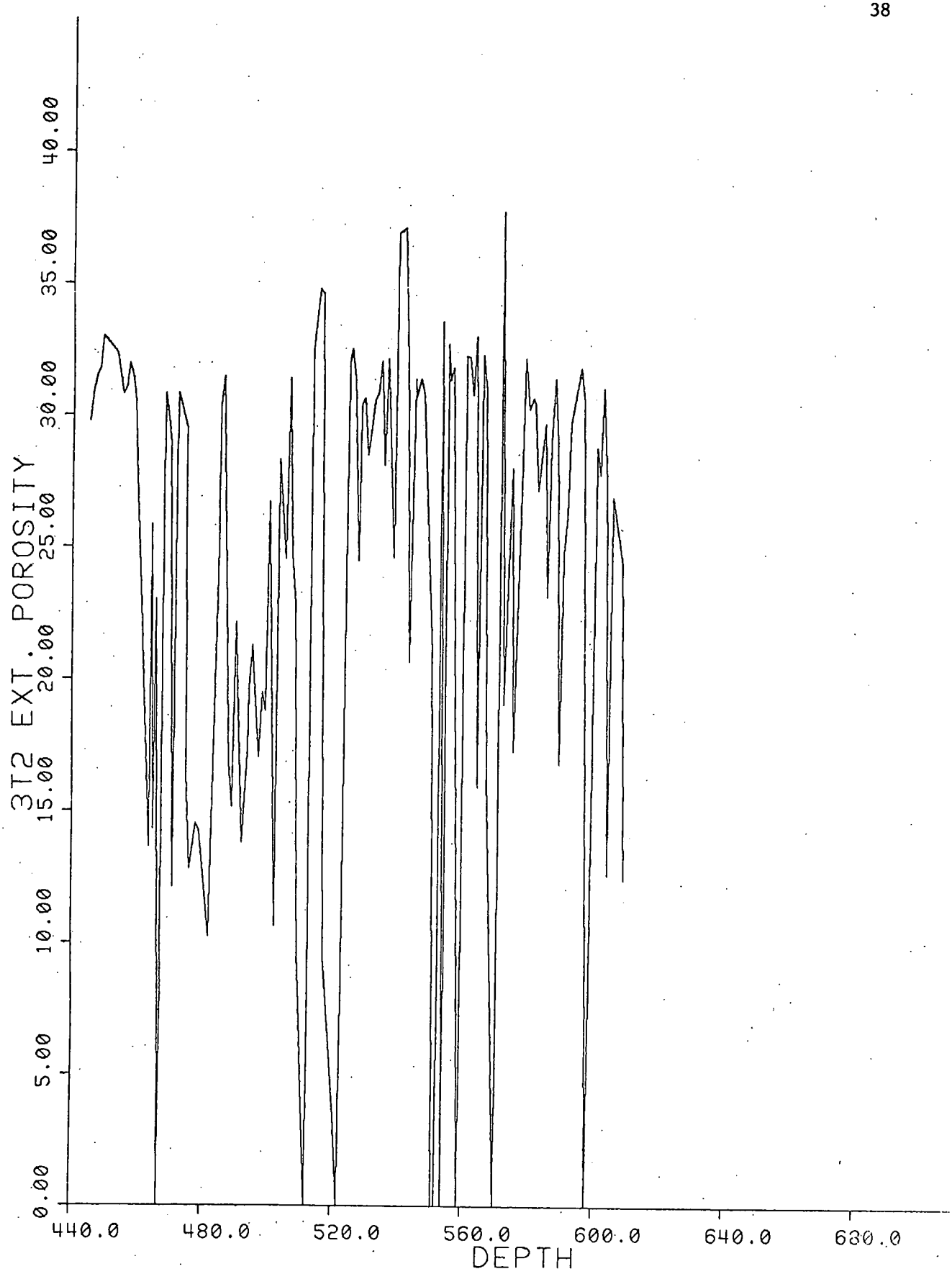
3T2 EXT. POROSITY
0.00
5.00
10.00
15.00
20.00
25.00
30.00
35.00
40.00
440.0
480.0
520.0
560.0
600.0
640.0
680.0
DEPTH

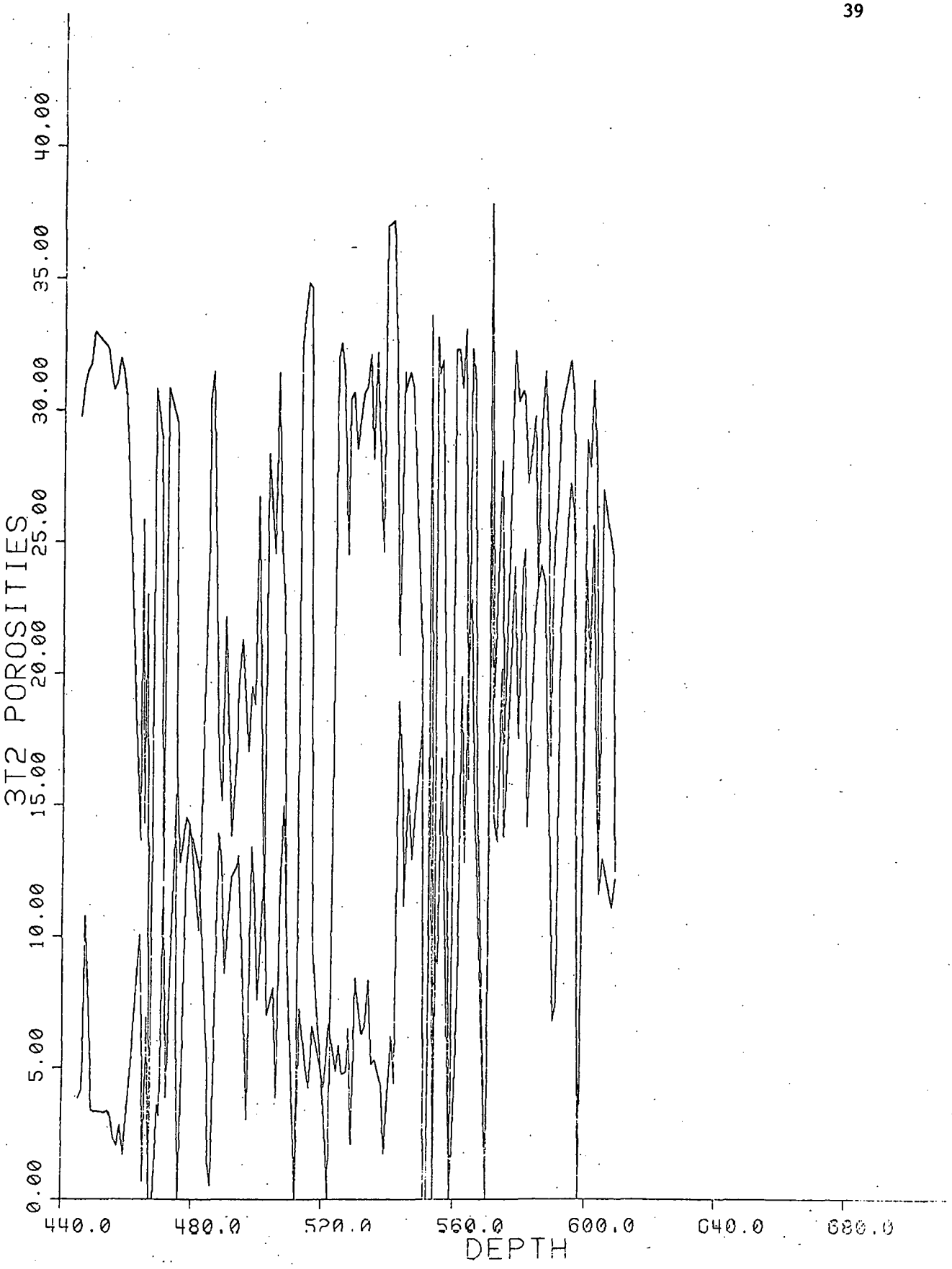
3T2 POROSITIES
0.00
5.00
10.00
15.00
20.00
25.00
30.00
35.00
40.00
440.0
480.0
520.0
560.0
600.0
640.0
680.0
DEPTH

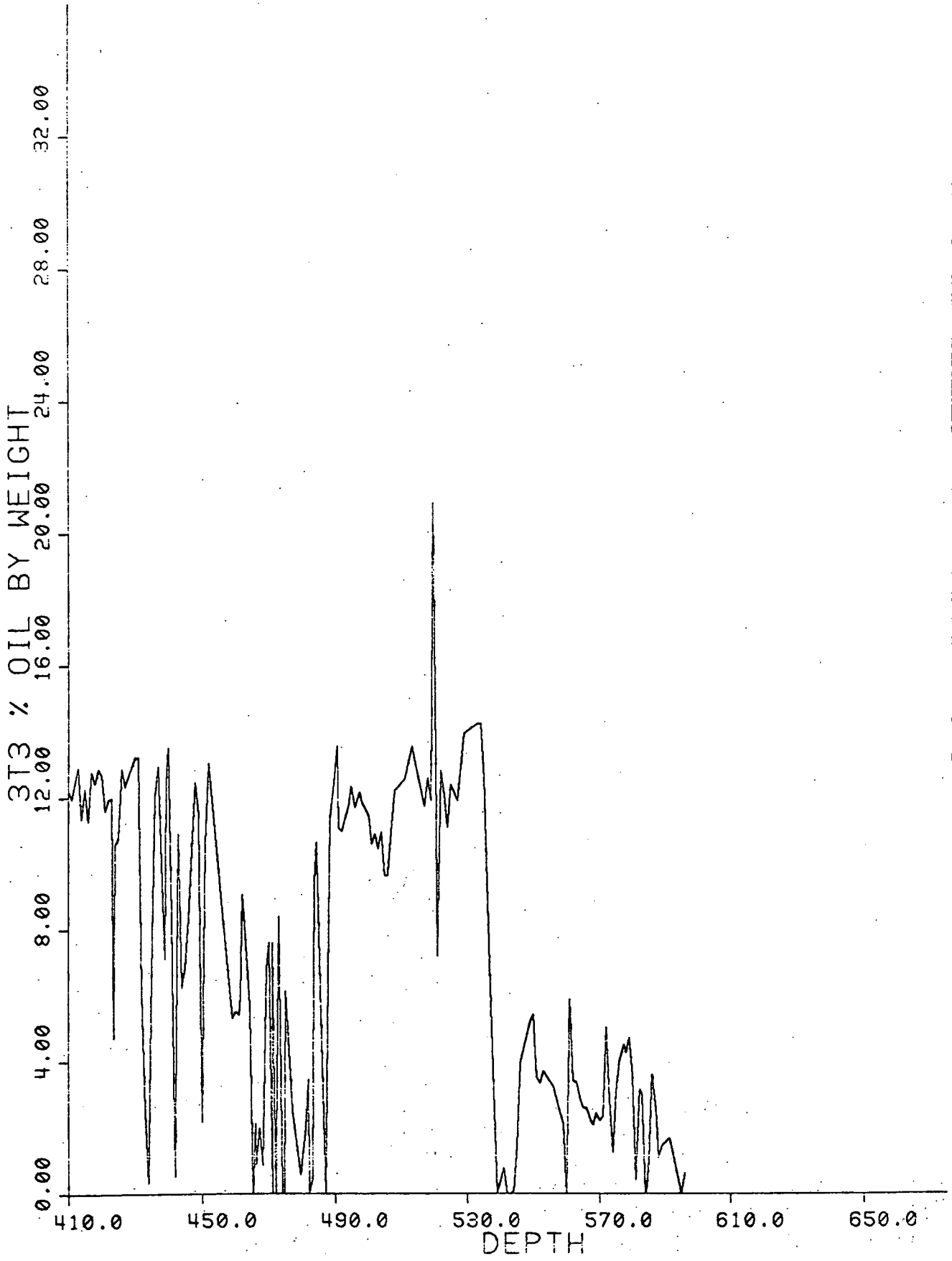
3T3 % OIL BY WEIGHT
0.00
4.00
8.00
12.00
16.00
20.00
24.00
28.00
32.00
410.0
450.0
490.0
530.0
570.0
610.0
650.0
DEPTH

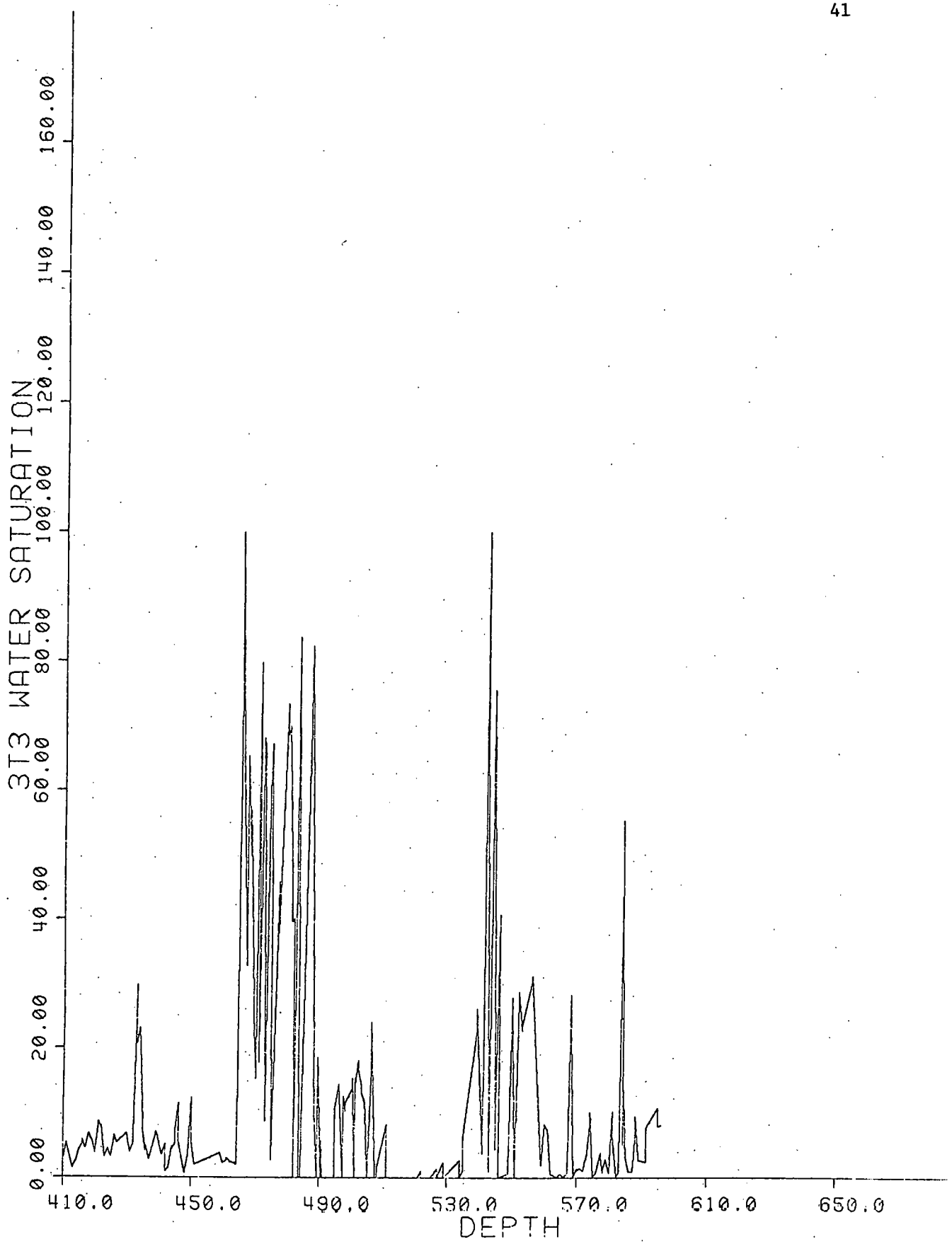
3T3 WATER SATURATION
0.00
20.00
40.00
60.00
80.00
100.00
120.00
140.00
160.00
410.0
450.0
490.0
530.0
570.0
610.0
650.0
DEPTH

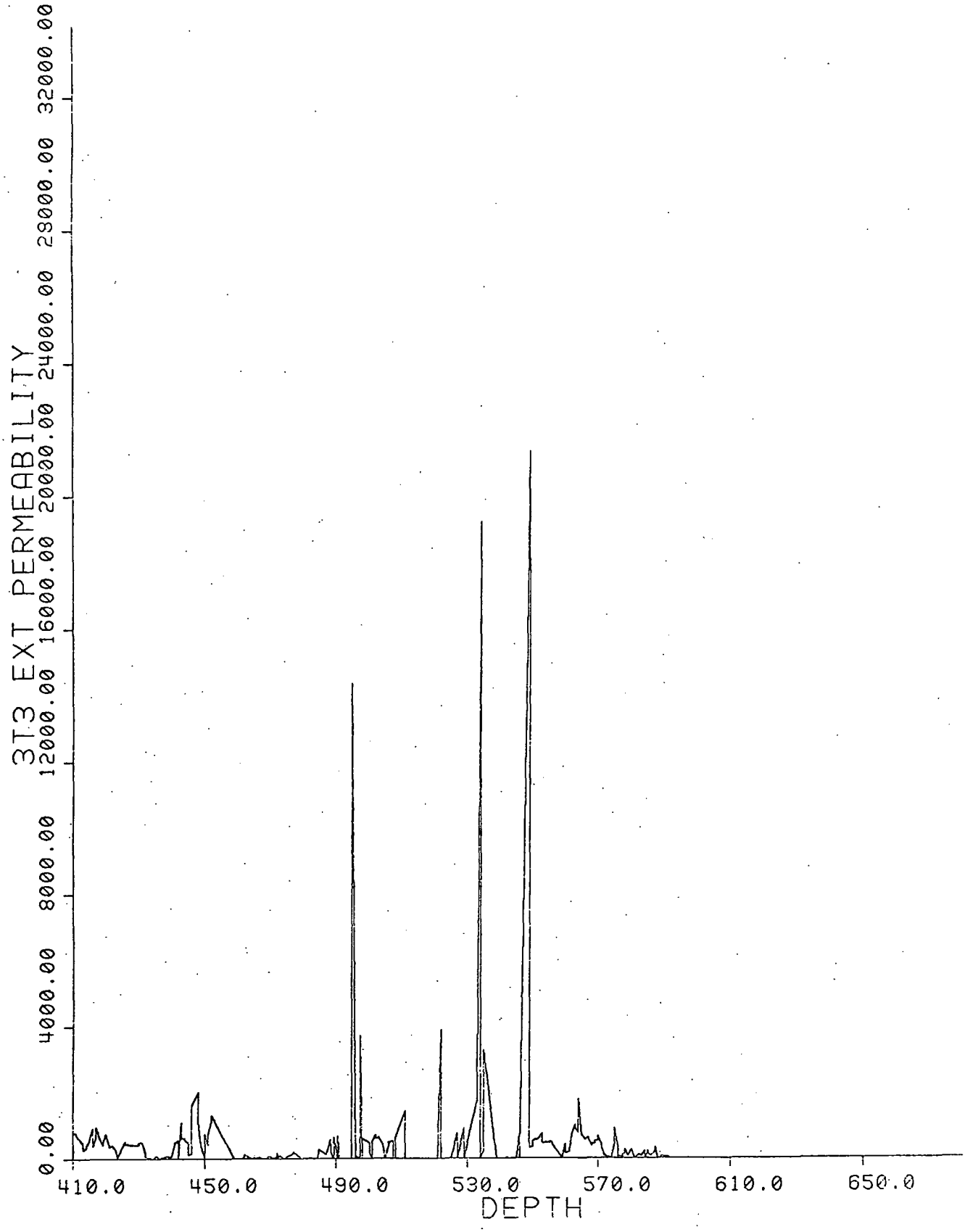
3T3 EXT PERMEABILITY
0.00
4000.00
8000.00
12000.00
16000.00
20000.00
24000.00
28000.00
32000.00
410.0
450.0
490.0
530.0
570.0
610.0
650.0
DEPTH

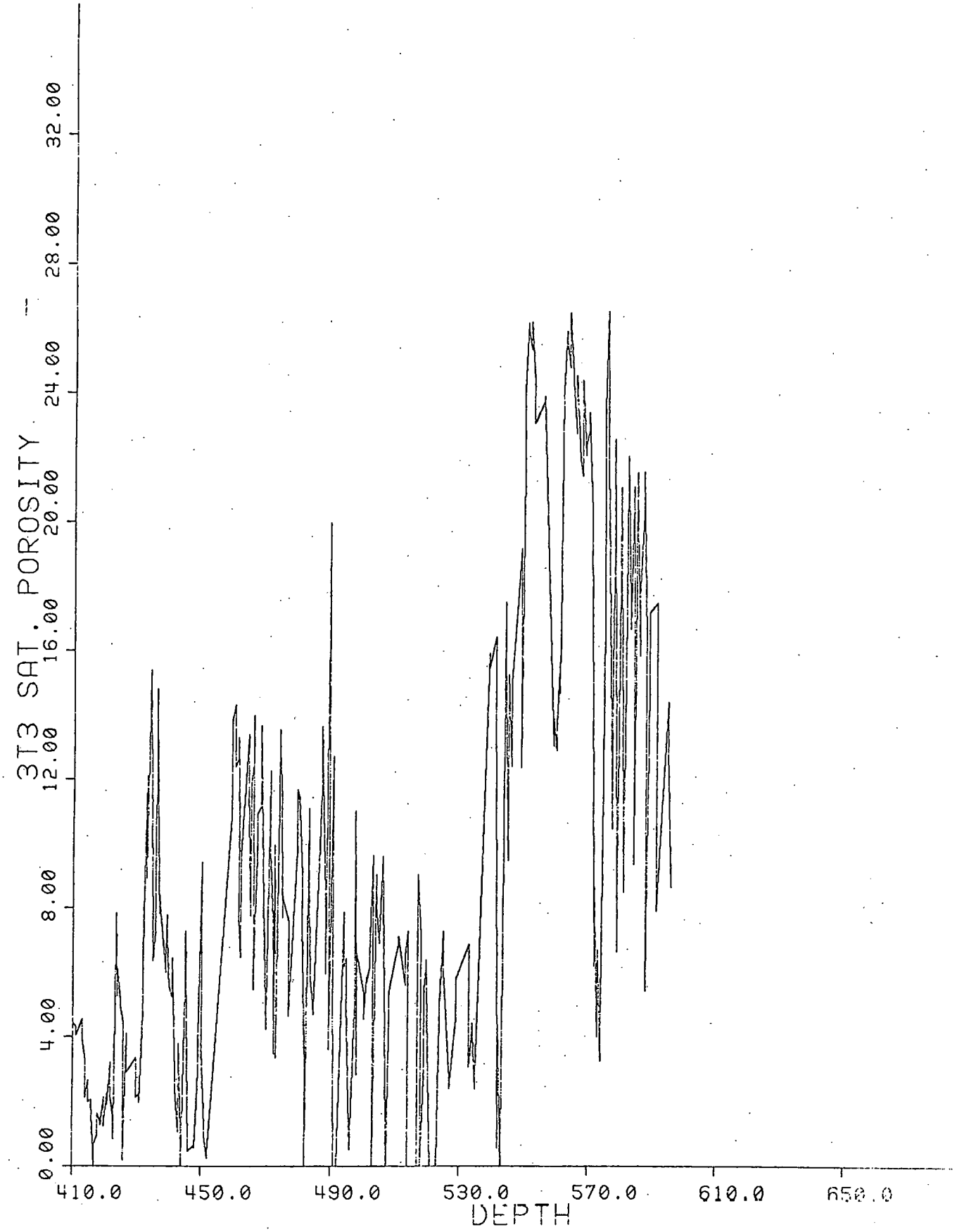
3T3 SAT. POROSITY
0.00
4.00
8.00
12.00
16.00
20.00
24.00
28.00
32.00
410.0
450.0
490.0
530.0
570.0
610.0
650.0
DEPTH

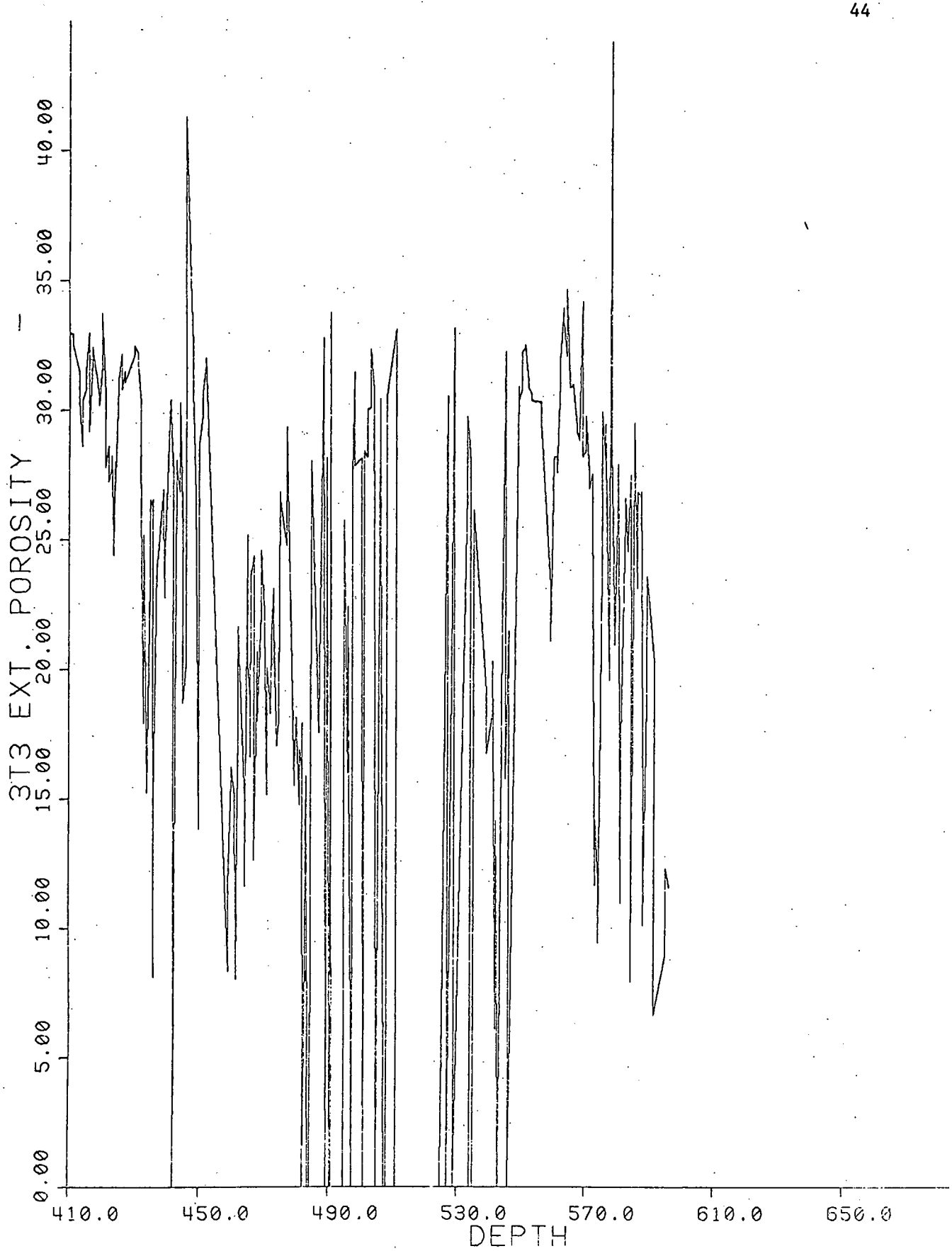
3T3 EXT. POROSITY
0.00
5.00
10.00
15.00
20.00
25.00
30.00
35.00
40.00
410.0
450.0
490.0
530.0
570.0
610.0
650.0
DEPTH

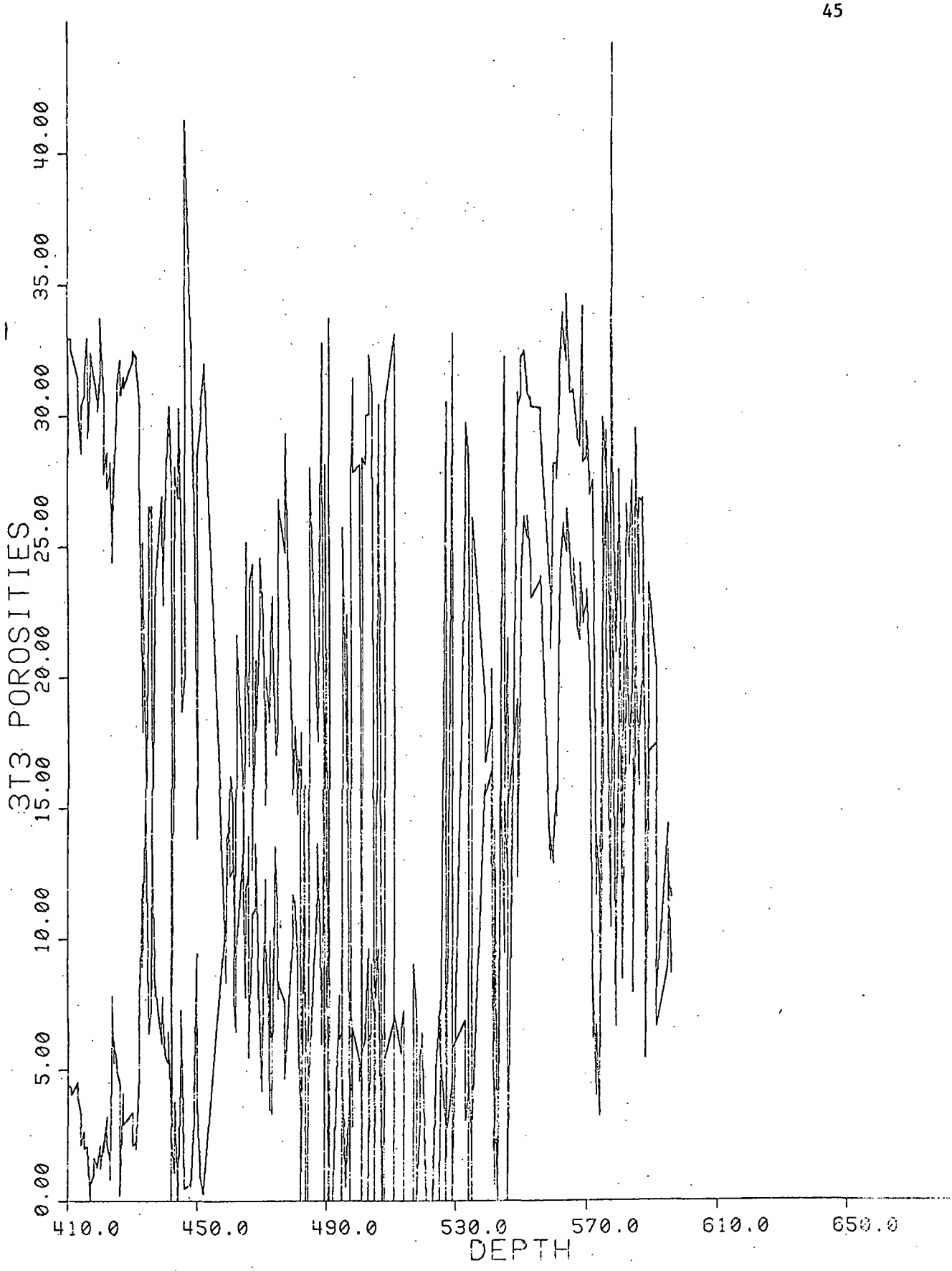
3T3 POROSITIES
0.00
5.00
10.00
15.00
20.00
25.00
30.00
35.00
40.00
410.0
450.0
490.0
530.0
570.0
610.0
650.0
DEPTH

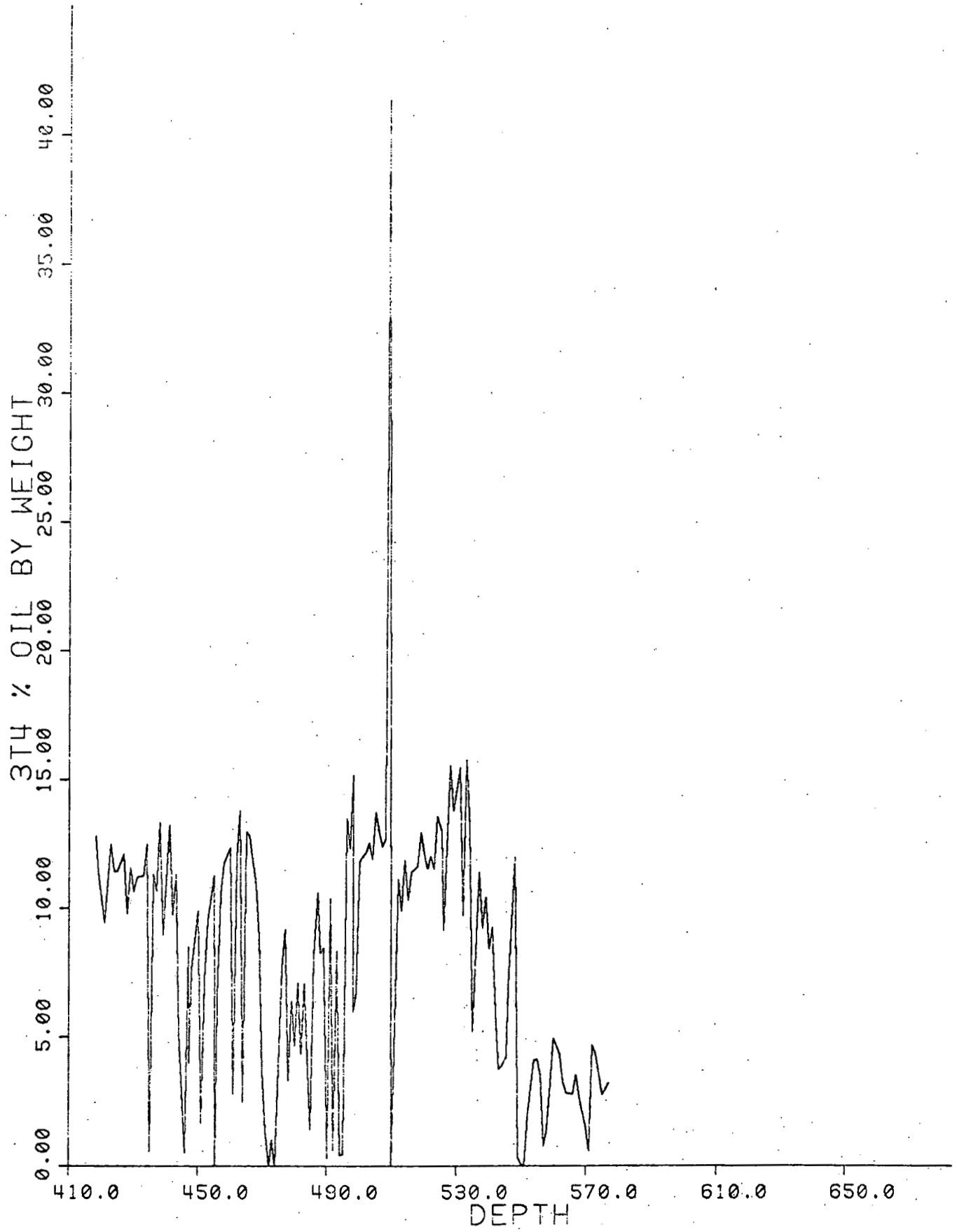
3T4 % OIL BY WEIGHT
0.00
5.00
10.00
15.00
20.00
25.00
30.00
35.00
40.00
410.0
450.0
490.0
530.0
570.0
610.0
650.0
DEPTH

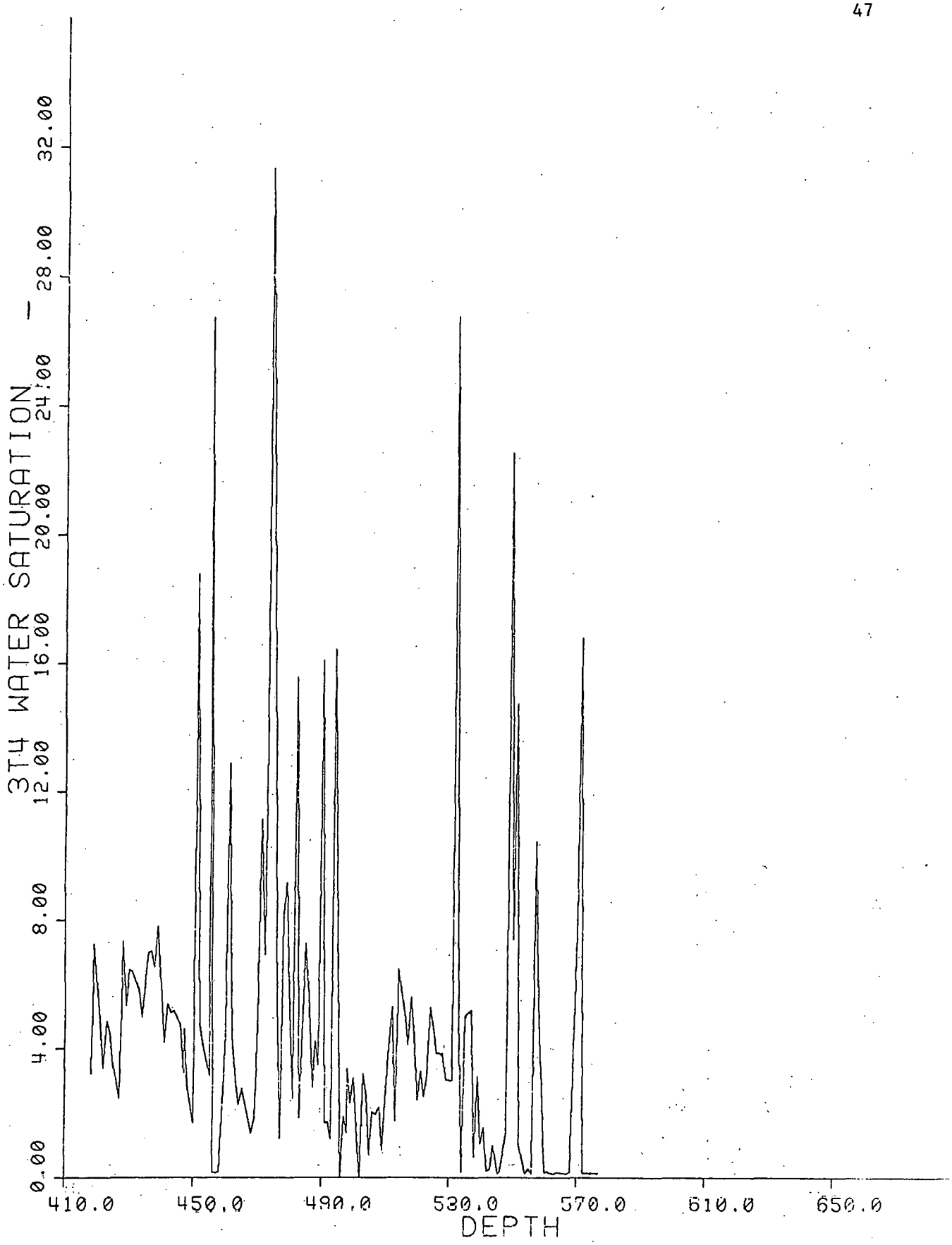
3T4 WATER SATURATION
0.00
4.00
8.00
12.00
16.00
20.00
24.00
28.00
32.00
410.0
450.0
490.0
530.0
570.0
610.0
650.0
DEPTH

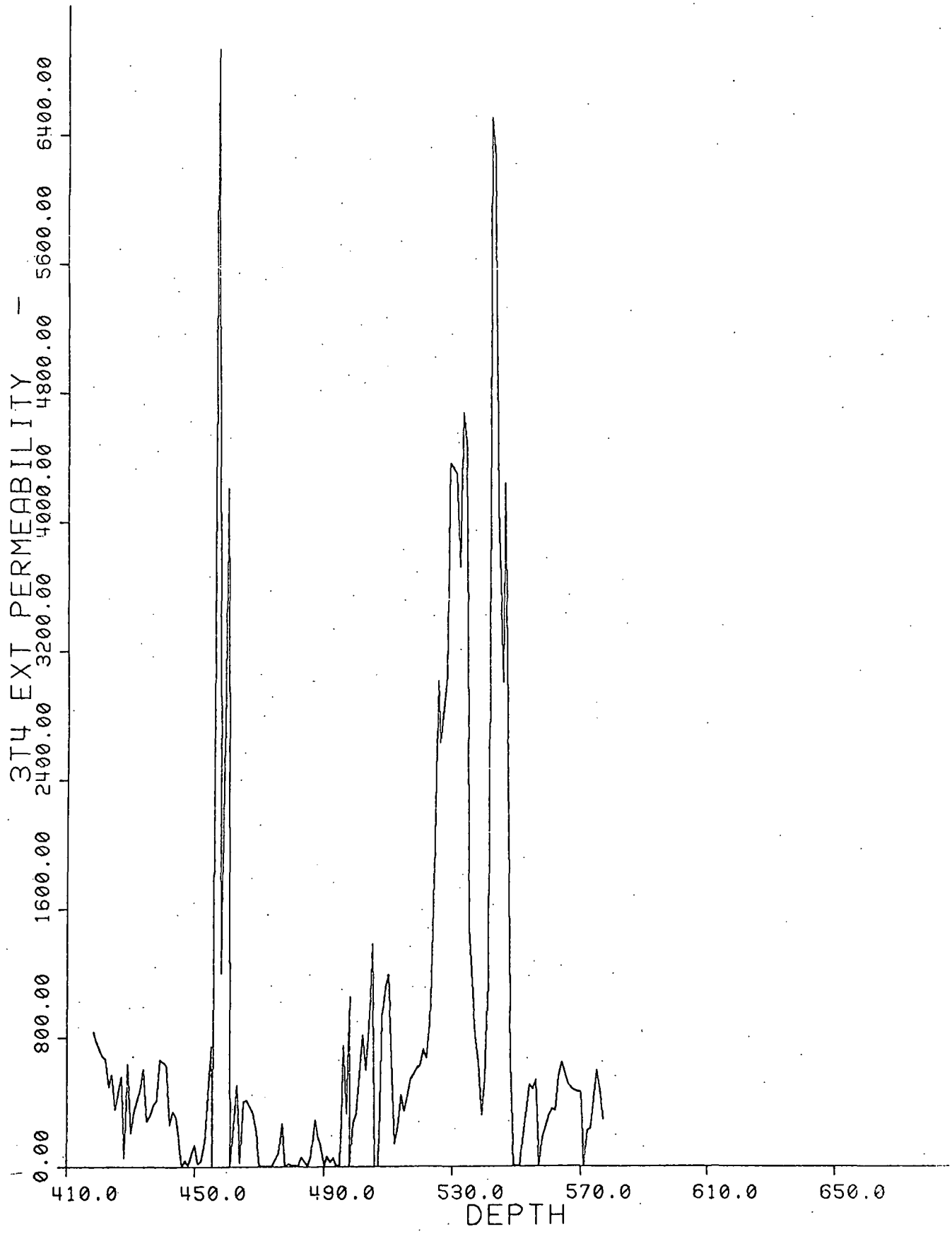
3T4 EXT PERMEABILITY
0.00
800.00
1600.00
2400.00
3200.00
4000.00
4800.00
5600.00
6400.00
410.0
450.0
490.0
530.0
570.0
610.0
650.0
DEPTH

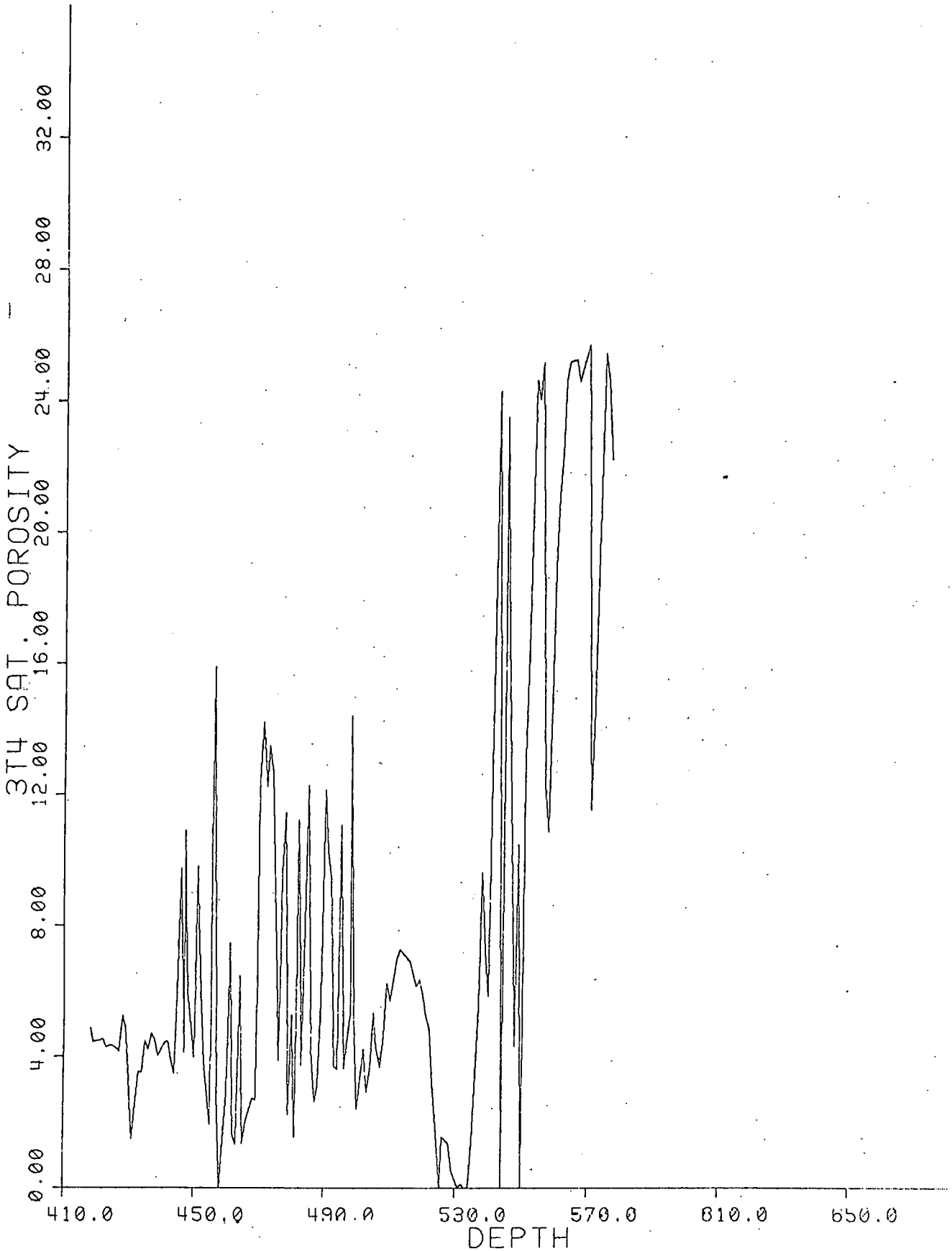
3T4 SAT. POROSITY
0.00
4.00
8.00
12.00
16.00
20.00
24.00
28.00
32.00
410.0
450.0
490.0
530.0
570.0
610.0
650.0
DEPTH

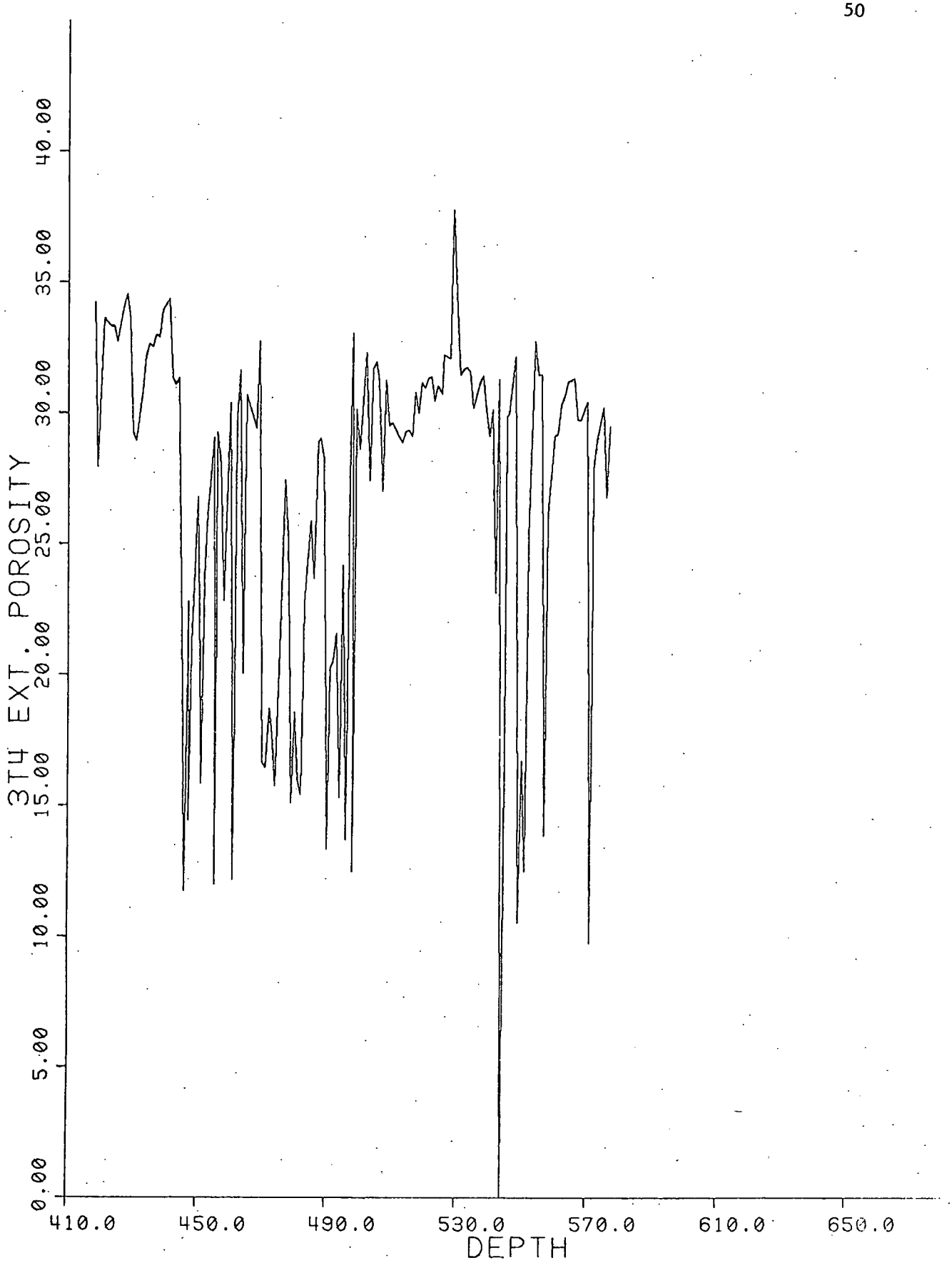
3TH EXT. POROSITY
0.00
5.00
10.00
15.00
20.00
25.00
30.00
35.00
40.00
410.0
450.0
490.0
530.0
570.0
610.0
650.0
DEPTH

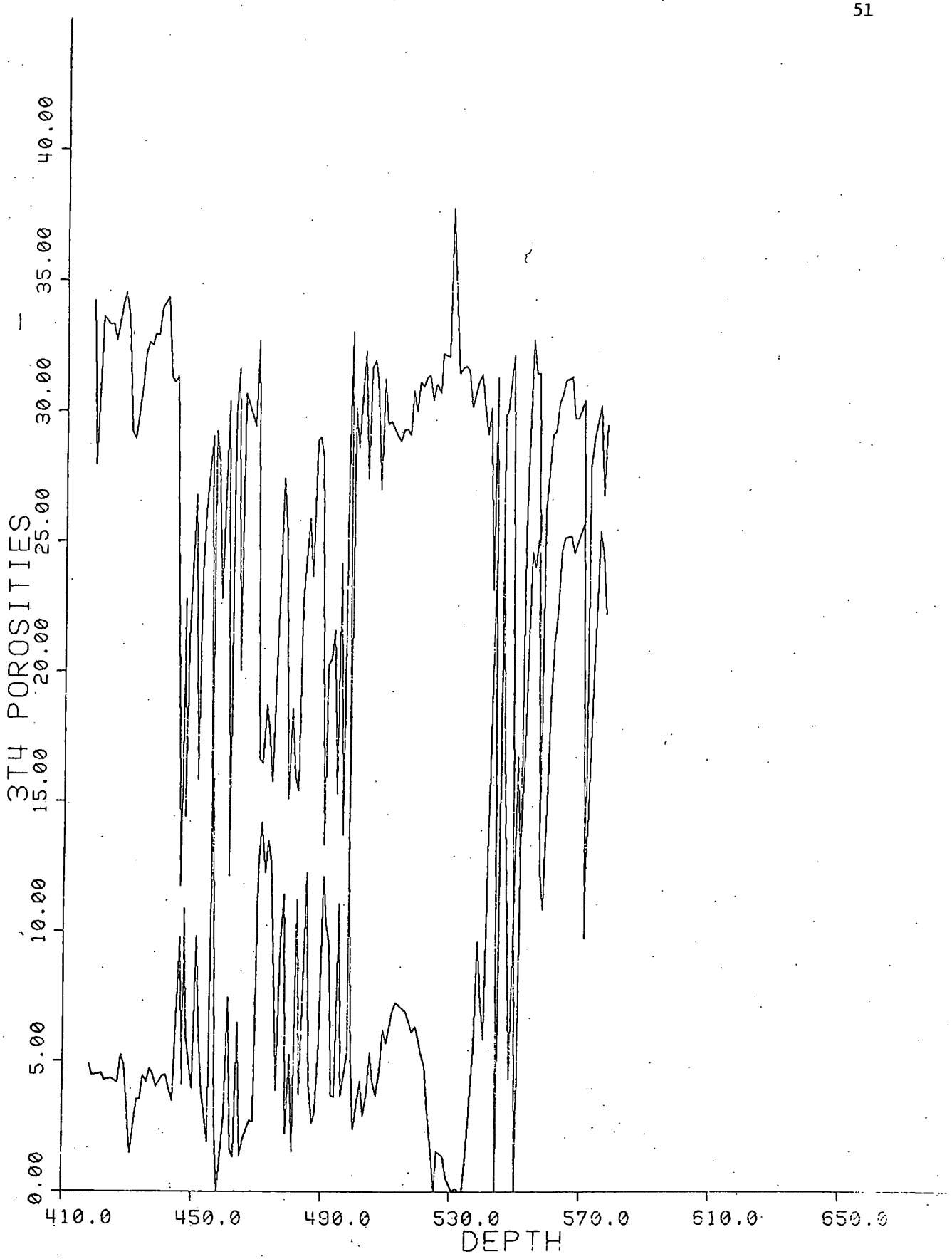
3T4 POROSITIES
0.00
5.00
10.00
15.00
20.00
25.00
30.00
35.00
40.00
410.0
450.0
490.0
530.0
570.0
610.0
650.0
DEPTH

## GOALS FOR FY 1979-80

An experimental program to measure relevant thermophysical properties of tar sand and bitumen properties has been initiated in this reporting period (10/1/78-11/1/79).

The program goals for FY 1979-80 are to complete the measurements of these properties and to report the findings in the open literature. Specifically, the scope of these measurements are as follows:

Viscosity:

The viscosity of bitumen already extracted from Utah open pit tar sand sites as a function of temperature, toluene content, and asphaltene/maltene content will be studied. In addition, the rheological (stress/strain-rate) behavior of selected bitumen/solvent combinations will be examined. This work is scheduled for completion in March, 1980.

Thermal Conductivity

Selected samples from the twelve identified regions are being tested for thermal conductivity as a function of temperature. This preliminary work is 50% complete. The effects of applied pressure, orientation and water saturation will be initiated in March, 1980, following the completion of the regional study. Parallel theoretical work in predicting the thermal conductivity is also in progress.

Specific Heat

Measurements of specific heat of samples from the twelve regions will be completed by February, 1980. Data analysis and repeatability studies will then be initiated to verify the results. From these measurements, specific heat values of the tar sand constituents will be predicted. These constituent values will be useful in predicting

specific heats of other tar sand samples. Since the specific heat values are temperature-dependent, this may lead to a more sophisticated model of bitumen specific heat values.

Relative Permeability

Comparison measurements are being arranged for with an outside agency. This is necessary due to the apparently insensitive results which have been measured to date. Any further decisions relating to the relative permeability measurement program will be deferred until the comparative results have been received. It may be necessary to investigate other methods of measuring relative permeability than have been used in this study to date.

## PERSONNEL FOR FY 78-79

W. R. Lindberg - Principal Investigator

I. K. Kim - Ph.D. Candidate, participated in design phases of thermal conductivity and specific heat apparatus.

T. Foster - Ph.D. Candidate, routine core analysis measurements, rewrote core analysis program and prepared data analysis routines for storing and presenting data, principal investigator of relative permeability study.

R. Christensen - M. S. Candidate, principal investigator for viscosity and specific heat studies, routine core analysis.

J. Winkel - undergraduate, senior

P. Tyrrell - Undergraduate, senior

D. Wall - undergraduate, senior

J. Lee - undergraduate, junior

R. Thomas - undergraduate, junior

J. Gilmer - undergraduate, junior

S. Ownbey - computer specialist

## REFERENCES

J. Anand, W. H. Somerton, E. Gowaa, "Predicting Thermal conductivities of formations from other known properties", SPE J., (1973) pp. 267-73

Bear, J., Dynamics of Fluids in Porous Media, American Elsevier Publishing Company, Inc., New York, (1972)

Brooks, R. H. and Corey, A. T., "Hydraulic properties of porous media," Hydrology Papers, Colorado State University, Fort Collins, CO, (March, 1964).

Brown, H. W., "Capillary pressure indication." Trans. AIME, 192, pp. 67-74, (1951).

Burdine, N.T., "Relative permeability calculations from pore-size distribution data." Trans. AIME, 198, pp. 71-77, (1953).

Carslaw and Jaeger, Conduction of Heat in Solids, 2nd Edition, Oxford Press, pp. 112-113, (1959).

Crane, R. A. and R. I. Vachon, "A Prediction of the bounds on the effective thermal conductivity of granular materials." I.J.H.M.T. 20, 711-723, (1977).

Eckert and Goldstein, Measurements in Heat Transfer, 2nd Edition, McGraw Hill, pp. 508-511, (1976).

Krischer, O., Uber die Bestimmung der Warmeleitfahigkeit der Warmokapazitat und der Warmeeindringzahl in einem Kurzzeitverfahren, Chem. Ing. Tech., Vol. 26, p. 42, (1954).

R. Krupiczka, "Analysis of thermal conductivity in granular materials", Inst. Chem. Engineering, pp. 122-144, (1967).

Powell, et al., Thermal Conductivity of Selected Materials, National Bur. Stds. Reference Data Series, NBS-8 (25 Nov. 1966).

Purcell, W. R., "Capillary pressures--their measurement using mercury and the calculation of permeability therefrom." Trans. AIME, 186, pp. 39-46, (1949).

Raznjevic, Handbook of Thermodynamic Tables and Charts, McGraw Hill, (1976).

Scheidegger, A.E., The Physics of Flow Through Porous Media, Second Edition, University of Toronto Press, Toronto, (1960).

Slobod, R. L., Chambers, A., and Prehn, W. L. Jr., "Use of centrifuge for determining connate water, residual oil, and capillary pressure curves of small core samples," Trans. AIME, 192, pp. 127-134, (1951).

Somerton, W. H., Keese, J. A., Chu, S.L., "Thermal behavior of unconsolidated oil sands," Soc. Pet. Eng. J., pp. 513 (1971).

Tye, R. P., "Thermophysical properties in electronic applications," in Directions of Heat Transfer in Electronic Equipment, ed. by Kraus, Bergles and Mollendorf (NSF Grant Eng. - 7701297), (1977).

Tye, R. P., Thermal Conductivity, Volumes I and II; Academic Press, New York, (1969).

Wyllie, M. R. J., and Gardner, G.H.F.; "The generalized Kozeny-Carman equation II. A novel approach to fluid flow", World Oil Sect., pp. 210-28, (1958).

# Appendix I

## Computer Program of Routine Data Analysis

## (written for Hewlett-Packard 2100 Mini-computers)

```
SCORES T=00004 IS ON CR00015 USING 00034 BLKS R=0216

0001  FTN4,L
0002        PROGRAM CORES
0003  C
0004  C                    WRITTEN BY M.W.THORNTON      APRIL 24, 1978.
0005  C                  REWRITTEN BY T.E.FOSTER        OCTOBER 30, 1978.
0006  C
0007  C *** USE THIS PROGRAM TO ENTER CORE DATA INTO FILE 'CORDAT'.  THE DATA
0008  C     IS USED TO CALCULATE FURTHER DATA WHICH IS ALSO STORED IN 'CORDAT'
0009  C     THE DATA IN THIS FILE CAN BE LISTED OR CROSS CORROLATED IN ANY
0010  C     MANNER.
0011  C
0012
0013        LOGICAL EDIT
0014        REAL L
0015        DIMENSION IPRAM(5), IDCB(144,2), DATA(64), NAME1(3), NAME2(3)
0016        DIMENSION CUSH(1), BUF(20),IARR(27)
0017  C
0018        EQUIVALENCE(DATA(3) , AFCT) , (DATA(4) , BFCT) , (DATA(5) , PFCT)
0019       1           ,(DATA(6) , OILG) , (DATA(7) ,PATHS) , (DATA(8) ,VISCS)
0020       2           ,(DATA(9) ,PATME) , (DATA(10),VISCE) , (DATA(11),DEPTH)
0021       3           ,(DATA(12),  L  ) , (DATA(13), DIAM) , (DATA(14),  PZS)
0022       4           ,(DATA(15), PVCS) , (DATA(16),  PS ) , (DATA(17),  VS )
0023       5           ,(DATA(18),  TS ) , (DATA(19),  WTS) , (DATA(20),  PZE)
0024       6           ,(DATA(21), PVCE) , (DATA(22),  PE ) , (DATA(23),  VE )
0025       7           ,(DATA(24),  TE ) , (DATA(25),  WTE) , (DATA(26),WTTHD
0026       8           ,(DATA(27),WTSAT) , (DATA(28),WTEXT) , (DATA(29),  H20)
0027       9           ,(DATA(30),  DIR)
0028       0           ,(DATA(33), RHOS) , (DATA(34), RHOE) , (DATA(35),RHOSW)
0029       1           ,(DATA(36), PHIS) , (DATA(37), PHIE) , (DATA(38),  A'S)
0030       2           ,(DATA(39),  AKE) , (DATA(40),  VO ) , (DATA(41),  SO )
0031       3           ,(DATA(42),  SW )
0032        DATA NAME1/2HCO, 2HRD, 2HAT/
0033        DATA NAME2/2HCO, 2HRD, 2HT2/
0034  C
0035        CALL RMPAR(IPRAM)
0036        LU = IPRAM
0037        CALL OPEN(IDCB(1,1),IERR,NAME1,0,0,15)
0038        CALL OPEN(IDCB(1,2),IER2,NAME2,0,0,15)
0039        CALL READF(IDCB(1,1),IERR,DATA,128,LEN,1)
0040        NUMB = DATA(1)*1
0041        NUMX = NUMB+1
0042   250  WRITE(LU,100) NUMB,NUMX
0043   100  FORMAT(2X,I3," SAMPLES HAVE BEEN ENTERED.",/
0044       1,5X,"TYPE 0 TO ENTER SAMPLE NO. ",I3,/
0045       2,5X,"TO EDIT A SAMPLE, ENTER THE SAMPLE NO.")
0046        READ(LU,*) IANS
0047   200  FORMAT(A2)
0048        IF (IANS .EQ. 0) GO TO 400
0049        ISAM = IANS
0050        IF(ISAM.GT.0.AND.ISAM.LE.900) GO TO 5000
0051        WRITE(LU,350)
0052   350  FORMAT(2X,"BAD SAMPLE NO.")
0053        GO TO 250
0054  C **  INPUTTING THE DATA
0055   400  ISAM = NUMX
0056        NUMX = NUMX + 1
0057        WRITE (LU,101) (DATA(I),I = 3,6)
0058   101  FORMAT (2X,"DO YOU WISH TO KEEP THESE SAME FOUR CALIBRATION"
0059       1 ," CONSTANTS ?"/2X,"A FACTOR = ",F7.3,/2X"B FACTOR = ",F6.1/2X,
0060       2  "PYCNOMETER FACTOR = ",F8.4/2X,"OIL GRAVITY = ",F5.2)
0061        READ (LU,200) IANS
0062        IF (IANS .EQ. 2HYE) GO TO 450
0063        WRITE (LU,102)
0064   102  FORMAT(2X,"ENTER THE A FACTOR,B FACTOR, PYCNOMETER FACTOR, AND "
0065       1        "OIL GRAVITY")
0066        READ (LU,*) (BUF(I),I = 1,4)
0067        GO TO 451
0068   450  DO 451 I = 1,4
0069        BUF(I) = DATA(I+2)
0070   451  CONTINUE
```

```
0071          GO TO 460
0072      455 WRITE (LU,103)
0073      103 FORMAT(2X,"DO YOU WISH TO CARRY THE ATMOSPHERIC PRESSURES AND AIR"
0074         1        " VISCOSITIES ?")
0075          READ (LU,200) IANS
0076          EDIT = .FALSE.
0077          IF (IANS .NE. 2HNO) GO TO 470
0078      460 WRITE (LU,104)
0079      104 FORMAT(2X,"ENTER THE ATMOSPHERIC PRESSURE AND VISCOSITY FOR THE "
0080         1       /2X,"SATURATED AND UNSATURED CASES.")
0081          READ (LU,*) (BUF(I),I = 5,8)
0082          EDIT = .FALSE.
0083      470 WRITE (LU,115)
0084      115 FORMAT("  WHAT IS THE ORIENTATION OF THE CORE? -- N OR W --  _")
0085          READ (LU,200) ICOR
0086          DIR = 0.
0087          IF (ICOR .EQ. 2HN ) DIR = 1.
0088          IF (ICOR .EQ. 2HW ) DIR = 4.
0089          IF (EDIT) GO TO 1150
0090          WRITE (LU,105)
0091      105 FORMAT(2X,"ENTER THE MEASURED DATA FROM THE SATURATED AND EXTRAC"
0092         1       "TED CORE,"/2X,"SEPARATED BY COMMAS, AND IN THE ORDER THEY A"
0093         2       "RE WRITTEN DOWN,"/2X,"STARTING WITH DEPTH.")
0094          READ (LU,*) (BUF(I),I = 9,23)
0095    COMIT WRITE (LU,106)
0096    C 106 FORMAT (2X,"IS THERE DATA TO BE RECORDED FROM THE CHIPS ?")
0097    C     READ (LU,200) IANS
0098    C     IF (IANS .NE. 2HNO) GO TO 420
0099    COMIT GO TO 1150
0100      420 WRITE (LU,107)
0101      107 FORMAT(2X,"ENTER THE MEASURED CHIP DATA IN THE ORDER THEY ARE WRI"
0102         1       "TTEN DOWN --"/2X,"STARTING WITH - THIMBLE WEIGHT -")
0103          READ (LU,*) (BUF(I),I = 24,27)
0104    C **  LOAD BUFFER INTO DATA ARRAY
0105     1150 DO 1200 J=1,27
0106          IF (BUF(J) .NE. -1.) DATA(J+2) = BUF(J)
0107     1200 IF (BUF(J) .EQ. -1.) BUF(J) = DATA(J+2)
0108          DATA(2) = ISAM
0109          WRITE (LU,110)
0110      110 FORMAT (2X,"DO YOU WANT TO CHECK YOUR TYPING ACCURACY ?")
0111          READ (LU,200) IANS
0112          IF (IANS .NE. 2HYE) GO TO 1400
0113    C **  DOUBLE CHECKING FOR ERRORS
0114     1199 ICOR = 2H**
0115          IF (DIR .EQ. 1.) ICOR = 2HN
0116          IF (DIR .EQ. 4.) ICOR = 2HW
0117          WRITE (LU,111) (BUF(J),J = 1,8), ICOR, (BUF(J),J = 9,27)
0118      111 FORMAT(" A FACTOR =",F7.3," B FACTOR =",F5.2," PYCNOMETER FACTOR"
0119         1       " =",F7.4," OIL GRAVITY =",F4.2//
0120         2 15X,"SATURATED",30X,"EXTRACTED"/10X,"PATH",5X,"VISCOSITY",21X,
0121         3 "PATH",5X,"VISCOSITY"/10X,F5.1,5X,F7.5,22X,F5.1,5X,F7.5//
0122         4 " ORIENT  DEPTH    LENGTH   DIAMETER"/A6,F8.1,5X,F5.2,5X,F5.2//
0123         5 32X,"SATURATED DATA"/13X,"P2",6X,"PYC",6X,"P",7X,"V",6X,"T"
0124         6,7X,"WT"/  15X,F6.1,3X,F6.3,3X,F5.2,3X ,F4.0,3X ,F5.1,3X ,F8.4/
0125         7/32X,"EXTRACTED DATA"/13X,"P2",6X,"PYC",6X ,"P",7X ,"V",6X ,"T"
0126         8,7X,"WT"/15X ,F6.1,3X ,F6.3,3X ,F5.2,3X ,F4.0,3X ,F5.1,3X ,F8.4/
0127         9/35X,"CHIP DATA"/12X,"THIMBLE WT",3X,"THIMBLE + SAT WT",3X,
0128         0 "THIMBLE + EXT WT   WATER"/14X,F7.3,8X,F8.3,11X,F8.3,7X,F4.2//
0129         1 "  DO YOU WANT TO CHANGE ANYTHING ?")
0130          READ (LU,200) IANS
0131          IF (IANS .EQ. 2HNO) GO TO 1400
0132     1198 WRITE (LU,112)
0133      112 FORMAT(" HOW MANY VALUES DO YOU WANT TO CHANGE ?"/" (TYPE '99' "
0134         1,      "TO ENTER ALL NEW DATA)")
0135          READ (LU,*) NUM
0136          IF (NUM .LE. 0) GO TO 1400
0137          IF (NUM .EQ. 99) GO TO 460
0138          WRITE (LU,113)
0139      113 FORMAT(" INPUT THE COLUMN NUMBER OF THE VALUE YOU WISH TO CHANGE"
0140         1," - COMMA -"/" AND THE NEW VALUE."/" DO THAT AS MANY TIMES AS"
0141         2," NECESSARY")
0142          READ (LU,*) (IARR(J),BUF(IARR(J)), J = 1, NUM)
```

```
0143          EDIT = .FALSE.
0144    C **  DOES THE ORIENTATION NEED TO BE CHANGED
0145          DO 1250 I = 1 , NUM
0146          IF (IARR(I) .EQ. 23) EDIT = .TRUE.
0147     1250 CONTINUE
0148          IF (EDIT) GO TO 470
0149          GO TO 1150
0150    C
0151    C
0152    C     * EQUATIONS FOR SATURATED SAMPLES
0153    C
0154     1400 WW = WTSAT - WTEXT - H2O
0155          IF (WW .LT. 0.) WW = 0.
0156          WO = 100. * WW / (WTSAT - WTTHM)
0157          IF (P2S .LE. 0. .AND. PYCS .LE. 0. .AND. PS .LE. 0. .AND.
0158         1    VS .LE. 0. .AND. TS .LE. 0. .AND. WTS .LE. 0. ) GO TO 1900
0159          VBS = PYCS * PFCT
0160          VSS = AFCT - BFCT * P2S / (1520. - P2S)
0161          RHOS = WTS / VBS
0162          PHIS = 100. * (VBS - VSS) / VBS
0163          IF (PHIS .LT. 0.) PHIS = 0.
0164          A1 = 2546.479 * VISCS * L * VS / (DIAM*DIAM * TS)
0165          PA = PATMS / 760.
0166          AKS = A1 * (PA / ((PS+PA)*(PS+PA) - (PA*PA)))
0167    C
0168    C     * EQUATIONS USING EXTRACTED CORE DATA
0169    C
0170          IF (P2E .LE. 0. .AND. PYCE .LE. 0. .AND. PE .LE. 0. .AND.
0171         1    VE .LE. 0. .AND. TE .LE. 0. .AND. WTE .LE. 0. ) GO TO 2000
0172    C
0173          VBE = PYCE * PFCT
0174          VSE = AFCT - BFCT * P2E / (1520. - P2E)
0175          RHOE = WTE / VBE
0176          RHOSC = WTE / VSE
0177          PHIE = 100. * (VBE - VSE) / VBE
0178          IF (PHIE .LT. 0.) PHIE = 0.
0179          IF (PHIE .GT. 100.) PHIE = 100.
0180          A2 = 2546.479 * VISCE * L * VE / (DIAM*DIAM * TE)
0181          AKE = A2 *(PATME/760.)/ ((PE + PATME/760.)**2 - (PATME/760.)**2)
0182          SW = 100.*100. * H2O * RHOS / ((WTSAT - WTTHM) * PHIE)
0183          SO = 100.* WO * RHOS / (OILC * PHIE)
0184          IF((SO+SW).LE.100.0) GO TO 2100
0185          SOO = SO
0186          SO = SOO * 100. / (SOO + SW)
0187          SW = SW * 100. / (SOO + SW)
0188          GO TO 2100
0189    C     * DEFAULTS FOR MISSING DATA
0190     1900 RHOS = 0.
0191          PHIS = 0.
0192          AKS = 0.
0193     2000 RHOE = 0.0
0194          PHIE = 0.0
0195          AKE = 0.0
0196          SO = 0.0
0197          RHOSC = 0.0
0198          SW = 0.0
0199    C **  WRITE THE DATA TO THE FILE
0200     2100 DATA(64) = 77.77
0201          CALL WRITF(IDCB(1,ISAM/501+1),IERR,DATA,128,MOD(ISAM-1,500)+1)
0202          WRITE(LU,2200) ISAM
0203     2200 FORMAT(2X,"DATA AND CALCULATIONS FOR SAMPLE ",I3," IN FILE.")
0204    C     * CONTINUE
0205          WRITE(LU,2400) NUMX
0206     2400 FORMAT(2X,"TYPE 0 TO ENTER NEXT SAMPLE (SAMPLE # ",I3," )"/
0207         1,7X,"NEW SAMPLE NO. TO EDIT ANOTHER SAMPLE.",/
0208         2,7X,"ANY NEGATIVE NUMBER TO STOP.")
0209          READ(LU,*) JANS
0210          IF (JANS .LT. 0) GO TO 9000
0211          IF (JANS .EQ. 0) GO TO 2401
0212          IF (JANS .GT. 900) WRITE (LU,350)
0213          ISAM = JANS
```

```
0214          GO TO 5000
0215    C     * CONTINUE TO NEXT SAMPLE
0216     2401 ISAM = NUMX
0217          NUMX = NUMX + 1
0218    C **  ERASE THE EXTRACTED CORE DATA
0219          DO 2501 JJ = 9, 23
0220     2501 BUF(JJ) = 0.
0221          ICOR = 2HXX
0222          GO TO 455
0223    C     * EDITING
0224     5000 CALL READF(IDCB(1,ISAM/501+1),IERR,DATA,128,LEN,MOD(ISAM-1,500)+1)
0225          WRITE(LU,114)
0226      114 FORMAT (" DO YOU WANT TO SEE THE DATA ?   _")
0227          AFCT = 10.824
0228          BFCT = 64.6
0229          PFCT = 1.2897
0230          OILG = 1.
0231          DO 5005 J=3,30
0232     5005 BUF(J-2) = DATA(J)
0233          READ(LU,200) IANS
0234     5009 IF(IANS .EQ. 2HYE) GO TO 1199
0235          GO TO 1198
0236    C     * COMPLETION
0237     9000 DO 9010 K=1,900
0238          CALL READF(IDCB(1,K/501+1),IERR,DATA,128,LEN,MOD(K-1,500)+1)
0239          IF(DATA(64).NE.77.77) GO TO 9020
0240     9010 CONTINUE
0241     9020 KK = K-1
0242          CALL READF(IDCB(1,1),IERR,DATA,128,LEN,1)
0243          DATA(1) = KK*1.0
0244          CALL WRITF(IDCB(1,1),IERR,DATA,128,1)
0245          CALL CLOSE(IDCB(1,1),IERR)
0246          CALL CLOSE(IDCB(1,2),IERR)
0247          WRITE(LU,9100)
0248     9100 FORMAT(10X,"*** END OF CORES ***"/10X,"TO RUN AGAIN --"/10X,
0249         1              "    :RU,CORES"/10X,"TO PRINT OUT THE DATA --"/10X,
0250         2              "    :RU,,1H","CROUT"/10X,"BEFORE YOU SIGN OFF THE "
0251         3 ,"COMPUTER"/10X,"LOAD 'LINDBERG #2' DISC -- AND"/10X,
0252         4              "    :RU,,1H","CREND")
0253          END
0254          END3
0255
```

```
&CROUT T=00004 IS ON CR=00015 USING 00010 BLKS R=0069

0001  FTN4,L
0002        PROGRAM CROUT
0003  C
0004  C                        WRITTEN BY T.E.FOSTER    NOV 10,1978
0005  C
0006  C  *** USE THIS PROGRAM TO LIST DATA IN CORDAT ***
0007  C
0008        DIMENSION IDCB(144,2),DAT(64),IPRAM(5),NAME(3),DAT2(64),DAT3(64)
0009        DIMENSION NAME2(3), IWELL(2), PRI(500), SEC(500), IORD(500)
0010        LOGICAL DONE
0011        DATA NAME/2HCO,2HRD,2HAT/, NAME2/2HCO,2HRD,2HT2/
0012  C  -  INITIALIZATION OF VARIABLES
0013        CALL RMPAR(IPRAM)
0014        LU = IPRAM(1)
0015        LST = LU
0016        ICOL1 = 11
0017        ICOL2 = 30
0018  C  -  DECIDE ON A PRINT-OUT FORMAT
0019        WRITE (LU,100)
0020    100 FORMAT ("  TYPE 1 FOR PRINT OUT OF RESULTS,"/
0021       1           7X, "2 FOR PRINT OUT OF ALL DATA IN A SAMPLE FILE.")
0022        READ (LU,*) MUCH
0023        WRITE(LU,101)
0024    101 FORMAT("  DO YOU WANT A HARD COPY OF THIS?   _")
0025        READ (LU,99) IANS
0026     99 FORMAT (2A2)
0027        IF (IANS .NE. 2HNO) LST = 12
0028        WRITE (LU,102)
0029    102 FORMAT("  TYPE IN THE NAME OF THE WELL YOU WANT TO LABEL THE ",
0030       1       "OUTPUT.")
0031        READ (LU,99) (IWELL(I), I = 1,2)
0032        IF (MUCH .EQ. 2) GO TO 3000
0033  C
0034        WRITE (LU,200)
0035    200 FORMAT("  ENTER FIRST SAMPLE, LAST SAMPLE TO BE LISTED.")
0036        READ (LU,*) IS1,IS2, IS3,IS4
0037        CALL OPEN (IDCB(1,1), IERR, NAME, 0,0,15)
0038        CALL OPEN (IDCB(1,2), IERR, NAME2,0,0,15)
0039  C  -  THE ORDER OF DATA PRINT-OUT
0040        N = IS2 - IS1 + 1
0041        N1 = IS4 - IS3 + 1
0042        IF (IS4 .EQ. 0) N1 = 0
0043        WRITE (LU,103)
0044    103 FORMAT("  THE DEFAULT SEQUENCE OF LISTING THE RESULTS IS BY INCR"
0045       1,"EASING DEPTHS"/"  WITH A SECONDARY ORDER OF ORIENTATION."/
0046       2 "  DO YOU WANT TO CHANGE THAT ?   _")
0047        READ (LU,99) IANS
0048        IF (IANS .NE. 2HYE) GO TO 10
0049  C *** CHANGING THE DEFAULT ORDER
0050        WRITE (LU,104)
0051    104 FORMAT("  ENTER THE COLUMN NUMBERS (FROM THE DATA SHEET) OF PRIM"
0052       1,"ARY, AND SECONDARY"/"  VARIABLES THAT YOU WANT THE RESULTS LIS"
0053       2,"TED BY.")
0054        READ (LU,*) ICOL1, ICOL2
0055        ICOL1 = ICOL1 + 2
0056        ICOL2 = ICOL2 + 2
0057  C *** LOADING UP THE ARRAYS FOR SORTING PURPOSES
0058     10 DO 15 I = 1, N
0059        ISAM = IS1 + I - 1
0060        CALL READF(IDCB(1,ISAM/501+1),IERR,DAT,128,LEN,MOD(ISAM-1,500)+1)
0061        PRI(I) = DAT(ICOL1)
0062        SEC(I) = DAT(ICOL2)
0063        IORD(I) = I
0064     15 CONTINUE
0065        IF (IS4 .EQ. 0) GO TO 16
0066        DO 16 I = 1, N1
0067        ISAM = IS3 + I - 1
0068        CALL READF(IDCB(1,ISAM/501+1),IERR,DAT,128,LEN,MOD(ISAM-1,500)+1)
0069        PRI(N+I) = DAT(ICOL1)
```

```
0070        SEC(N+I) = DAT(ICOL2)
0071        IORD(N+I) = N+I
0072     16 CONTINUE
0073  C *** REARRANGING IORD FOR THE PROPER PRINT-OUT ORDER
0074        DO 30 I = 1, N+N1-1
0075        DONE = .TRUE.
0076        DO 25 J = 1, N+N1-I
0077        IF (PRI(IORD(J)) .LT. PRI(IORD(J+1))) GO TO 25
0078        IF (PRI(IORD(J)) .EQ. PRI(IORD(J+1))) GO TO 20
0079        DONE = .FALSE.
0080        ITEMP = IORD(J)
0081        IORD(J) = IORD(J+1)
0082        IORD(J+1) = ITEMP
0083        GO TO 25
0084     20 IF (SEC(IORD(J)) .LT. SEC(IORD(J+1))) GO TO 25
0085        DONE = .FALSE.
0086        ITEMP = IORD(J)
0087        IORD(J) = IORD(J+1)
0088        IORD(J+1) = ITEMP
0089     25 CONTINUE
0090        IF (DONE) GO TO 31
0091     30 CONTINUE
0092  C *** NOW LIST OUT THE DATA IN THIS DETERMINED ORDER
0093     31 DO 1000 K = 1, N+N1
0094        KK = IORD(K) + IS1 - 1
0095        IF(IORD(K) .GT. N) KK = IORD(K) - N + IS3 - 1
0096        IPAGE = (K-1) / 26 + 1
0097        CALL READF(IDCB(1,KK/501+1),IERR,DAT,128,LEN,MOD(KK-1,500)+1)
0098        JSAM = DAT(2)
0099        IDIR = DAT(30)
0100        ICOR = 2H**
0101        IF (IDIR .EQ. 1) ICOR = 2HN
0102        IF (IDIR .EQ. 4) ICOR = 2HW
0103        IF (MOD(K-1,26) .EQ. 0) WRITE (LST,300) (IWELL(I),I = 1,2), IPAGE
0104   300 FORMAT("1",5/,46X,5"*","    CORE ANALYSES    ",5"*"/
0105      1              51X,      "NAME OF WELL:   ",2A2,42X,"PAGE ",I2//
0106      2 11X,"NO.  ORIENT  DEPTH",5X,"RHO-S  RHO-E  RHO-SC",5X,"PHI-S  "
0107      3 ,"PHI-E",6X,"K(S)     K(E)",7X,"WO",5X,"SO",5X,"SW",7X,"NO."//)
0108        WRITE(LST,500) JSAM, ICOR, DAT(11), (DAT(I), I = 33,42), JSAM
0109   500 FORMAT (9X,I4,5X,A2,X,F3.1,5X,3(F5.3,2X),3X,2(F5.2,2X),3X,
0110      1         2(F6.1,2X),3X,3(F5.2,2X),3X,I4/)
0111  1000 CONTINUE
0112        CALL CLOSE (IDCB(1,1), IERR)
0113        CALL CLOSE (IDCB(1,2), IERR)
0114        GO TO 9000
0115  C
0116  3000 WRITE (LU,3100)
0117  3100 FORMAT ("  ENTER FIRST, LAST SAMPLES TO BE LISTED.")
0118        READ (LU,*) JSAM, KSAM
0119        KD = (KSAM - JSAM+1) / 3
0120        IF ((KD*3) .NE. (KSAM - JSAM+1)) KD = KD + 1
0121        CALL OPEN (IDCB, IERR, NAME, 0, 0, 2)
0122  C
0123        DO 3150 JJ = 1, KD
0124        IR1 = JSAM + JJ * 3 - 3
0125        IR2 = IR1 + 1
0126        IR3 = IR1 + 2
0127        CALL READF (IDCB, IERR, DAT , 128, LEN, IR1)
0128        CALL READF (IDCB, IERR, DAT2, 128, LEN, IR2)
0129        CALL READF (IDCB, IERR, DAT3, 128, LEN, IR3)
0130        WRITE (LST,3160) IR1, IR2, IR3
0131  3160 FORMAT (2X,3(7X,"SAMPLE ",I3,8X)///)
0132        DO 3500 K = 1, 43
0133        L = K
0134        IF (K .EQ. 43) L = 64
0135        WRITE (LST,3200) L, DAT(L), L, DAT2(L), L, DAT3(L)
0136  3200 FORMAT (2X,3(" DATA(",I3,") = ",F10.4,2X))
0137  3500 CONTINUE
0138        WRITE (LST,3600)
0139  3600 FORMAT ("1")
0140  3150 CONTINUE
```

```
0141          CALL CLOSE (IDCB, IERR)
0142  C
0143   9000 WRITE(LU,3601)
0144   3601 FORMAT(10X,"*** END OF CROUT ***"/10X,"TO RUN AGAIN --"/10X,
0145         1                "    :RU,CROUT"/10X,"TO INPUT OR EDIT DATA --"/10X,
0146         2                "    :RU,",1H","CORES"/10X,
0147         3 "TO SIGN OFF THE COMPUTER, LOAD 'LINDBERG #2' DISC AND --"/10X,
0148         4                "    :RU,",1H","CREND")
0149          END
0150          ENDS
```

```
@CRPLT T=00004 IS ON CR00015 USING 00010 BLKS R=0069

0001  FTN4,L
0002        PROGRAM CRPLT
0003  C
0004  C                     WRITTEN BY TOM FOSTER    JUN 14,1979
0005  C
0006  C  *** USE THIS PROGRAM TO PLOT DATA IN CORDAT ***
0007  C
0008        DIMENSION IDCB(144,2),DAT(64),IPRAM(5),NAME(3),IXL(3),IYL(10)
0009        DIMENSION NAME2(3), DEPTH(500), QUANT(500), QUAN2(500), IWELL(2)
0010        COMMON ICOM(170)
0011        LOGICAL DONE
0012        DATA NAME/2HCO,2HRD,2HAT/, NAME2/2HCO,2HRD,2HT2/
0013        DATA IXL/2HDE,2HPT,2HH /
0014  C  -  INITIALIZATION OF VARIABLES
0015        CALL RMPAR(IPRAM)
0016        LU = IPRAM(1)
0017        LST = LU
0018        ICOL1 = 11
0019  C
0020        WRITE (LU,200)
0021    200 FORMAT(" ENTER FIRST SAMPLE, LAST SAMPLE TO BE PLOTTED.")
0022        READ (LU,*) IS1,IS2 ,IS3,IS4
0023        CALL OPEN (IDCB(1,1), IERR, NAME, 0,0,15)
0024        CALL OPEN (IDCB(1,2), IERR, NAME2,0,0,15)
0025  C  -  THE ORDER OF DATA PRINT-OUT
0026        N = IS2 - IS1 + 1
0027        N1 = IS4 - IS3 + 1
0028        IF (IS4 .EQ. 0) N1 = 0
0029        WRITE (LU,103)
0030    103 FORMAT(" WHAT ARE THE COLUMN NUMBERS OF THE QUANTITIES YOU WANT"
0031       1       ," PLOTTED"/" VERSUS DEPTH?  _")
0032        READ (LU,*) ICOL2, ICOL3
0033        WRITE (LU,104)
0034    104 FORMAT(" WHAT LABEL DO YOU WANT ON THOSE QUANTITIES?")
0035        READ (LU,99) (IYL(I),I = 1,10)
0036     99 FORMAT(10A2)
0037  C *** LOADING UP THE ARRAYS FOR SORTING AND PLOTTING PURPOSES
0038     10 DO 15 I = 1, N
0039        ISAM = IS1 + I - 1
0040        CALL READF(IDCB(1,ISAM/501+1),IERR,DAT,128,LEN,MOD(ISAM-1,500)+1)
0041        DEPTH(I) = DAT(ICOL1)
0042        QUANT(I) = DAT(ICOL2)
0043        IF (ICOL3 .NE. 0) QUAN2(I) = DAT(ICOL3)
0044     15 CONTINUE
0045        IF (IS4 .EQ. 0) GO TO 16
0046        DO 16 I = 1, N1
0047        ISAM = IS3 + I - 1
0048        CALL READF(IDCB(1,ISAM/501+1),IERR,DAT,128,LEN,MOD(ISAM-1,500)+1)
0049        DEPTH(N+I) = DAT(ICOL1)
0050        QUANT(N+I) = DAT(ICOL2)
0051        IF (ICOL3 .NE. 0) QUAN2(N+I) = DAT(ICOL3)
0052     16 CONTINUE
0053  C *** REARRANGING 'DEPTH' AND 'QUANT'S FOR PROPER PLOTTING
0054        DO 30 I = 1, N+N1-1
0055        DONE = .TRUE.
0056        DO 25 J = 1, N+N1-1
0057        IF (DEPTH(J) .LE. DEPTH(J+1)) GO TO 25
0058        DONE = .FALSE.
0059        TEMP = DEPTH(J)
0060        DEPTH(J) = DEPTH(J+1)
0061        DEPTH(J+1) = TEMP
0062        TEMP = QUANT(J)
0063        QUANT(J) = QUANT(J+1)
0064        QUANT(J+1) = TEMP
0065        IF (ICOL3 .EQ. 0) GO TO 25
0066        TEMP = QUAN2(J)
0067        QUAN2(J) = QUAN2(J+1)
0068        QUAN2(J+1) = TEMP
0069     25 CONTINUE
```

```
0070          IF (DONE) GO TO 31
0071       30 CONTINUE
0072       31 CALL CLOSE (IDCB(1,1), IERR)
0073          CALL CLOSE (IDCB(1,2), IERR)
0074    C *** NOW PLOT THE CORRECTLY ORDERED QUANTITIES
0075          CALL MODE(0,1.,1.,1.)
0076          IF (ICOL3 .NE. 0) CALL SCAN(DEPTH,QUAN2,N+N1,441)
0077          CALL SCAN(DEPTH,QUANT,-(N+N1),441)
0078          CALL MODE(-8,XMIN,DX,XORG)
0079          WRITE (LU,333) XMIN,DX,XORG
0080      333 FORMAT (3F12.3)
0081          CALL MODE(-9,YMIN,DY,YORG)
0082          WRITE (LU,333) YMIN,DY,YORG
0083          CALL DRAW(DEPTH,QUANT,N+N1,441)
0084          IF (ICOL3 .NE. 0) CALL DRAW(DEPTH,QUAN2,N+N1,441)
0085          CALL AXES(5.1,IXL,20.2,IYL)
0086          CALL DRAW(0.,0.,1,9000)
0087          CALL DRAW(0,0,0,9999)
0088          STOP
0089          END
0090          ENDS
```

# Appendix II

## Specific Heat Measurement

## (Theory and Procedure)

## INTRODUCTION

Knowledge of the specific heat of tar sands is needed to help accurately model the thermal behavior of most tar sand bitumen recovery techniques.

Several difficulties arise when attempting to measure the specific heat of materials such as tar sand. First, tar sand is a very non-homogeneous material. To overcome this difficulty, large samples must be used. The second drawback deals with the lack of related information, such as thermal conductivity or thermal diffusivity, since most calorimeters require that information. Another difficulty lies with the need to measure specific heat over a wide range of temperatures. The necessary temperature range is from room temperature to recovery temperature (approximately 250°C).

The overall goal of this project is to predict the heat capacity of a tar sand sample when the bitumen-water-sand concentrations are known. This generalization from site specific measurements is important for future site identification field studies when detailed measurements may not be possible. Specific heat measurements of the constituents of tar sand are also important to the numerical models also being employed.

The topics of discussion within this section include: 1) description of apparatus, 2) supporting theory, 3) experimental procedure, 4) depth specific data, 5) apparatus accuracy, 6) discussion and conclusion.

Apparatus

Several conventional colorimeters were considered for the present application. Common drop colorimeters and dewar experiments were discarded when the knowledge of thermal conductivity or the use of samples were required. Instead, an apparatus developed by Krischer (1954), and discussed in Eckert and Goldstein (1976), was decided upon. The present experimental apparatus, based on this concept, is shown in Figure 8.

The machine operates by sandwiching foil heaters between a stack of equally thick layers of sample. After an initial period of time a quasi-stationary condition sets up which can be described by parabolic temperature profiles. Once the time-temperature history has been established, the specific heat can be determined as a function of temperature.

Heat losses from the stack to the surroundings proved to be the greatest experimental difficulty. To reduce the heat loss, guard heaters were placed directly on the ends of the sample, as well as a couple of inches away from the circular sides.

The sample thickness seemed to play an important role in the success of the experiment. The thinner the sample the lower the heat loss and smaller the temperature difference across the sample. Samples one inch thick provided an easily controllable heat loss together with an adequate temperature difference.

Theory

Modelling the transient temperature history has been described by Carslow and Jaeger (1959). Although cylindrical samples are used, the

large diameter and insulated sides allows the model to represent an infinite slab bounded by two parallel planes. The model to be represented assumes a constant heat flux into a solid at L, where the thickness extends from zero to L (Figure A-1). All surfaces not exposed to the direct heat flux are considered adiabatic.

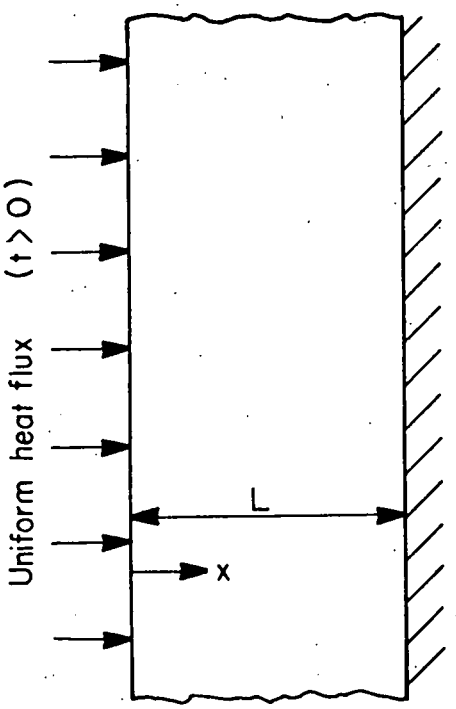


Figure A-1. One-dimensional model of transient heating of slab with uniform heat flux at one boundary and an adiabatic wall at the other boundary.

The temperature distribution within the sample can be described as follows.

$$T(x,t) = \frac{qt}{\rho CpL} + \frac{qL}{k}\left(\frac{3x^2-L^2}{6L^2}\right) - \frac{2}{\pi^2}\sum_{n=1}^{\infty}\frac{(-1)}{n^2}\exp\left(\frac{-\alpha n^2\pi\tau}{L^2}\right)\cos\frac{n\pi x}{L} \qquad \text{(A-I)}$$

Where

T = temperature excess (T(x,0)=0)
q = heat flux per surface area
t = time
ρ = density
Cp = specific heat
L = sample thickness
K = thermal conductivity
α = thermal diffusivity
x = dist from heater

Equation (1) consists of two parts. The first part describes the parabolic steady temperature profile while the second part describes the transient initial temperature distribution. The transient term is plotted in Figure A-2.

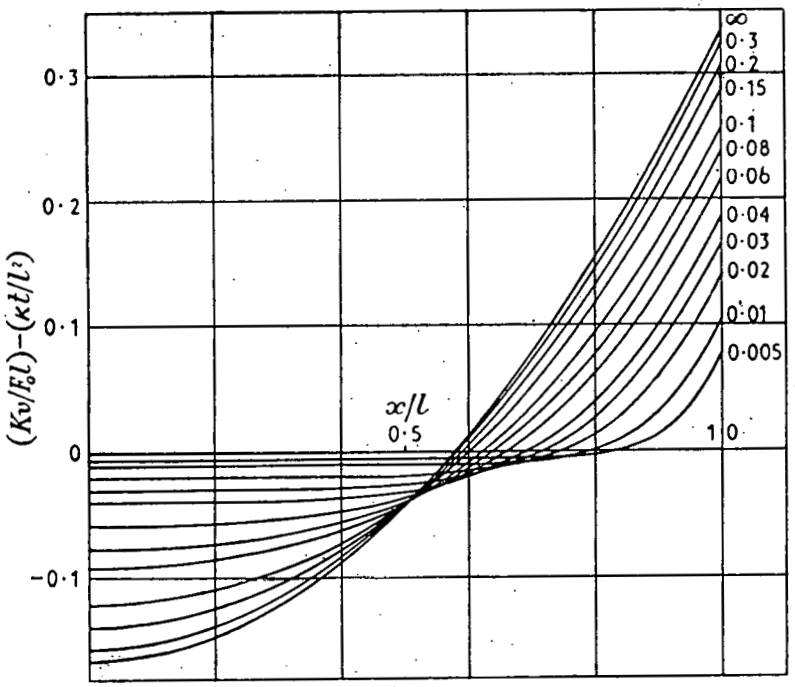


Figure A-2. Transient temperature distribution for slab of Figure A-1 (from Carslaw and Jaeger, 1959), as a function of Fourier modulus.

Notice from Figure A-2 that the temperature profile becomes parabolic when the Fourier time constant $\frac{(\alpha\tau)}{L^2}$ approaches infinity. Note also that for values of the Fourier time constant greater than -3 the transient term has all but disappeared. Therefore, given enough initial time, a parabolic temperature profile will set up within the slab. Assuming now that the Fourier time constant is infinity, equation (A-1) will reduce to equation (A-2) as shown below,

$$T = \frac{qt}{\rho CpL} + \frac{qL}{k}\,\frac{3x^2-L^2}{6L^2} \qquad \text{(A-2)}$$

At a representative point in the sample, equation (A-2) may be differentiated with respect to time. One may then solve for the specific heat:

$$Cp = \frac{q}{\rho L} \left(\frac{\partial t}{\partial T}\right)_x \qquad \text{(A-3)}$$

this equation is valid only if Cp is a slowly varying function of temperature, that is:

$$\frac{\rho L T}{\dot{q}} \frac{dCp}{dT} \left(\frac{\partial T}{\partial t}\right)_x << 1.$$

This condition must be checked for each test run in order to validate the results.

From Figure A-2, equation (A-3) is valid only when the Fourier modulus ($\alpha t/L^2$) is greater than .3. The actual transient time may be determined from this condition. If we assume a value of one for the Fourier modulus, one may estimate the "transient set-up time",

$$t = L^2/\alpha = \frac{L^2 \rho Cp}{k} .$$

For representative values of tar sand properties:

$k = 1.0$ Btu/hr-ft-°F,

$Cp = .4$ Btu/lbm-°F,

$\rho = 130$ lbm/ft$^3$,

$L = .08$ ft,

the transient set-up time, t, is 20 minutes.

## EXPERIMENTAL PROCEDURE

The primary function in running the experiment is to determine the time-temperature history of the sample. The history is obtained by monitoring the temperature at the center of the stack (Figure 8) every five minutes. Monitoring continues until a desired center temperature is reached. A set-up time of 30 minutes is allowed to be certain a parabolic temperature profile exists within the sample. Once the desired temperature has been reached an appropriate curve fit is applied to the time-temperature data. The derivative of the curve along with known constants will result in the specific heat as a function of time.

The entire apparatus including sample mounted thermocouples, and guard heaters is placed in a refrigerator until the sample temperature drops well below room temperature. Since 30 minutes are allowed to set up a parabolic profile, starting the temperature below room temperature allows room temperature data to be calculated. Three thermocouples are located in positions so that heat loss can be monitored. One thermocouple, located on the end, is matched with the center temperature so the heat flux is evenly distributed. The end thermocouple matches the center with the help of end guard heaters. Radial heat loss is monitored by two thermocouples on the diameter and controlled by the radial guard heater. A good experiment occurs when the center thermocouple, the end thermocouple and the two radial thermocouples all indicate the same temperature. A voltmeter monitors the heat flux to the stack, and Variacs control the heat flux to the stack and guard heaters.

## APPARATUS OPERATION

Two separate materials were tested to verify the accuracy of the experimental apparatus. The first, paraffin, has a known specific heat of 0.69 Btu/lbm°F (2.9 KJ/Kg°K) at 68°F (20°C) (Raznjevic, 1976). The experiment was conducted without the use of guard heaters. Assuming the specific heat is equal to a linear function of temperature, a result of 0.5985 Btu/ibm°F (2.5KJ/Kg°K) was obtained. The experimental error was about 13 percent.

The second material tested was plexiglas G. The specific heat was given as 0.35 Btu/lbm°F (1.47 KJ/Kg°K) (Plasticraft, 1976). Two sets of tests were run, one using a sample three inches in diameter and one-half inch thick, and the other four inches in diameter and one inch thick. The larger the sample, the more accurate the results. Again, no guard heaters were used, however, a test result of 0.3676 Btu/ibm°F (1.5KJ/Kg°k), only five percent from known values, was obtained.

Since the accuracy on both materials seemed good, tar sand was the next material tested. Guard heaters were not used on plexiglas G or paraffin because low temperatures were being studied. It is good practice, however, to use the guard heaters since end and radial heat losses effect the results to a large degree.

As an example of the experimental procedure and results, the specific heat tests of Region 9 will be presented. Four tests were run on the same sample at different heating rates in order to determine repeatability. Three of the trials are shown in Figure A-3, where the measured temperature is the temperature at the plane of symmetry in the

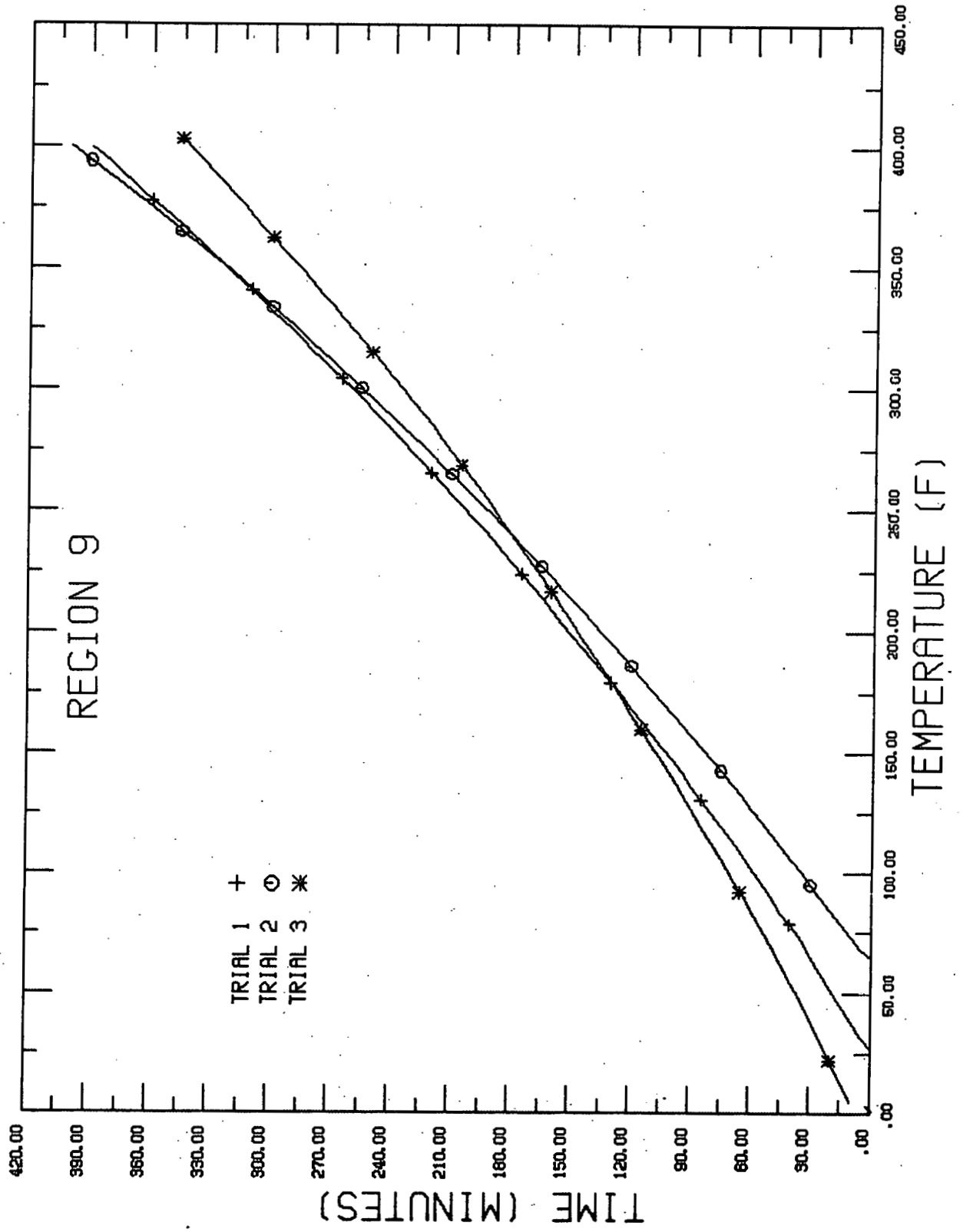


Figure A-3 Experimental temperature-time histories at the core centerline in specific heat apparatus. Region 9. Trials 1-3 are at three heater voltages: 100, 95, 90, respectively.

center of the stack. A convenient test of repeatability is to define a normalized temperature, T*:

$$T^* = \frac{(T-T_i)}{\dot{q}} = \frac{1}{pLC}\,(t-t_i)$$

and to plot T* vs. $(t-t_i)$ as is shown in Figure A-4. The curves should lie exactly on top of each other if the same starting temperature, $T_i$, is the same for all cases ($t_i$ is the time corresponding to $T_i$). It is seen that some variation is encountered at the longer times, but generally, the tests are quite repeatable. The temperature-time history is then curve-fit (in the least-squares sense) with varying degrees of polynomials. The resulting equation, T(t), is differentiated with respect to time. The differentiated result is then used in Equation 3, allowing one to obtain the predicted specific heat:

$$Cp = \frac{\dot{q}}{\rho L}\,\frac{\partial t}{\partial T}_x . \qquad (3)$$

For the example of Region 9, the resulting prediction is:

$$Cp = -1.664(10^{-2})T^2 + 6.22T = 763.0$$

for a cubic curve-fit for the temperature-time experimental data.

A test of the sensitivity of the order of the polynomial curve-fit one predicted specific heat is shown in figure A-5. It is seen that there is little difference in predicted results for polynomial curve-fits above a cubic, except at the two ends, where agreement is still satisfactory. The error introduced by a linear temperature dependence on specific heat is much higher than for the higher-order expressions, and is thus an inadequate model of specific heat.

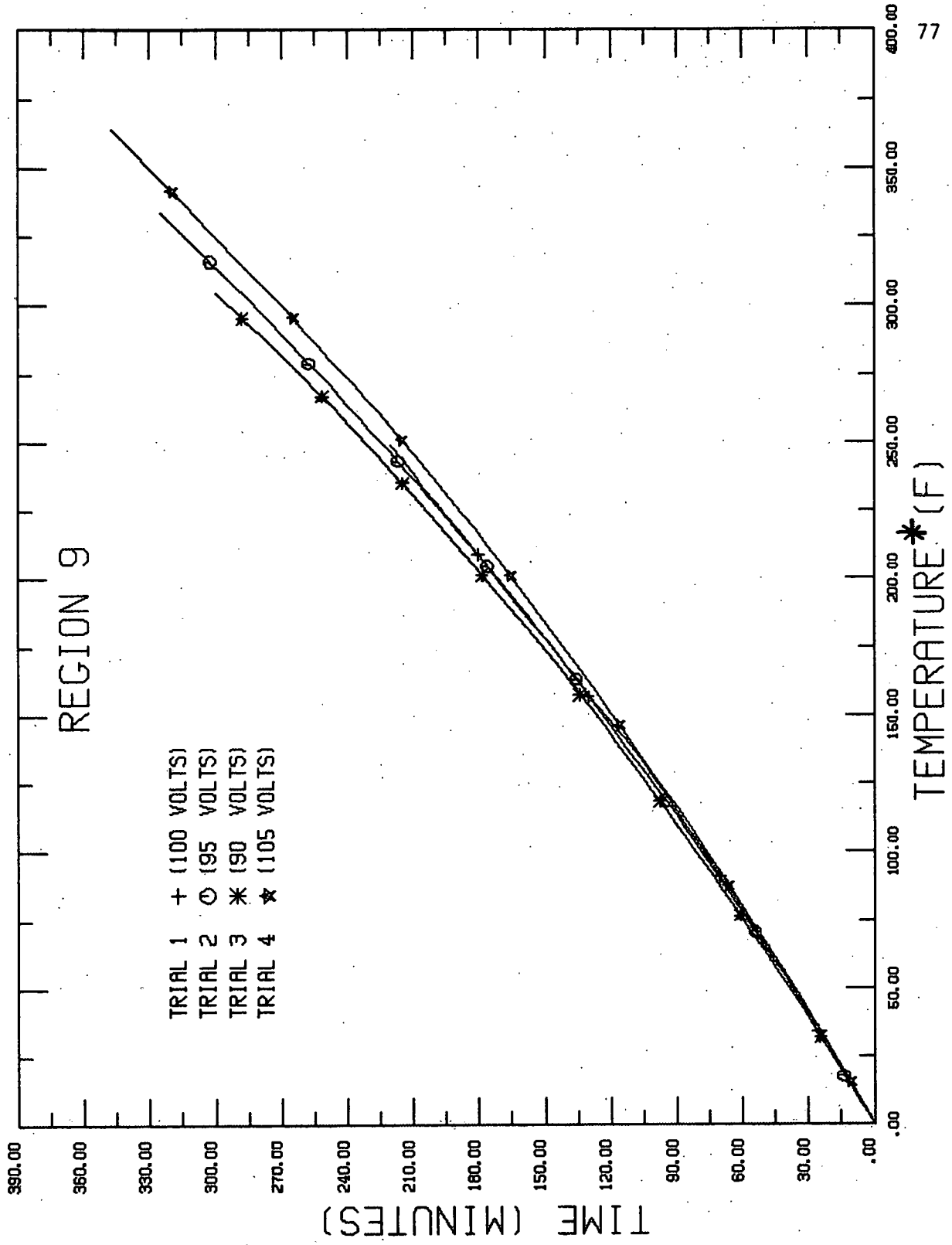


Figure A-4 Normalized temperature-time histories using the data of Figure A-4, $T^*=(T-Ti)/\dot{q}$

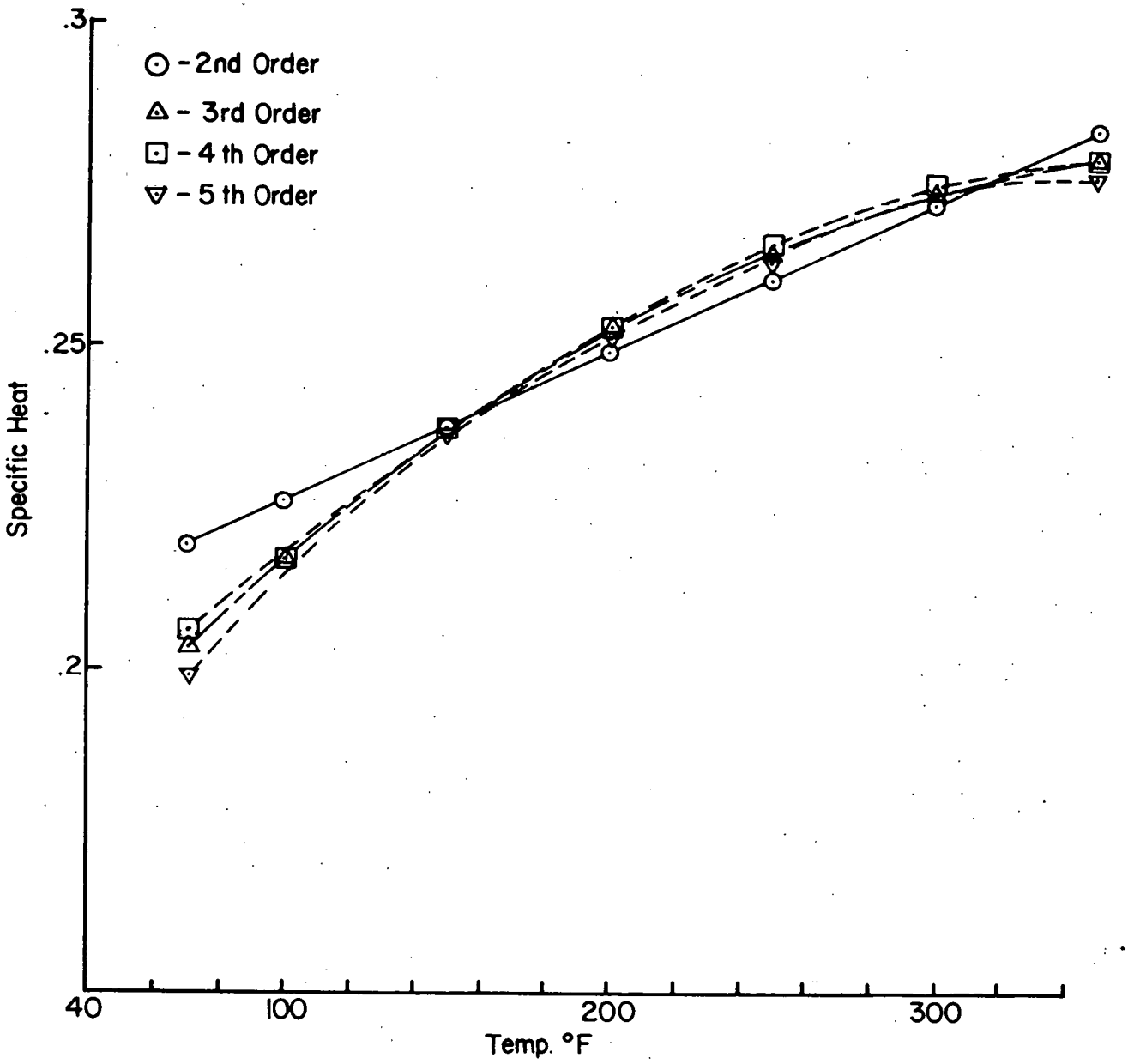


Figure A-5 Test of the sensitivity of predicted specific heat values from various orders of polynomial curve-fits of experimental data, for Region 8.

## SUMMARY AND CONCLUSIONS

An experimental system for measuring the specific heat of tar sands has been developed and tested. The system adequately accommodates the need for large samples, a range of temperatures and the fact that no other property values (such as thermal conductivity) are necessary.

Most of the identified regions of the three test bores have been tested for specific heat, but the data is still to be considered preliminary until further analysis and testing is completed.

Two observations may be noted at this time. First, the specific heat of tar sand is a strong, non-linear function of temperature. This observation has been consistently true for all measurements to date. Second, the large dependence of specific heat on temperature seems to indicate that the bitumen is behaving like it was melting at increasing temperature, so that the specific heat measurement was reflecting a latent heat effect with increasing temperature. This observation is quite speculative, but has some support in the viscosity measurements which are being made at the same time.

# Appendix III

## Thermal Conductivity Measurement

## (Theory and Procedure)

## INTRODUCTION

In order to evaluate the feasibility of in-situ tar sands development, it is necessary to measure thermal conductivities of tar sand samples. Several methods are used for measuring thermal conductivity, depending on limitations of sample size, temperature range of the test, sample homogeniety and expected conductivity range. Three methods will be presented and discussed as possible candidates for the measurement of thermal conductivity of tar sand samples: the guarded hot plate method, the axial rod method, and the comparative method.

From considerations as are pointed out in the review of techniques, an apparatus has been selected, designed, constructed and tested which uses the comparative method of determining thermal conductivity.

### Survey of Methods for Determining Thermal Conductivity

The comparative method and alternative methods for determining thermal conductivity will be discussed in this section. A general survey of thermal conductivity and its measurement has been given by Tye (1969). Figure A-6 is a summary of the applicable ranges of thermal conductivity and temperature which is appropriate for each measurement method. It is seen that the comparative method is the only approach for materials having thermal conductivities between 1 and 10 W/m-°C, which is the expected range of thermal conductivities for tar sand.

The other two techniques, the axial rod and guarded plate, will be discussed for reference purposes and to point out the limitations these methods impose.

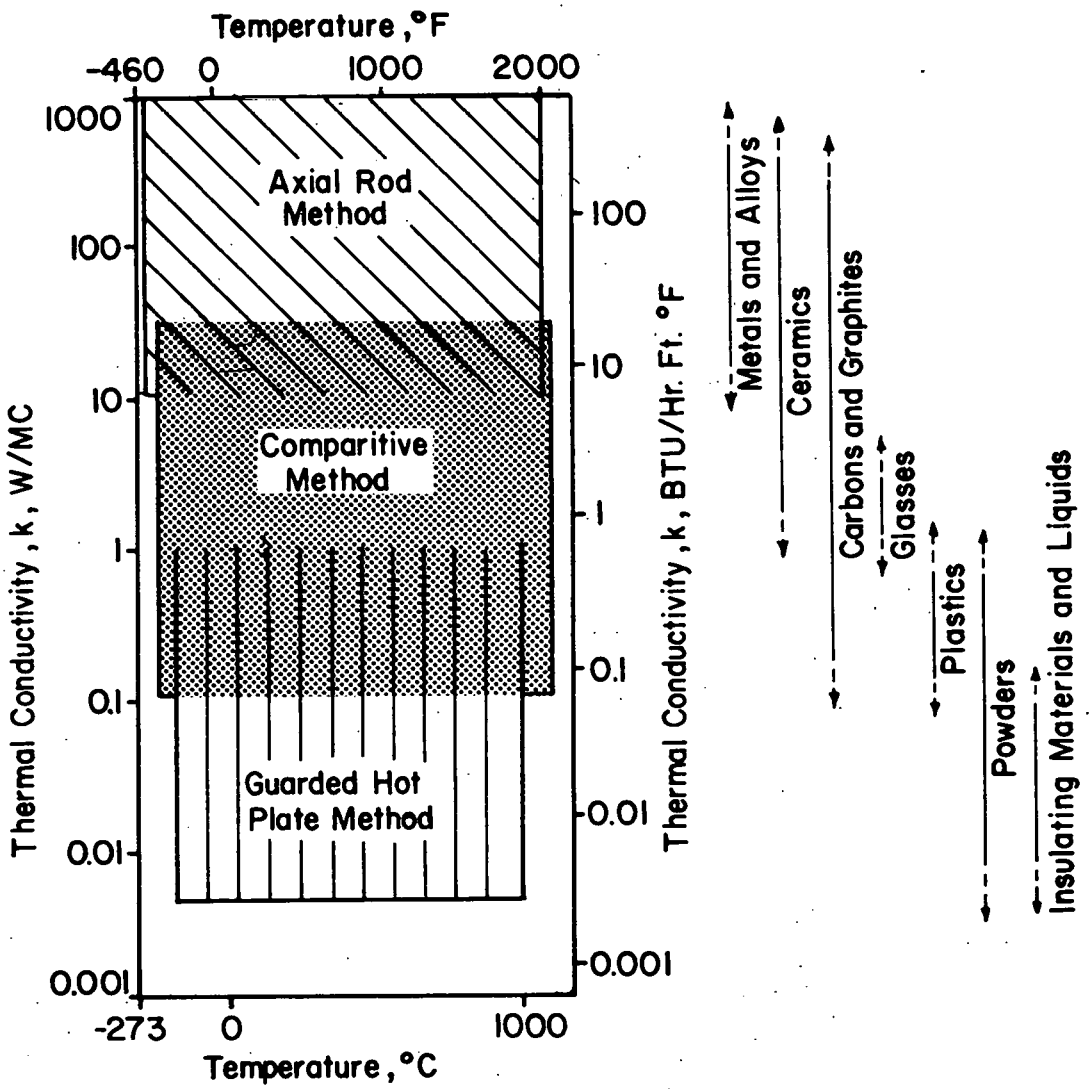


Figure A-6 Summary of applicable ranges of thermal conductivity which is appropriate for each measurement method (from Tye, 1977).

Guarded Plate Method:

The guarded plate method is described in ASTM Standard C177 and is schematically shown in Figure A-7. Standard C177 uses a guarded hot plate which has metal surface plates and a gap between the sample and the guard. The heater is sandwiched between two identical samples. The entire assembly is then placed between two heat sinks. Pressure may be applied to the entire apparatus by an external axial load. For high temperature operation, insulating discs or auxiliary heaters are placed between the samples and the heat sinks. Thermal conductivity may then be calculated by the following equation:

$$k_{sample} = \frac{Q/A}{(dT/dx)_1 + (dT/dx)_2}$$

where Q is the power supplied to the main heater, A is the heater surface area, and (dT/dx) are the measured temperature gradients in the two samples.

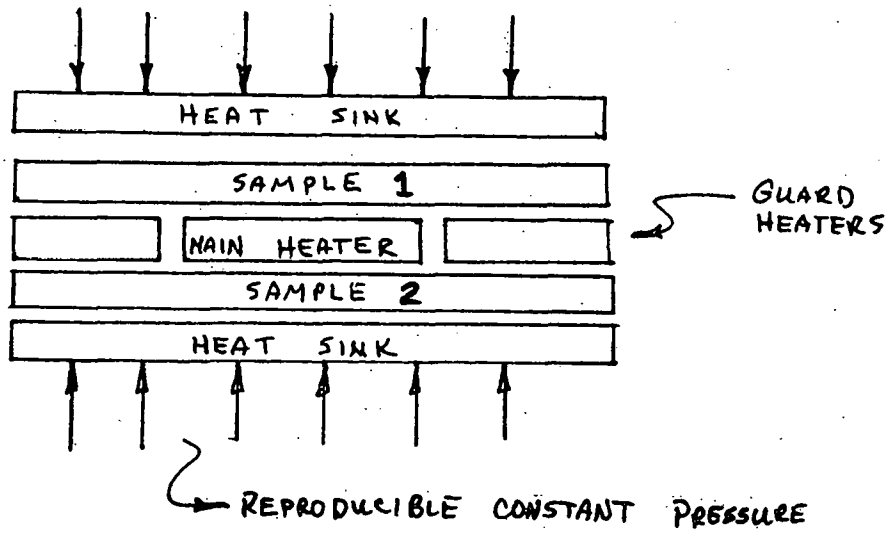


Figure A-7. Guarded hot plate method for determining thermal conductivity of low conductivity materials.

The expected range of thermal conductivity for this method to be applicable is between .02 and 2.W/m-°C. Sample thickness to diameter ratios are approximately 1:6. The design basically provides measurable amounts of heat flux in low conductivity samples without causing excess temperature gradients. A one-sample, guarded hot plate is a variation of this method and essentially utilizes only one side of the apparatus discussed above.

The difficulties encountered in this method when it is applied to the upper conductivity limit values (1-2 W/m-°C) are: radial losses in the samples, two-dimensional effects and the need for large samples (both to account for inhomogenieties and measureable temperature gradients). When applied to tar sand samples, sample slabs of the order of 15 cm. in diameter would be required in order to provide 2.5 cm. thick samples (a necessity due to the inhomogeniety problem).

Axial Rod Method

This technique is shown in Figure A-8, and is composed of a long circular test sample located between a heater and a heat sink. The guard heater is placed around the sample and is separated from the sample by insulation. The range of applicability of this method is from 10 to 1000 W/m-°C. For samples in the 1-2 W/m-°C range, this approach requires very efficient insulation, complex guard heater design and control, and very sensitive heat flux measurements. These problems usually make this method inappropriate for measurements of conductivities in the expected range of tar sand samples. The attractive features include the sample size and the effective averaging out of non-homogenieties due to the sample length.

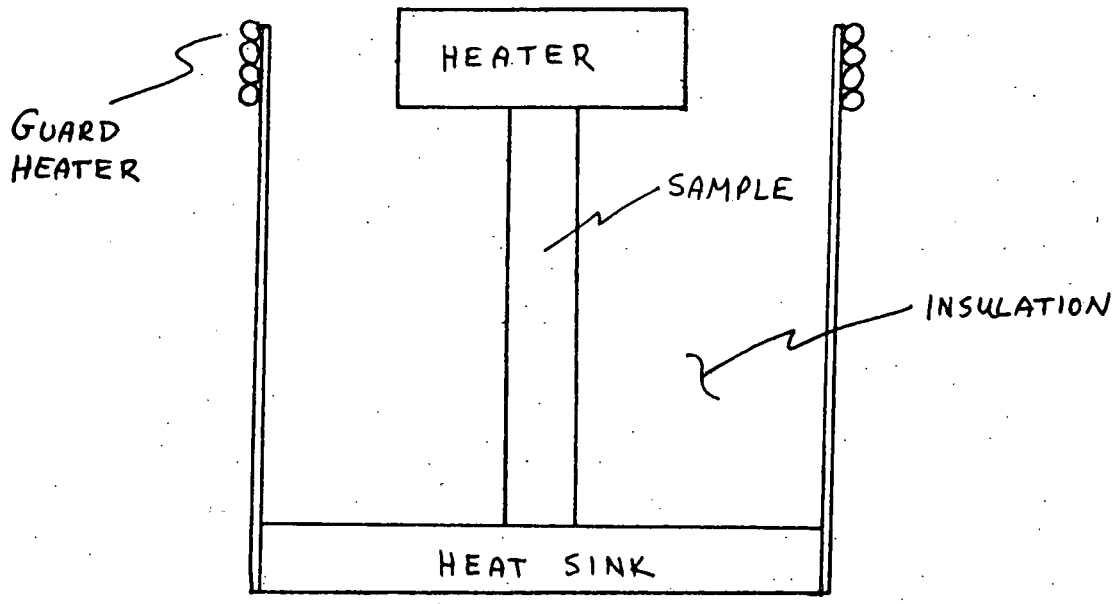


Figure A-8. Axial rod method of measuring thermal conductivity of high conductivity samples

Comparative Method

The comparative method differs from the guarded hot plate methods because the heat flux is not determined from the measured electrical input to a guarded heater. Instead, a reference standard of known conductivity is placed in thermal contact with the test specimen. A temperature difference is set up across the stack and the heat flux is determined by applying Fourier's law of conduction to the standard (see Figure A-9).

The stack may consist of either one or two reference standards and the test sample. The stack order would be either a sample-standard or a standard-sample-standard configuration. Heat transfer through the stack is controlled by the main stack heater above the top standard

and an auxillary heater/heat sink combination below the stack. Radial heat losses from the stack is controlled by a cylindrical guard heater.

If one assumes no heat losses, the heat flux calculated through the reference standard is equal to the heat flux through the test sample. The equation for determining the sample conductivity is:

$$k_{sample} = \frac{k_{standard}\ (\Delta T/\Delta x)\ standard}{(\Delta T/\Delta x)\ sample}$$

where $k_{standard}$ is known at its average temperature, and $(\Delta T/\Delta x)$ is the measured temperature gradient in either the standard or the sample. In the case of elevated temperature measurements, where there is appreciable heat losses, the two-standard configuration is preferable, where the heat flux through the sample may be determined by averaging the heat fluxes through the two standards.

The comparative method has two disadvantages that introduce added error into the conductivity measurement which are not associated with the guarded hot plate methods. First, there is a possibility of a mismatch between the conductivities of the reference standard and the sample. This case then causes widely different temperature differences between the sample and the standards. The second disadvantage is the presence of a contact resistance between the sample and the standard, which must be accounted for by careful measurements of the temperature gradients within each element of the stack.

The advantages of the comparative method include the fact that it is well-suited to measure materials with thermal conductivities in the range between 1 and 10 W/m-°C, it is independently calibrated, and the method allows for a sample size more easily constructed from typical

tar sand core samples. In addition, the apparatus is relatively simple to construct and use.

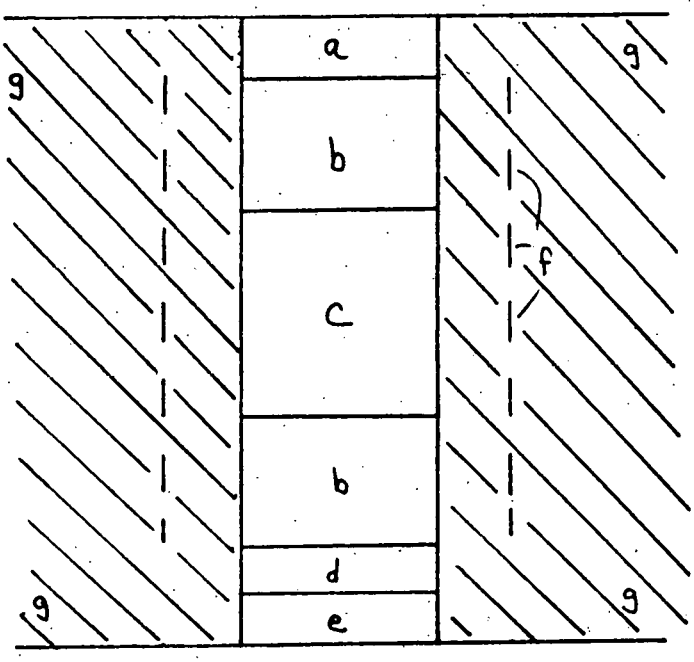


a) main heater
b) standards
c) specimen (sample)
d) auxiliary heater
e) heat sink
f) guard heaters
g) insulation

Figure A-9. Comparative method for determining thermal conductivity, showing the two comparison standard configuration.

Experimental Apparatus and Procedure

The comparative method was selected to best suit the expected conductivity range and non-homogeneous nature of tar sand samples. An experimental comparative method apparatus has been designed, built and tested. The device has been found to be effective in a temperature range between 20°C and 150°C with thermal conductivity calibration errors at ± 3%, which is within the design goal of ± 5%.

Apparatus Description

The apparatus consists of a stack of three elements: two Pyrex 7740 reference standards and the tar sand sample to be tested. Pyrex 7740 is a homogeneous material whose thermal conductivity is known as a function of temperature (see Figure A-10). Pyrex 7740 serves as the top and bottom reference standard while the tar sand sample is aligned in the middle. The standards and sample all are 19 mm. in diameter, 28.6 mm. long and have two .4 mm. holes drilled in them for thermocouple placement. The resulting stack arrangement is shown in Figure A-11.

Heat transfer through the stack is accomplished using a heater at the stack top and a heat sink at the bottom. The heat sink is composed of a reservior with internal running water from a temperature controller in series with a thin foil heater, which allows base temperatures to exceed the boiling temperature of water. A cylindrical guard and insulation surround the stack to prevent radial heat losses. The guard, a thin-walled metal cylinder, has a heater at the top and a heat sink at the bottom. The guard heat sink is composed of copper tubing welded to the cylinder and a small heater adjacent to the copper coils, which serves the same function as the stack heat sink. All four heat sources/

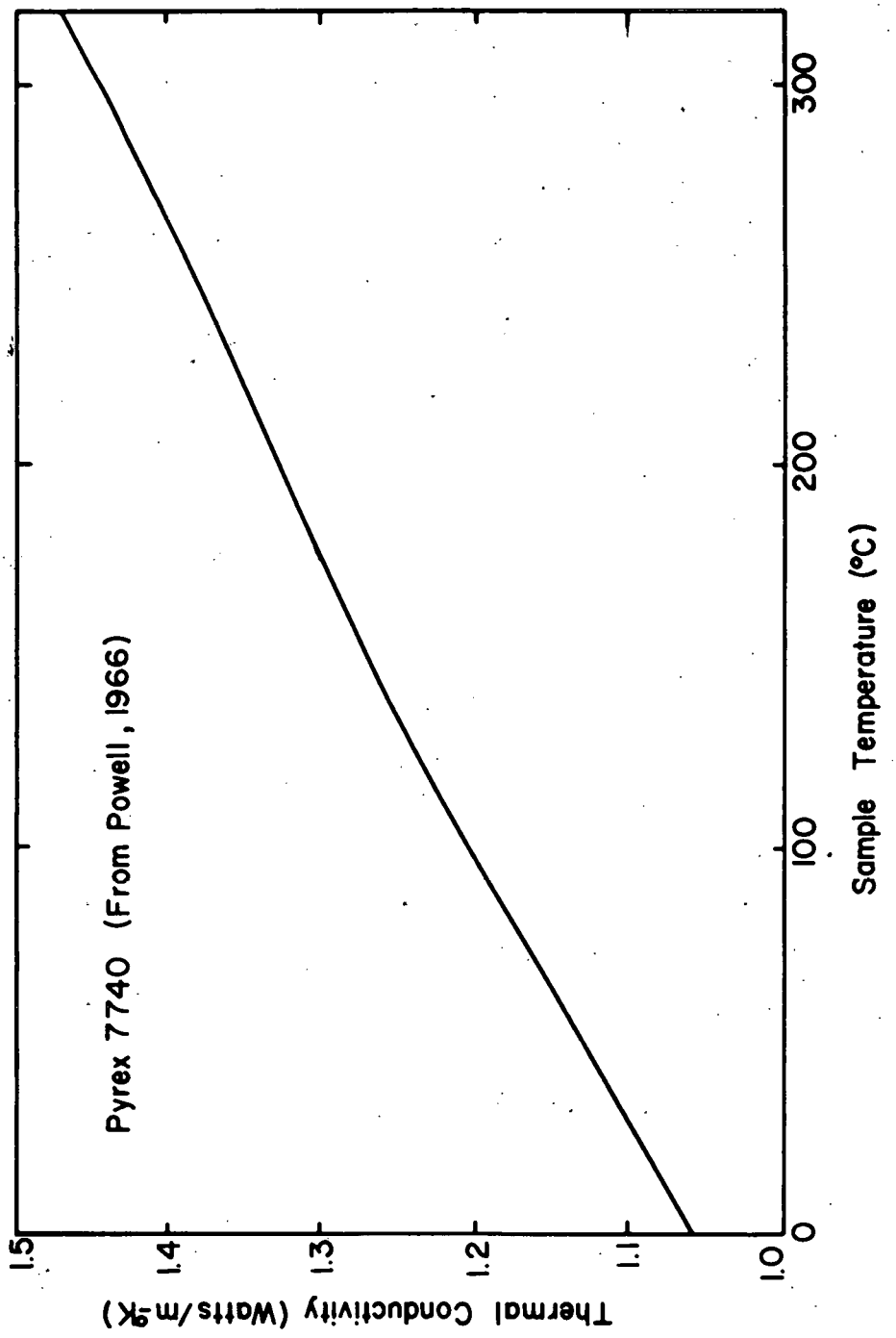


Figure A-10 Thermal conductivity of Pyrex 7740, for use as a comparative standard.

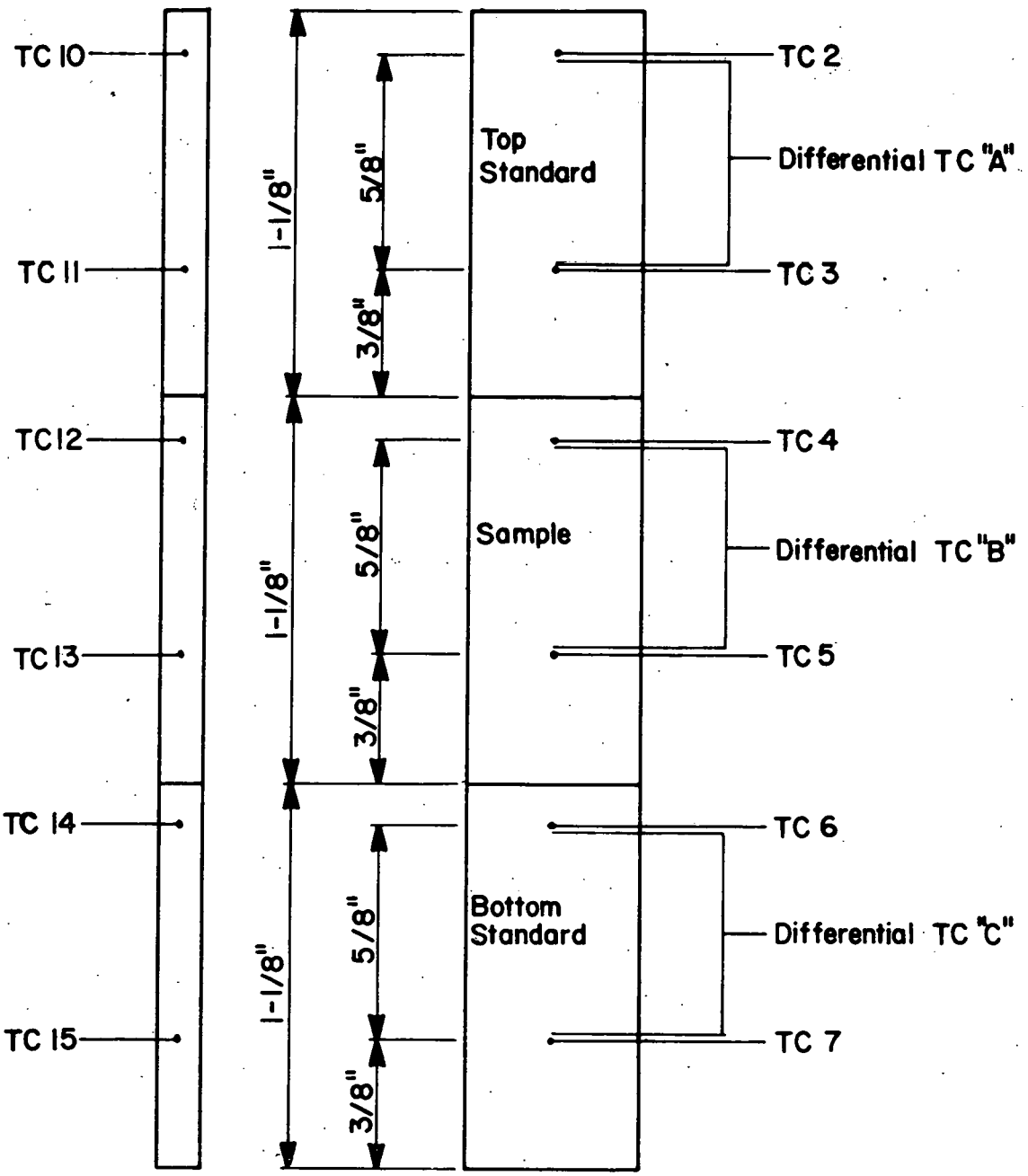


Figure A-11 Detailed view of thermal conductivity and one side of guard, showing dimensions and thermocouple (TC) locations.

sinks are variable and are used to provide controllable temperature gradients within the stack and guard. All temperatures are measured using iron-constantan thermocouples, and the temperature differences in each stack element are measured using differentially arranged thermocouples. A schematic of the overall arrangement of the apparatus is shown in Figure 9, while Figure A-11 shows a detailed view of the stack and associated thermocouple arrangement.

Calibration Procedure

The conductivity device was calibrated using a Pyrex 7740 standard in place of a tar sand sample. The thermal conductivity of the center standard was determined experimentally as a function of the average temperature of the sample and compared to the known conductivity at that temperature (see Figure A-10). The conductivity of the test standard was examined at average stack temperatures ranging from 50°C to 120°C. Experimental accuracy was determined to be within $\pm$ 3% when compared withthe published conductivity data.

Experimental Results and Discussion

The measured temperatures at the interior locations within the stack are shown in Figure A-12 for three temperature levels for a tar sand sample test. Fourier's law may be applied to each of the three stack elements:

$$q = k_i(T_i)A\frac{\Delta T_i}{L_i}$$

where $q_i$ is the heat transfer rate through each element, $k_i(T_i)$ is the thermal conductivity of each element (evaluated at the average temperature of the element), A is the cross-sectional area of the stack,

$\Delta T_i/L$ is the temperature gradient within each element.

It will be noted in Figure A-12 that the conductivities of the sample do not exactly match the standard conductivities (since dT/dx is not the same). If the mismatch is not too significant, this difference does not create any real problems. Care must be taken to keep heat losses to a minimum, however, and this is accomplished by adjusting the guard temperature to closely match the stack temperature profiles.

Even with care, there is some heat loss from the stack to the surroundings so that the heat flux through the top (hot) standard, $q_1$, is greater than the heat flux through the bottom (cold) standard, $q_3$. The heat flux through the sample is estimated by taking an average of $q_1$ and $q_3$:

$$q_2 = \text{qsample} = \frac{1}{2}(q_1 + q_3)$$

The thermal conductivity of the sample, then is:

$$k_2(T_2) = \text{ksample}(T_2) = \frac{q_2 L_2}{A\ \Delta T_2}$$

It will also be noted from Figure A-12 that there is a significant contact resistance between the test sample and the comparison standards (as reflected by the temperature at each interface). This resistance presents no experimental problems if the temperature gradient within the sample is independently measured. Extrapolation methods to estimate interface temperatures do not yield valid results due to this contact resistance.

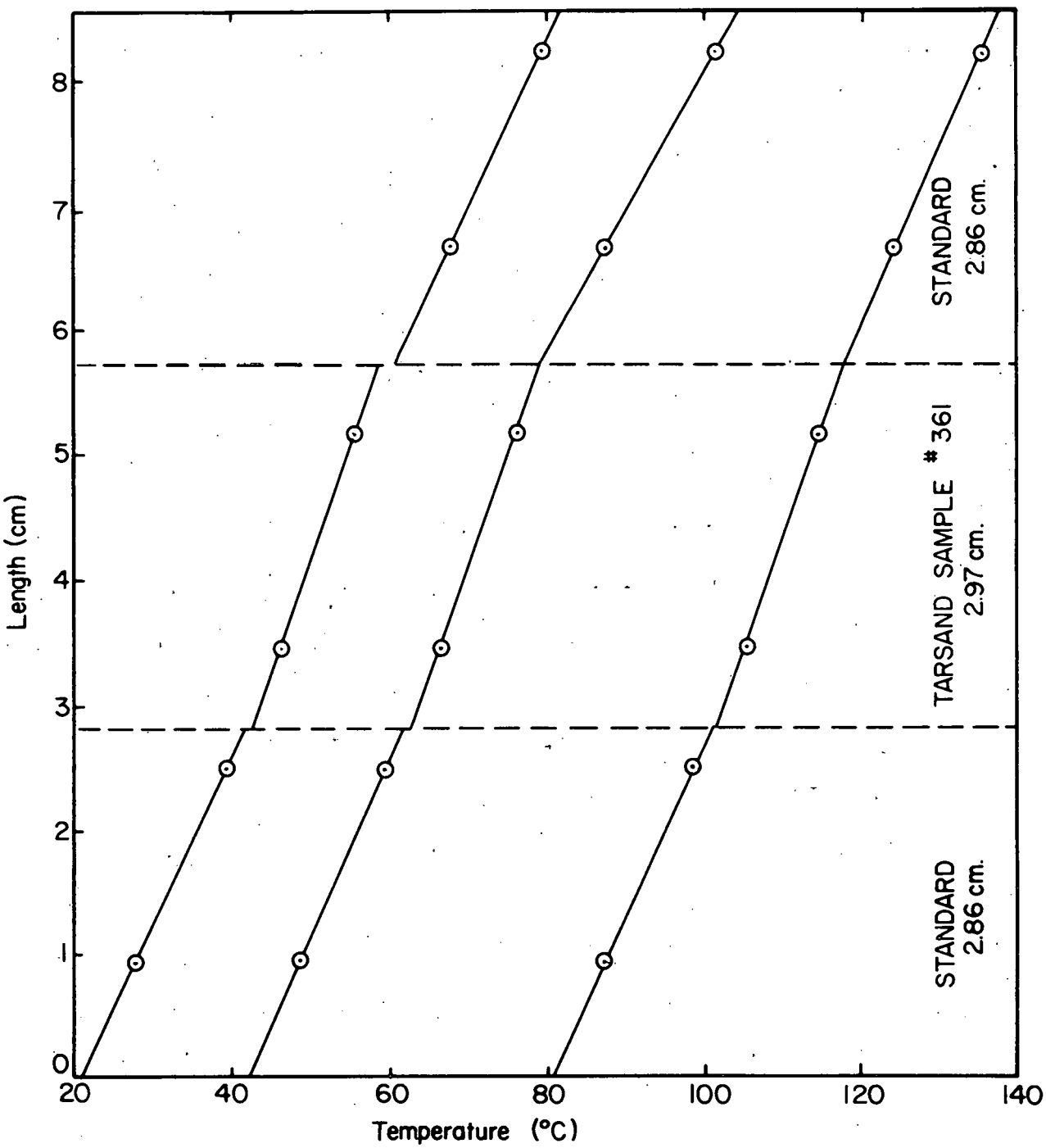


Figure A-12 Temperature profiles within the thermal conductivity stack for Sample Number 361.

The experimental procedure involved an initial setting of input heat flux to the sample heater and heat sink temperature(via. temperature controlled water circulation). When a steady-state was reached within the stack and the guard temperatures were adequately watched with corresponding stack temperatures ($\pm$ .5°C), the stack temperatures were recorded. The system was then adjusted for a higher operating temperature and the process was repeated. Higher operating temperatures were reached by increasing the heat sink temperature. The set of stack temperatures at each steady-state setting were then used in the calculation procedure previously discussed to predict thermal conductivity.

In order to reach average sample temperatures over 100°C the heat sink operation must be modified to increase the sink temperature. This is accomplished by adding a foil heater between the sink and the stack and effectively adding a controllable resistance at that point. This change of operating mode has introduced some systematic error which is being addressed by an improved heater design.

As examples of the experimental results, two tests are shown in Figure 3 for samples whose properties are tabulated in Table IV. The systematic drop in conductivity at the higher temperatures is apparent, but the conductivity measurements fall within $\pm$ 5% of the average. This variability should be reduced with improved high temperature methods.

# Appendix IV

## Relative Permeability Measurements

## (Theory and Procedure)

# INTRODUCTION

Relative permeability curves for tar sand samples have been generated through a multi-step procedure based on theoretical and empirical results. The curves were calculated from capillary pressure measurements which were obtained from a mercury injection apparatus. This particular technique was used because of the speed, ease, and availability of the mercury injection apparatus as compared to measuring relative permeability directly. The accuracy of this technique is subject to question and the results seem to warrant further testing and independent checking.

This report summarizes the procedure for calculating relative permeability from capillary pressure. The various techniques of measuring capillary pressure are considered. The calculated values of relative permeability from the present procedure are presented and discussed.

## The Use of Capillary Pressure to Determine Relative Permeability

Because of the time, expense, and difficulties involved with trying to measure relative permeabilities directly (W. Rose, personal communication), an approach has been used to deduce relative permeability from measurements of capillary pressure. The theoretical basis for such an approach was developed through the work of numerous authors, including Burdine (1953) and Wyllie and Gardner (1958). Brooks and Corey (1964) compiled the work of these authors together with experimental data of their own to form a technique of calculating relative permeability from capillary pressure measurements. This technique, summarized below,

has been used on the tar sand cores to obtain relative permeability curves. Bear (1975) also summarized the results presented by Brooks and Corey (1964). Scheidegger (1960) reviews some other techniques.

From a large number of experimental data, Brooks and Corey (1964) observed that the effective saturation $S_e$ (defined as $S_e = \frac{S - S_{w_o}}{1 - S_{w_o}}$, $S_{w_o}$ being the irreducible wetting saturation) is related to capillary pressure, $P_c$, by

$$S_e = \frac{P_b}{P_c}^{\lambda} \quad \text{for } P_c \geq P_b \,, \tag{1}$$

where $\lambda$ and $P_b$ are characteristic constants of the medium. $\lambda$ is a number which characterizes the pore-size distribution and $P_b$, the bubbling pressure, is a measure of the maximum pore-size forming a continuous network of flow channels within the medium. Substituting equation (1) into the equations derived by Burdine (1953) and Bear (1975).

$$k_{rw} = S_e^2 \frac{\int_0^{S_e} \frac{dS}{P_c^2}}{\int_0^1 \frac{dS}{P_c^2}} \tag{2}$$

and

$$k_{rw} = (1 - S_e)^2 \frac{\int_{S_e}^1 \frac{dS_e}{P_c^2}}{\int_0^1 \frac{dS_e}{P_c^2}} \tag{3}$$

yields:

$$k_{rw} = (S_e)^{\frac{2 + 3\lambda}{\lambda}} = S_e^{\varepsilon} \,, \quad \varepsilon = (2 + 3\lambda)/\lambda \tag{4}$$

and

$$k_{rnw} = (1 - S_e)^2 (1 - S_e^{\frac{2 + \lambda}{\lambda}}). \tag{5}$$

So after experimentally determining $\lambda$, $P_b$, and $S_{w_o}$, relative permeability curves may be generated using equations (4) and (5).

The quantities $\lambda$ and $P_b$ are obtained by plotting $S_e$ versus $P_c$ on a log-log scale. Plotted this way, $\lambda$ is the slope of the straight line region of the curve, and $P_b$ is the value of $P_c$ at which the straight line approximation intercepts $S_e = 1$. To plot $S_e$, however, the value of $S_{w_o}$ must be known since S is the only saturation measured directly. To determine $S_{w_o}$, various values of $S_{w_o}$ are assumed and the corresponding $S_e$'s are plotted versus $P_c$. The value of $S_{w_o}$ which causes the $S_e$ versus $P_c$ curve to be the best straight line approximation (when plotted on a log-log scale) is the $S_{w_o}$ selected. So with the correct $S_{w_o}$ selected, $\lambda$ and $P_b$ can be calculated and the relative permeability curves may be generated from equations (4) and (5).

The Measurement of Capillary Pressure

There are a number of ways to measure capillary pressure, including the restored state, mecury injection and centrifuge methods. Some authors who have reviewed the various ways include Brown (1951), Purcell (1949), and Slobod, et. al. (1951). The restored state method is a standard and reliable method, but unfortunately, it is extremely slow, taking several weeks to obtain one capillary pressure curve. The mercury injection and centrifuge methods are both much faster and the U.W. mineral engineering department has a mercury injection apparatus which is being used for this series of tests.

Since the surface tension and wetting angle of mercury is different from that of water and oil, curves generated by the mercury injection

method must be compensated to correspond with the restored state method. The equation for capillary pressure is:

$$P_c = \frac{2\sigma\cos\theta}{r} \qquad (6)$$

where $\sigma$ is the surface tension, $\theta$ is the wetting angle, and r is the radius of curvature of the fluid. Using a surface tension and wetting angle for mercury of 480 dynes/cm and 140° together with a surface tension and wetting angle for water of 70 dynes/cm and 0°, Purcell (1949) determined the ratio of capillary pressures for a given pore size to be approximately 5. Using this ratio he found fair agreement between the mercury injection apparatus and the restored state displacement cell.

Brown (1951) found that much better agreement could be reached if that ratio were allowed to vary with values ranging between 5.4 and 8.3. For limestone he found the average ratio to be 6.4 and for sandstone, the average was 7.2. Since most of the core analysis done deals with sandstone, a ratio of 7.2 was picked.

The ratio of 7.2 enables the pressure versus saturation data from the mercury injection apparatus to be converted to a capillary pressure curve which can be manipulated into relative permeability curves in accordance with the previous section.

Accuracy of Results

Since the above procedure is a multi-step process based on a number of theoretical and empirical results, it would be desirable to check these calculated relative permeability curves against a standard relative permeability measuring device. Unfortunately, no such device is readily available. However, it was possible to check the procedure

of determining $S_{w_o}$, $\lambda$, and $P_b$. This procedure will be discussed below.

Brooks and Corey (1964) presented data of capillary pressure versus saturation along with their calculated values of $S_{w_o}$, $\lambda$, and $P_b$. This data was used to compare our calculations of $S_{w_o}$, $\lambda$, and $P_b$ with Brooks and Corey, Figure A-13 shows the plot of $S_e$ versus $P_c$ for an assumed $S_{w_o} = 0$. As can be seen, the plot is not very straight. As the value of $S_{w_o}$ is increased, the plots become straighter. Figure A-14 shows the plot of $S_e$ versus $P_c$ for $S_{w_o} = 0.166$, which is a much straighter plot. Increasing $S_{w_o}$ further does not improve the straight line fit. The slope and intercept of the straight region in Figure A-14 is $\lambda = 3.45$ and $P_b = 40$, respectively. Brooks and Corey's $\lambda$ and $P_b$ were 3.7 and 41 respectively for an $S_{w_o}$ of 0.167, in quite close agreement with the technique presented here.

## RESULTS AND DISCUSSION

Since wells 3T2, 3T3, and 3T4, were divided into a total of twelve regions, a representative depth from each region was picked for relative permeability measurement. To date, four regions have been tested. Relative permeability curves of the four measured regions are shown in Figure 4. The corresponding capillary pressure curves are shown in Figures A-15 through A-18. It can be seen in Figure 4 that the relative permeability curves are all very similar. The measured values of $S_{w_o}$ and $\lambda$ which are used to calculate relative permeability are shown in Table A-1.

| Region | $S_{w_o}$ | $\lambda$ |
|---|---|---|
| 1 | 0. | .43 |
| 3 | 0.001 | .37 |
| 6 | 0.007 | .53 |
| 7 | 0. | .34 |

Table A-1. Calculated values of $S_{w_o}$ and from capillary pressure measurements.

The four cores which have been measured cover the range of consistency from very loose sandstone to shale. Since the relative permeabilty curves are nearly identical for these four different cores, a few possibilities suggest themselves: the pore-size distribution, as reflected in similar values of $\lambda$, is the same order for all samples, the experimental and numerical procedure for determining $\lambda$ and $S_e$ is inadequate to resolve the material differences, or Burdine's theory is an inadequate representation of the relevant processes. In any case, measuring more regions would quite likely produce similar relative permeability curves.

Further testing of the measurement technique is necessary. The procedure for calculating $S_{wo}$ and $\lambda$ has already been checked as has been previously described. The capillary pressure measurements and the procedure for calculating relative permeability remains unchecked. This can perhaps be most easily checked by an independent agency. In addition, the use of a material completely different from tar sand, such as packed glass beads, in the mercury injection apparatus is currently being tested and will be compared to similar tests which have been reported by Brooks and Corey (1964). Another procedure for calculating relative permeability from capillary pressure is also under current investigation.

| Region | Well | Depth | Rho-S | Rho-E | Rho-SG | Phi-S | Phi-E | K(S) | K(E) | Wo | So | Sw |
|---|---|---|---|---|---|---|---|---|---|---|---|---|
| 1 | 3T4 | 427 | 2.045 | 1.756 | 2.664 | 4.19 | 34.09 | 6.2 | 559.8 | 12.10 | 72.57 | 2.46 |
| 3 | 3T4 | 520 | 2.077 | 1.836 | 2.659 | 5.88 | 30.97 | 4.8 | 629.1 | 12.15 | 81.52 | 2.41 |
| 6 | 3T3 | 472 | 2.233 | 2.132 | 2.609 | 7.80 | 18.27 | 11.4 | 42.2 | 0.0 | 0.0 | 68.11 |
| 7 | 3T3 | 502 | 2.056 | 1.828 | 2.613 | 6.45 | 30.03 | 52.8 | 619.8 | 10.89 | 74.58 | 16.91 |

Table A-2. Routine core measurement results for regions where relative permeability measurements were made.

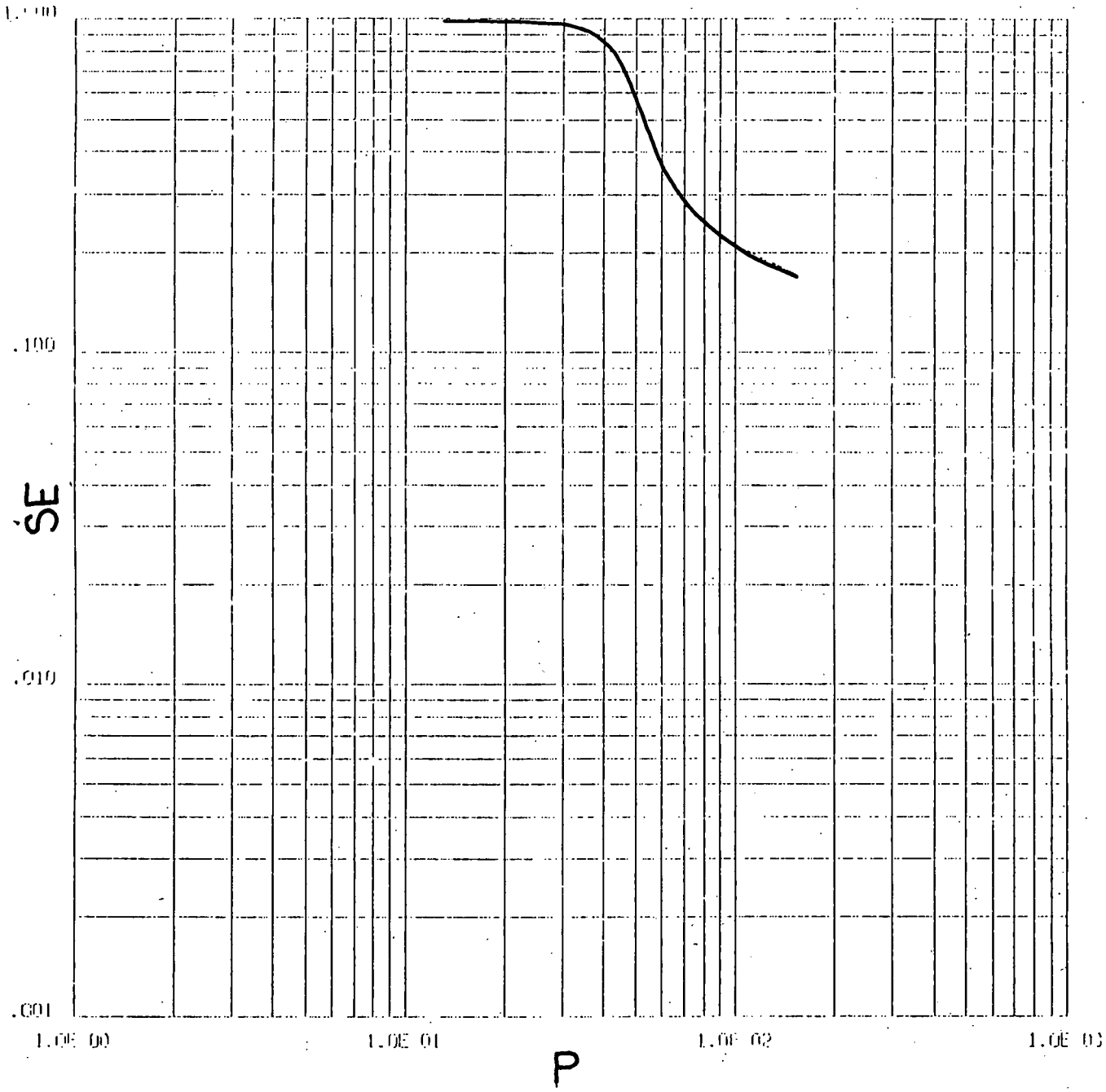


Figure A-13 Effective saturation vs. capillary pressure for $S_{w_o} = 0.0$ (from Brooks and Corey, 1964).

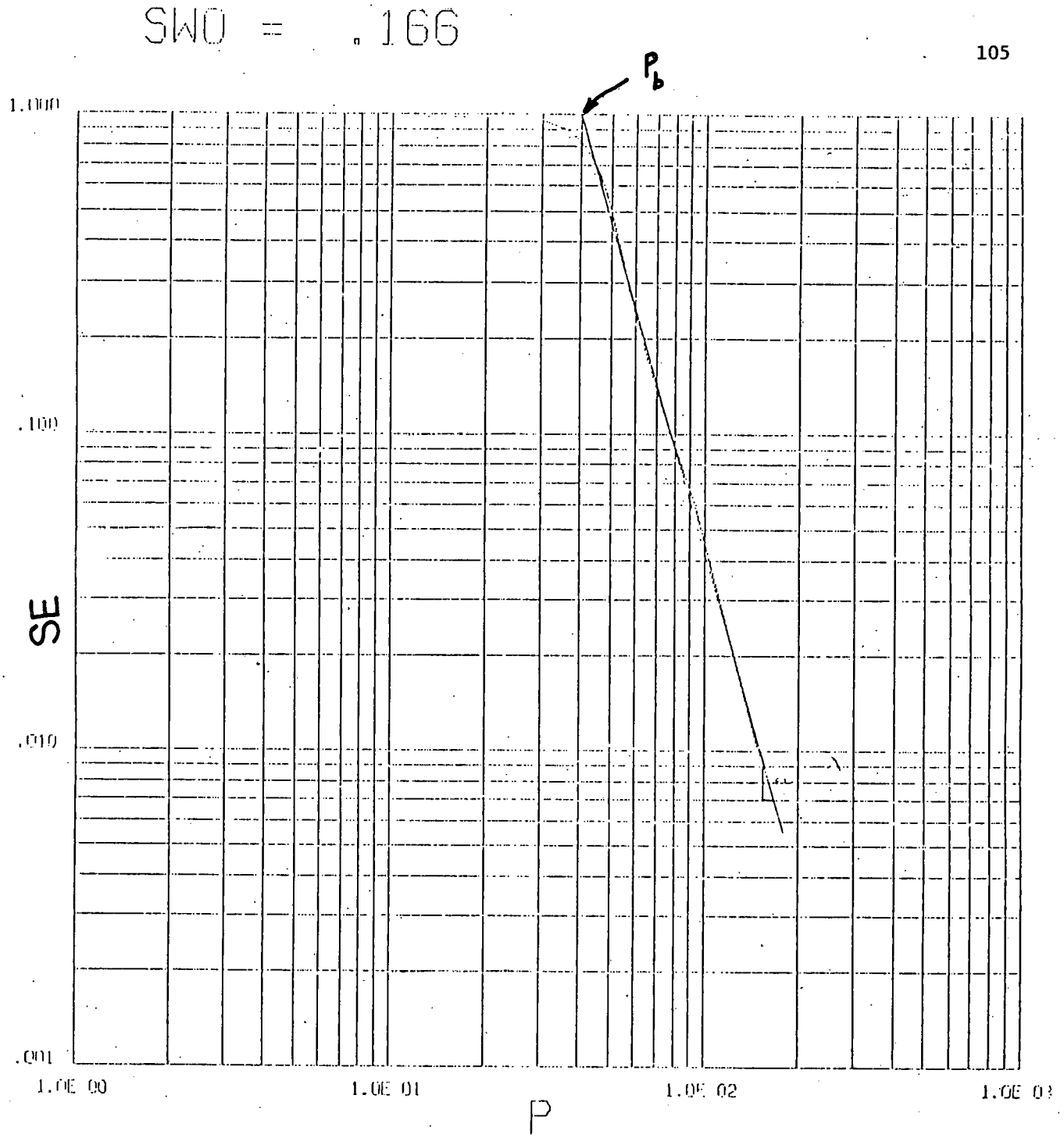


Figure A-14 Effective saturation vs. capillary pressure for $S_{w_o}$ = .166 (from Brooks and Corey, 1964).

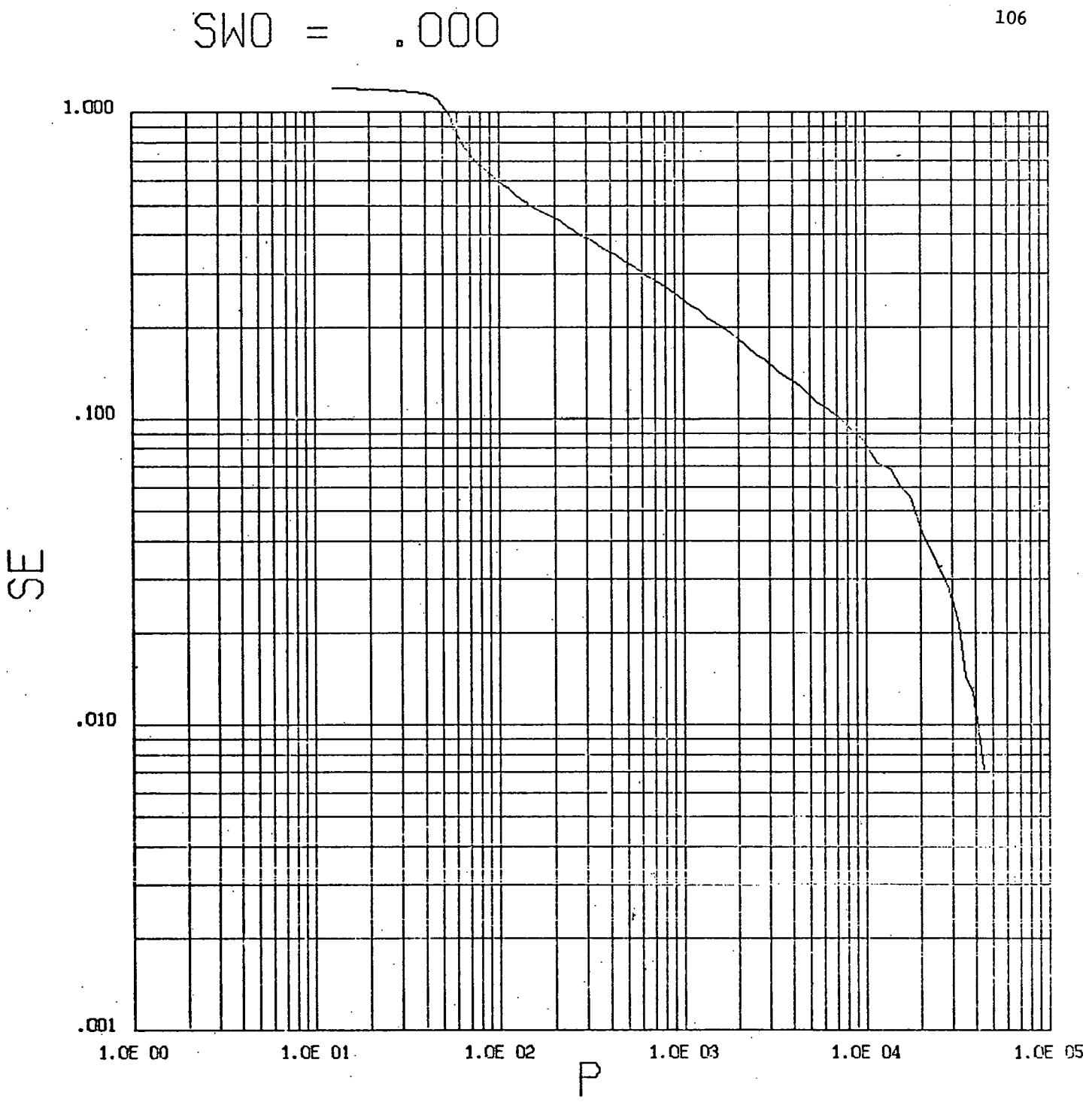


Figure A-15 Effective saturation vs. capillary pressure for $S_{w_o}$ = 0.0 (measured in Region 1).

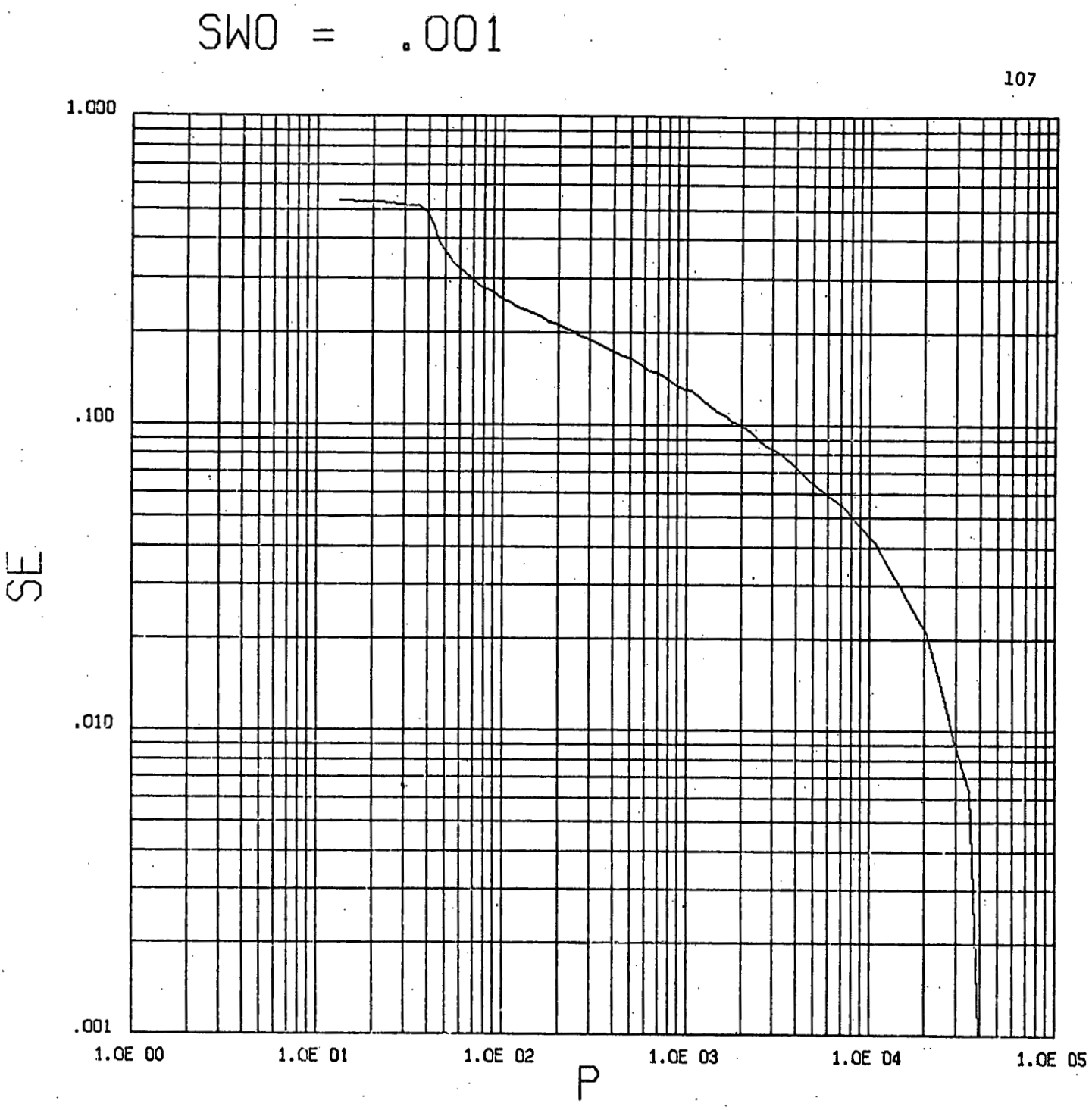


Figure A-16 Effective saturation vs. capillary pressure for $S_{wo}$ = .001 (measured in Region 3).

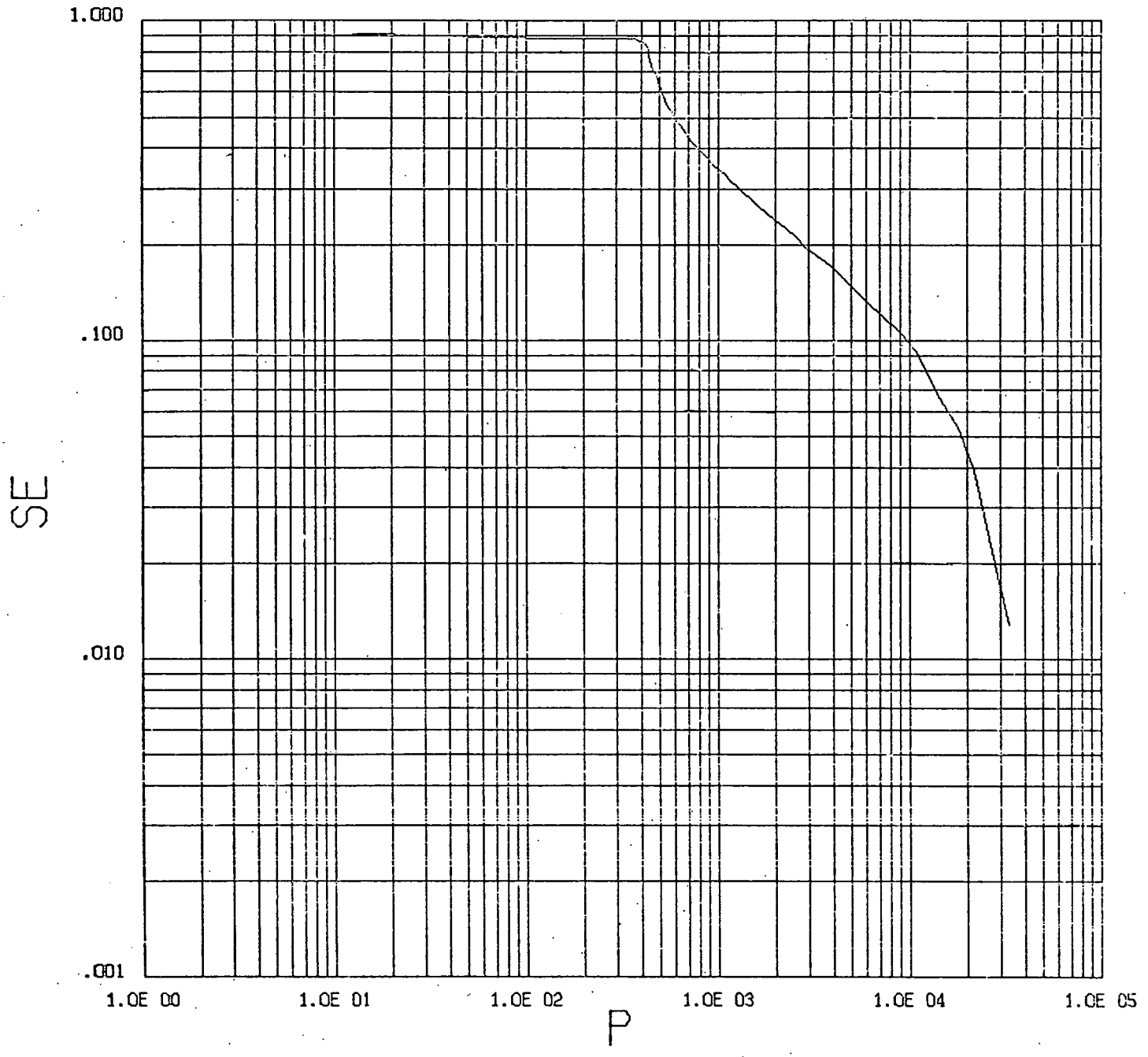


Figure A-17 Effective saturation vs. capillary pressure for $S_{w_o}$ = .007 (measured in Region 6).

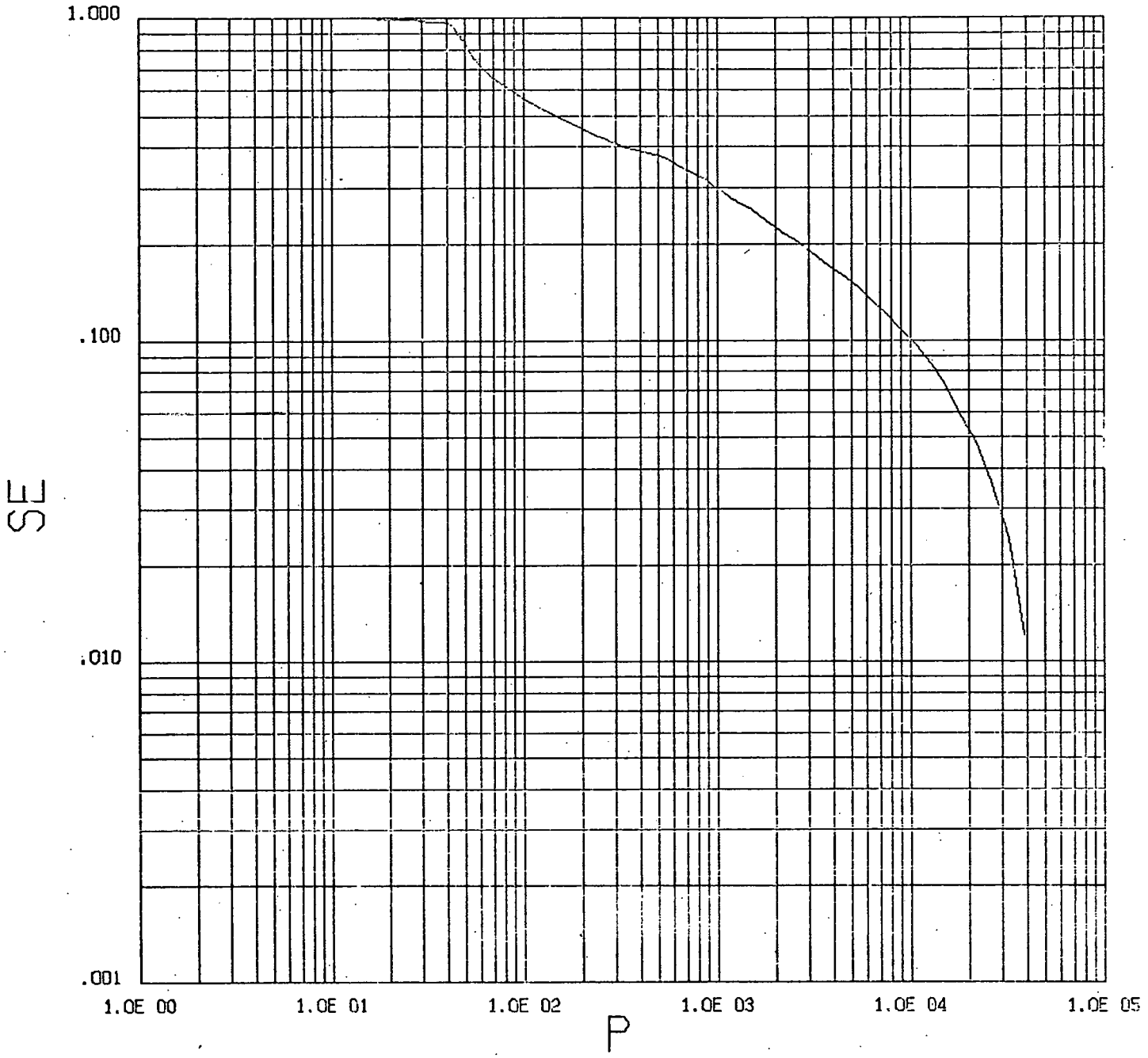


Figure A-18 Effective saturation vs. capillary pressure for $S_{w_o}$ = 0.0 (measured for Region 7).